AD 687294

December 1968

Final Report

EXISTING STRUCTURES EVALUATION
Part II: Window Glass and Applications

Prepared for:
OFFICE OF CIVIL DEFENSE
OFFICE OF THE SECRETARY OF THE ARMY
WASHINGTON, D.C. 20310

STANFORD
RESEARCH
INSTITUTE

SRI

MENLO PARK
CALIFORNIA

Final Report

SUMMARY OF EXISTING STRUCTURES EVALUATION
Part II: Window Glass and Applications

December 1968

Contract No.
OCD-DAHC20-67-C-0136

OCD Work Unit
No. 1126C

Prepared for:

OFFICE OF CIVIL DEFENSE
OFFICE OF THE SECRETARY OF THE ARMY
WASHINGTON, D.C. 20310

STANFORD
RESEARCH
INSTITUTE

MENLO PARK
CALIFORNIA

By:

J.H. Iverson
Public Works Systems

OCD Review Notice

This report has been reviewed by the Office of Civil Defense and approved for publication. Approval does not signify that the contents necessarily reflect the views and policies of the Office of Civil Defense.

SUMMARY

Introduction

This report covers one portion of a research project to evaluate existing NFSS structures for resistance to combined nuclear weapons effects. The objective of this investigation was to determine the response of windows to air blast overpressures generated by nuclear explosions, including glass fragment data (weights, velocities, numbers produced, and spatial densities) that could be used to predict statistically the effects of window glass failure on humans.

Glass, a brittle material, conforms to elastic theory to the point of failure. Unfortunately, the usual methods of structural analysis based on material ultimate strength or breaking stress were found to be inapplicable to glass panes. Glass strength depends almost completely on flaws or defects. Therefore, failure strongly depends on the probabilities of the number, size, and location of flaws.

Incipient Failure Load Prediction

Windows exposed to explosions were found to behave similarly to a simple oscillator. Thus, the differential equation of motion for a single-degree-of-freedom system with no damping was usable. Window glass response predictions were based on a load-deflection relationship. The loading with about 50 percent probability of causing failure was reported.

The analytical work was begun with a theoretical load-deflection equation for large deflections of plates since deflections from one to

seven times the glass thicknesses were found in test data. The equation, which includes both bending and membrane action, was then modified slightly (in the membrane term) to fit available static test data. Failure loads, which serve as end points to the equation for various pane sizes and thicknesses, were selected from design data. Thus, a static resistance function describing window response including failure was established.

Data relating breaking stress to various loading rates were used to select 1.8 as the ratio of dynamic to static failure loads.

The air blast loading function selected was the pressure-time relationship that describes the interaction of a nuclear blast wave with the front face of a closed rectangular structure. The clearing distance was set equal to zero for side-face loading.

A computer program was developed that numerically solved the differential equation of motion using the Newmark β Method. The resistance function and the loading function were included in the program as subroutines. Inputs to the program include window size and load parameters. The print-out includes the load causing incipient failure and a complete time-history of the response, if desired. The results of several runs were plotted. Figure S-1 provides predictions of the free-field overpressure with a 50 percent probability of causing incipient failure in windows containing sheet glass subjected to front-face loading. Similar figures for side-on loading and for plate glass are included in the report.

Glass Fragment Characteristics

Data on weight, velocity, and spatial density of glass missiles resulting from window failure caused by a nuclear explosion were reported for Operation Teapot tests. Glass missiles emanating from multipane windows having either steel or wood frames were trapped in Styrofoam absorbers.

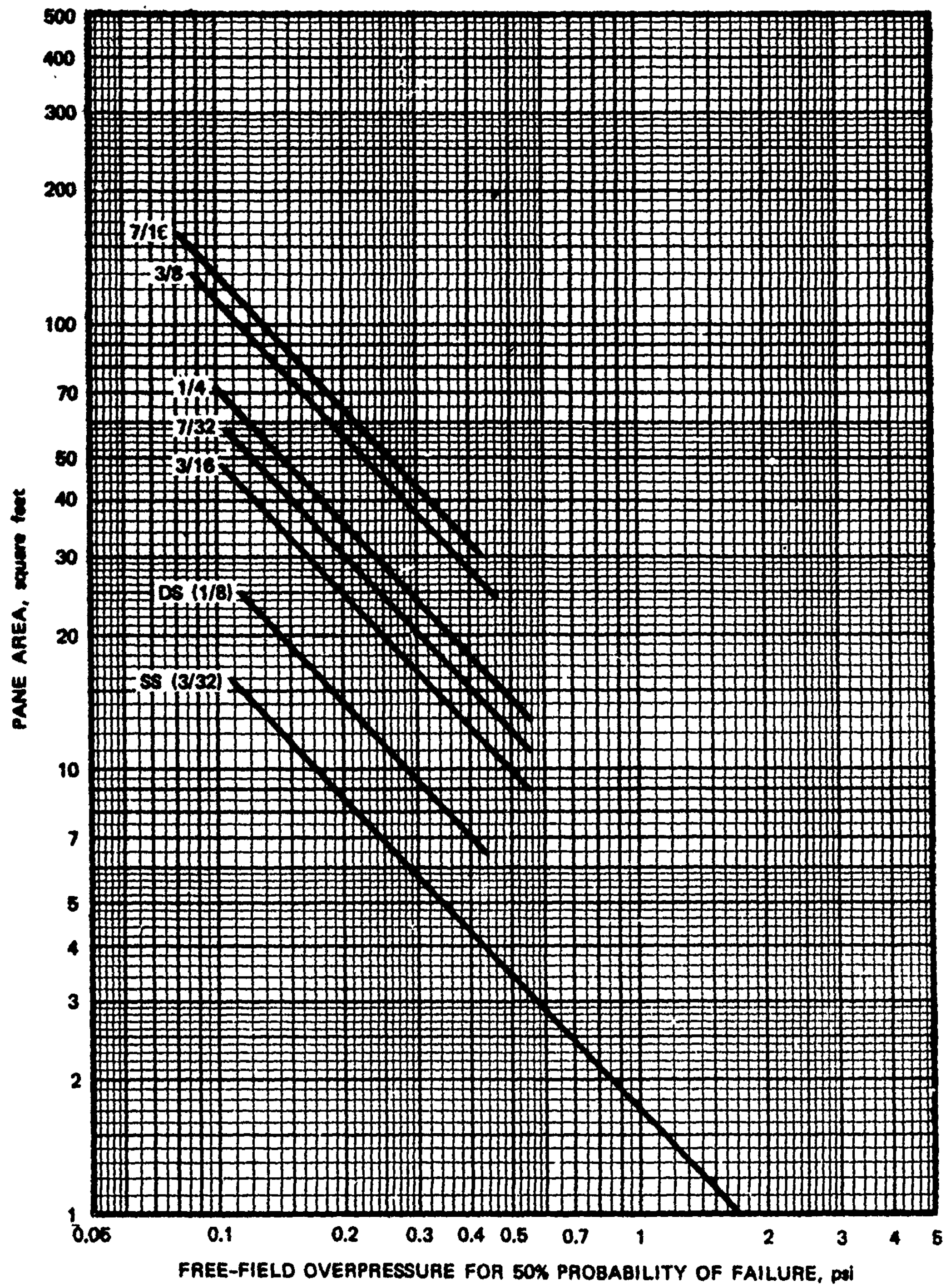

FIG. S-1 SHEET GLASS INCIPIENT FAILURE PRESSURES FOR FRONT-FACE LOADING AS A FUNCTION OF PANE AREA AND THICKNESS

These test data were used to develop the curves presented in Figure S-2, which can be used to predict average and geometric mean fragment weights. The geometric mean fragment weight was found to be indicative of the most likely fragment weight. The average fragment weight is needed in calculations of the number and spatial density of fragments.

The spatial density of fragments very near a window can be estimated by

$$N_0 = \frac{\gamma h}{\bar{M}} \tag{S-1}$$

where N_0 is the spatial density of fragments zero feet from a window (units are fragments per area), γ is the unit weight of glass (0.090 lb/in^3), h is the pane thickness, and $\bar{M}$ is the average fragment weight. The total number of fragments produced by a given window may be found by multiplying N_0 by the total glass area of the window.

The spatial density of fragments 10 feet from a window (N_{10}), based on the Operation Teapot data, can be found by using Figure S-3.

Fragment velocities calculated in this report were based on Bowen's (1961) translation model. Examples of some calculated velocities appear in Table S-1.

The procedures described above for estimating incipient failure and weights, spatial densities, numbers, and velocities of fragments were applied to windows in 14 buildings located in San Jose and Palo Alto, California, which were part of the National Fallout Shelter Survey (NFSS). The results can be found in Chapter VII of the report.

Biological Considerations

Figure S-4, adapted from work by Bowen, et al. (1956), is presented to relate fragment characteristics to injuries. This figure is presented for illustrative purposes only, since original work on the biological

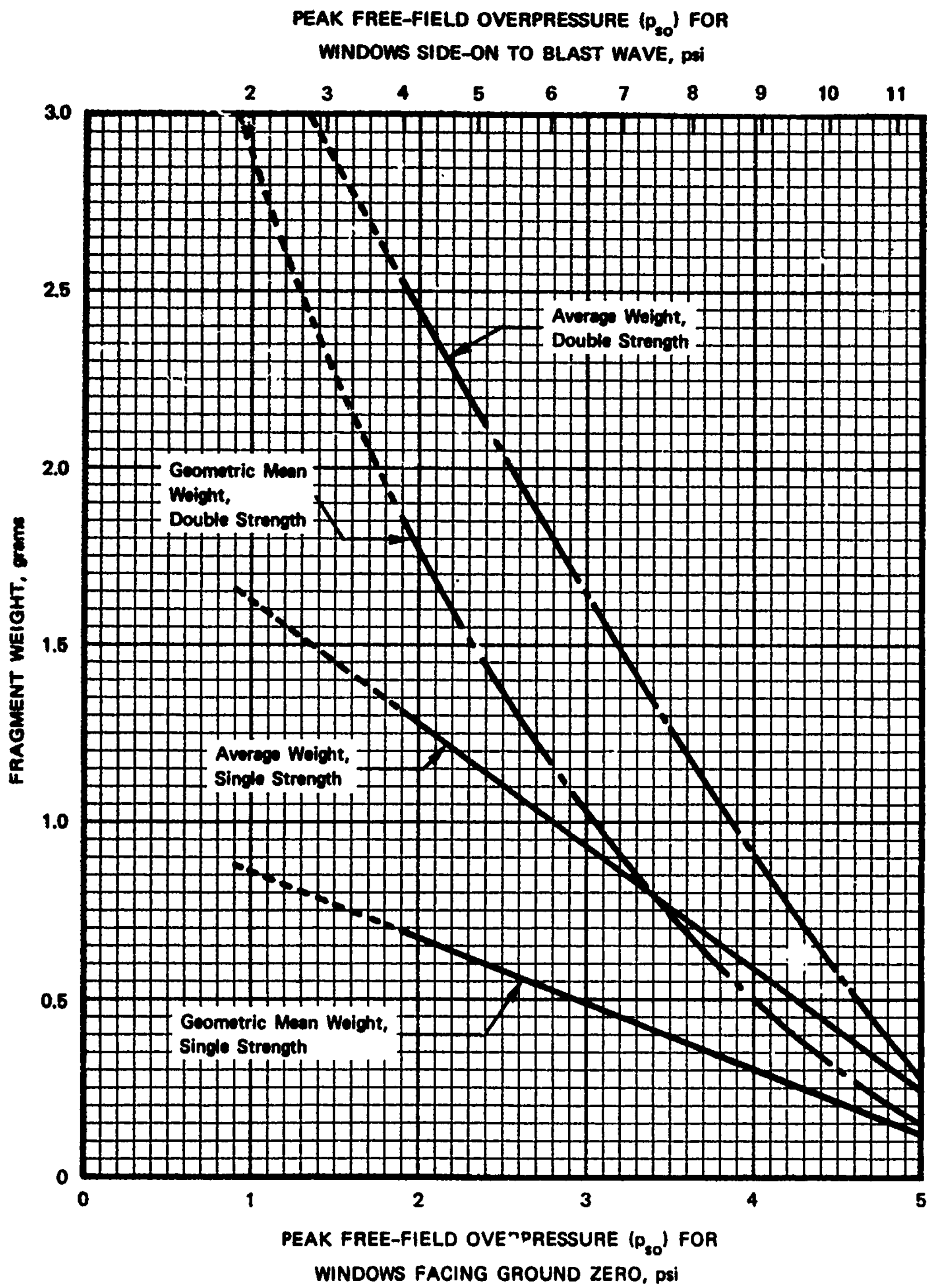

FIG. S-2 FRAGMENT WEIGHT PREDICTIONS

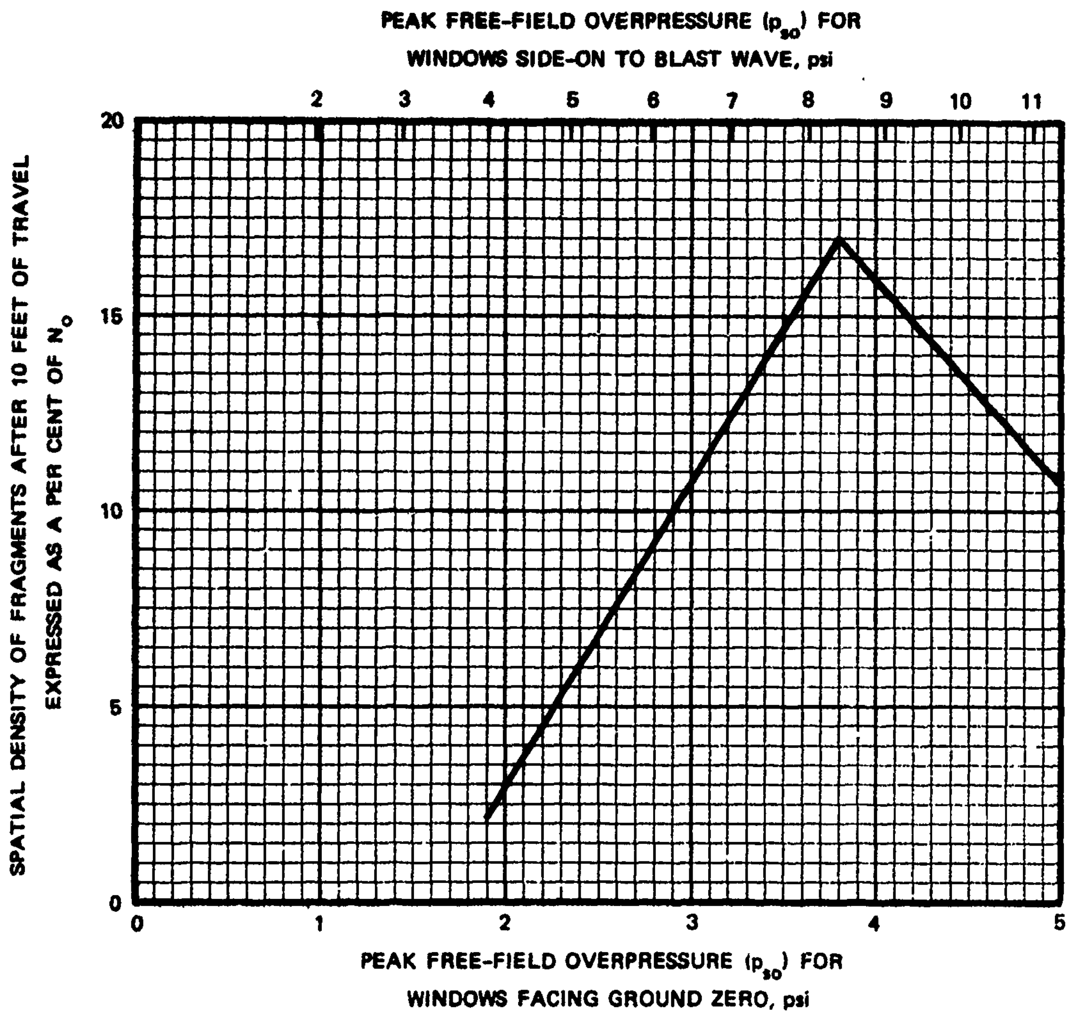

FIG. S-3 SPATIAL DENSITY PREDICTIONS AFTER 10 FEET OF TRAVEL AS A FUNCTION OF OVERPRESSURE

Table S-1

FRAGMENT WEIGHT AND VELOCITY PREDICTIONS FOR OVERPRESSURES ABOVE INCIPIENT FAILURE

	Free Field Overpressure (psi) Front Facing	Free Field Overpressure (psi) Side Facing	Geometric Mean Fragment Weight M_{50}, (gm)	Average Fragment Weight $\overline{M}$, (gm)	Velocity of Geometric Mean Weight Fragment After 10 Feet of Travel (fps)*
Single strength	2.0	4.2	0.67	1.27	87
	3.0	6.5	0.48	0.93	132
	5.0	11.4	0.12	0.24	238
Double strength	2.0	4.2	1.85	2.43	92
	3.0	6.5	1.07	1.63	130
	5.0	11.4	0.14	0.28	234
3/16-in. sheet	2.0	4.2	4.3	5.6	93
	3.0	6.5	2.1	3.3	138
	5.0	11.4	0.14	0.28	234
1/4-in. sheet	2.0	4.2	9.8	13.0	94
	3.0	6.5	4.2	6.6	139
	5.0	11.4	0.14	0.28	234

* Velocities are given for a weapon yield of 1 Mt, ambient atmospheric pressure of 14.7 psi, and speed of sound in undisturbed air of 1126 fps.

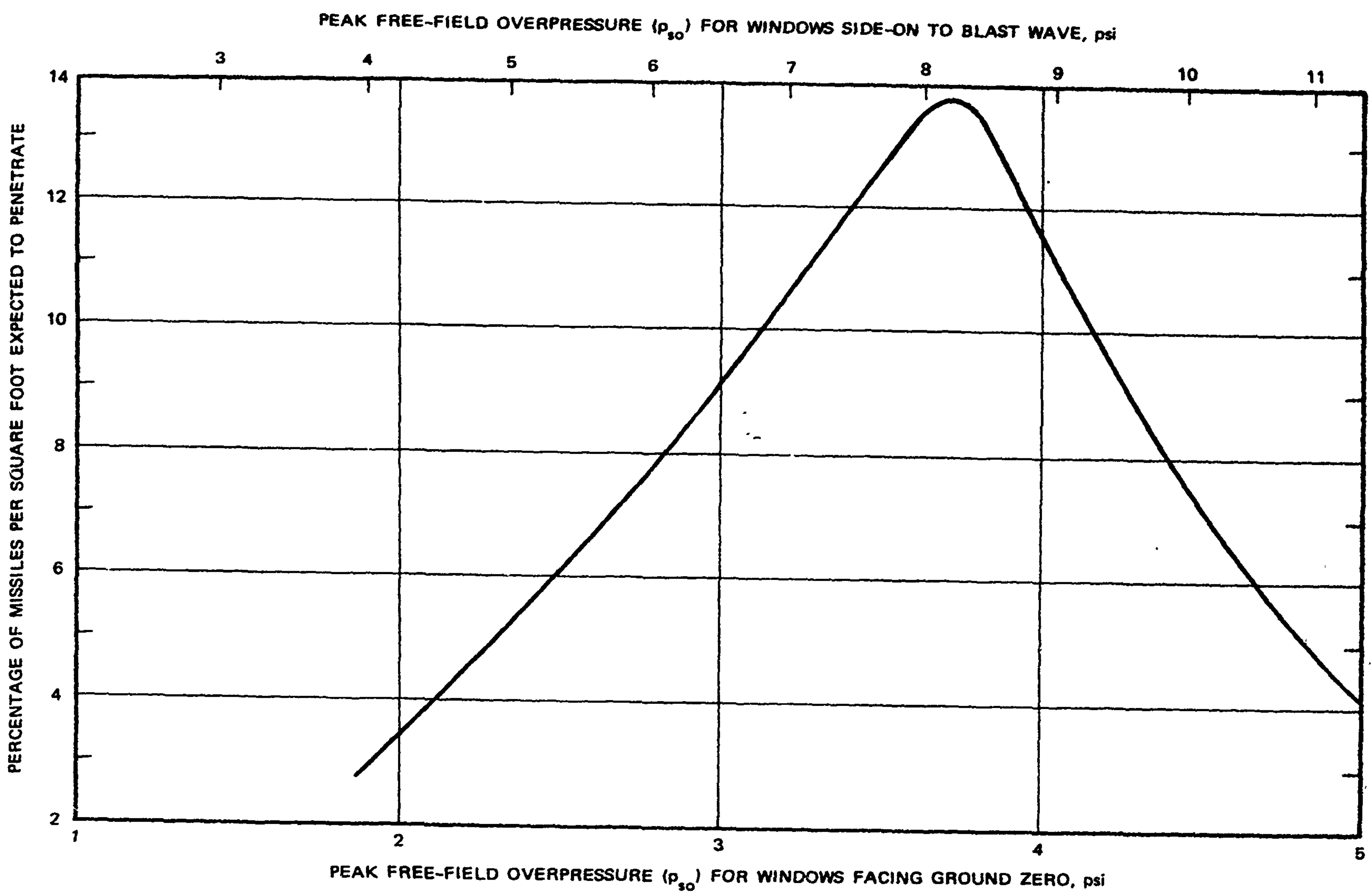

FIG. S-4 EXPECTED FREQUENCY OF PENETRATION AS A FUNCTION OF PEAK OVERPRESSURE*

* Computed for glass missiles occurring about 10 feet behind windows in house walls facing blast. Penetration criterion derived from dog abdomen studies.

aspects of flying glass missiles was outside the scope of this investigation.

Other Work

Five appendixes are included in the report. Appendix A provides the Uniform Building Code approach to selecting the minimum glass thickness for a window; common window types and sizes are recorded in Appendix B; test data on the modulus of rupture of glass may be found in Appendix C; Appendix D contains general information on various dynamic loadings to windows in relation to nuclear explosion, conventional explosion, shock tube, and sonic boom tests; and figures describing the elapsed time between loading and failure for windows are in Appendix E.

Final Report

EXISTING STRUCTURES EVALUATION
Part II: Window Glass and Applications

December 1968

SRI Project No. MU-6300-020

Contract No. OCD-DAHC20-67-C-0136

OCD Work Unit No. 1126C

Prepared for:

OFFICE OF CIVIL DEFENSE
OFFICE OF THE SECRETARY OF THE ARMY
WASHINGTON, D.C. 20310

STANFORD RESEARCH INSTITUTE

MENLO PARK CALIFORNIA

By:

J.H. Iverson
Public Works Systems

OCD Review Notice

This report has been reviewed by the Office of Civil Defense and approved for publication. Approval does not signify that the contents necessarily reflect the views and policies of the Office of Civil Defense.

FOREWORD

This report is one of a series covering research of a continuing nature under a project for blast resistance evaluation of existing structures in the National Fallout Shelter Survey (NFSS) inventory of the U.S. Office of Civil Defense (OCD).

The objective is to develop an evaluation method for estimating blast resistance and the cost-effectiveness of structure modifications to improve blast protection.

The evaluation method differs from vulnerability analysis techniques by carrying along significant statistical yardsticks (e.g., on strengths of materials) in the calculations sufficient to meet the needs of shelter operations research or war-gaming. It differs from protective design/analysis by aiming at a 50% probability basis, rather than the 90%-99% probability basis intended in design/analysis methods.

The results expected of the evaluation method will provide inputs for systems analyses related to performance of structures and effects on shelterees. For the latter purpose, the evaluation method results will include data on fragments and their sizes, masses, accelerations, velocities, and displacements.

The approach used for the continuing research was to develop an evaluation method for each of several structural elements (e.g., window glass, walls, and slabs), including reaction load-time history, and then for structural frames.

The research includes applications to specific buildings, such as those selected in a statistically adequate sample of NFSS structures under another OCD project, thereby making possible various extrapolations to the overall NFSS structures picture.

ABSTRACT

This report covers one portion of a research project to evaluate existing National Fallout Shelter Survey (NFSS) structures for resistance to combined nuclear weapons effects. The objective of this investigation was to determine the response of windows to air blast overpressures generated by nuclear explosions, including glass fragment characteristics (weights, velocities, numbers produced, and spatial densities) that could be used to predict statistically the effects of window glass failure on humans.

The analysis leading to the presentation of graphs, which can be used to predict the free-field overpressure at incipient failure for sheet and plate glass, was based on the theoretical load-deflection equation for large deflections of plates, modified by test results found in the literature. Glass panes were changed to equivalent single-degree-of-freedom systems in the analysis. The analysis was also used to estimate the time to failure for windows at various overpressures. Methods for predicting glass fragment characteristics were obtained empirically from Operation Teapot nuclear test data. The procedures for estimating incipient failure overpressures and fragment weights, spatial densities, numbers, and velocities were applied to windows in 14 buildings (located in San Jose and Palo Alto, California) that were part of the NFSS.

CONTENTS

Preceding page blank

CONTENTS

FIGURES

FIGURES

TABLES

TABLES

I INTRODUCTION

Relationship to Parent Investigation

This report covers one portion of a research project to evaluate existing NFSS structures for resistance to combined nuclear weapons effects. In the overall program, an analytical approach is taken to the evaluation of the blast protection available in existing buildings and is related to confidence levels and people-damage.

If a structure were examined to determine its response to a range of air blast overpressures, the lowest overpressure causing building damage would be that associated with window glass failure.* Glass failure is not structurally detrimental; however, if the glass fragments accelerated by air blast attain sufficient velocity, the injury to humans is of major concern. Thus, the need existed for a study of window† behavior, ranging from the overpressure causing incipient failure to the overpressure causing failure of the wall containing the window.

Objective

The objective of this investigation was to determine the response of windows to air blast overpressures generated by nuclear explosions, including development of output useful in estimating the probability and degree of injury to humans caused by glass fragments. It was expected

---

* Failure is defined as the dislodging of pieces of glass or frame from their original position in a window.

† Even though the precise definition of a window is an opening in a wall of a building to admit light, or light and air, the term window as used herein is the opening, including one or more glass panes mounted in a sash (casement or frame).

that such an investigation could be profitably used by others to make statistical predictions of the effects of window glass failure on humans in specific situations. The following sequence of effort was used to achieve the objective:

- Development of a method to predict incipient window failure (Chapter II)
- Development of a method to predict number, weight, and spatial density of fragments (Chapter III)
- Reporting of a method to predict the velocity of glass fragments (Chapter IV)
- Use of the above methods to predict human injuries (Chapter V)
- Application of the incipient failure and fragment number, weight, spatial density, and velocity prediction procedures to 14 NFSS structures (Chapter VII)

Types of Glass[1-3*]

Glass is basically a product of the fusion of silica. The principal compounds added during the manufacturing of window glass are soda to improve quality and lime to improve chemical durability, thus soda-lime-silica or more commonly soda-lime glass. Further classification of soda-lime glass is done on the basis of differences in the manufacturing processes. Sheet glass, one type of soda-lime glass sometimes referred to as window-sheet, is drawn from large melting tanks and annealed. Annealing is a process of controlled cooling from a suitable temperature to prevent or remove objectionable stresses. Polished plate glass, another type of soda-lime glass, is manufactured from rolled sheets that are

---

* Superscripts refer to the references listed at the end of this report.

annealed, cooled, and then mechanically ground and polished to produce flat, parallel, and bright surfaces. Float glass, a type of plate glass, is manufactured by floating molten glass on a dead flat surface of molten metal where it flows to a uniform thickness.

Sheet glass and polished plate are the most commonly used, accounting for the major portion of glass in existing buildings. Therefore, they are the two types that are conside ed in this report. Tables 1 and 2 indicate the weights, thicknesses, and maximum sizes of sheet and plate that are available commercially. Other types of glass such as tempered, safety, laminated, and wire glass are available, but they are not discussed in this report since their use is generally limited to special applications.

A design procedure for the selection of glass for windows is given in Appendix A. Common window types and sizes and associated glass sizes are given in Appendix B.

Properties of Glass

Glass, which is both homogeneous and isotropic, qualifies as a brittle material. It conforms to elastic theory to the point of fracture; that is, either fracture occurs or the specimen returns to its original shape on release of applied loads.[2] One property agreed on in current literature is that glass always fails in tension.

The ultimate tensile strength of glass[5-7] theoretically approaches 3 million psi. Experimentally, values exceeding 1 million psi have been observed in fine fibers. That such tensile strengths are not achieved in use is evidenced by considering modulus of rupture values as approximate peak tensile strengths, then noting that the σ_r* values for glass

* Symbols are explained in the Notation section; only special usages will be defined in the text.

Table 1

SHEET GLASS SPECIFICATIONS

Type	Thickness (in.) Nominal	Range	Approximate Weight per Square Foot Ounces	Pounds	Maximum Size (in.)
Single strength	3/32	(.085-.097)	19	1.20	40 X 50
Double strength	1/8	(.117-.131)	26	1.60	60 X 80
3/16" heavy sheet	3/16	(.182-.200)	40	2.51	120 X 84
7/32" heavy sheet	7/32	(.212-.230)	45	2.82	120 X 84
1/4" heavy sheet	1/4	(.240-.260)	52	3.23	120 X 84
3/8" heavy sheet	3/8	(.356-.384)	77	4.78	60 X 84
7/16" heavy sheet	7/16	(.400-.430)	86	5.36	60 X 84

Source: Reference 4.

Table 2

PLATE GLASS SPECIFICATIONS

Type	Thickness (in.) Nominal	Tolerance	Approximate Weight per Square Foot (pounds)	Maximum Size (in.)
Float	1/4	±1/32	3.24	122 X 200
Regular plate	1/8	±1/32	1.64	76 X 128
Regular plate	1/4	±1/32	3.28	127 X 226
Regular plate	5/16	±1/32	4.10	127 X 226
Regular plate	3/8	±1/32	4.92	125 X 281
Regular plate	1/2	±1/32	6.56	125 X 281
Regular plate	3/4	+1/32 -3/64	9.85	120 X 280
Regular plate	1	+3/64 -1/16	13.13	74 X 148

Source: Reference 4.

laths* (Table C-1) are all under 50,000 psi, or less than 5 percent of the observed tensile strength of fibers.

Glass strength depends almost completely on flaws or defects[2,5-8] most of which are found on the surface. If glass were ductile, yielding near the flaws would tend to equalize somewhat the stress concentrations before failure. Since glass is brittle and does not yield, stress concentrations at flaws are not relieved, and failure is caused by the propagation of one of the flaws. The flaw size that causes failure or the number of flaws in a specimen is a matter of probability. This is the reason for the wide dispersion of strength values reported in tests and for the difficulty in predicting the performance of an individual specimen within reasonably close limits. Therefore, a standard deviation value or a coefficient of variation is usually reported with an average value of the ultimate tensile strength, load carrying capacity, or modulus of rupture of glass.

Flaws or defects in glass can occur in several forms:[2,3,6,9,10] submicroscopic voids, bubbles, foreign matter on the surface of reheated glass, and mechanical damage. The usable strength of plate glass is reduced by the process of grinding and polishing the surfaces.[1] Other factors affecting strength are moisture, temperature, duration of stress, age, and induced stresses. It would have been desirable to place a strength adjusting factor on each variable but such information was not found in the literature; however, a few comments on some of the variables were found. In one series of static tests on panes,[11] it was found that only 85 percent of the established failure pressure was required to cause failure when a surface scratch appeared on the tension side. Temperature variations within the range of interest of this report were found to have

---

* A standard glass lath used in determining the modulus of rupture of glass is 10 in. long, 1-1/2 in. wide, and 1/4 in. thick.

little effect on strength.[2,12] The strength of a lath or pane is sometimes reduced by as much as one-half if its edges are rounded by grinding instead of cut as they usually are.[12]

Strength values are purposely not reported here since a further discussion of strength related to glass panes is found in Chapter II. Necessary values for material properties of glass were found in several references.[2-4,6,13] The values selected for use are:

- Modulus of elasticity, $E = 10^7$ psi
- Poisson's ratio, $\nu = 0.23$
- Unit weight, $\gamma = 0.090$ lb/in^3 $\approx$ 155 lb/ft^3

Acknowledgments

The author gratefully acknowledges the assistance and guidance of H. L. Murphy, C. K. Wiehle, and L. Seaman of Stanford Research Institute. In addition, a special acknowledgment is due J. L. Bockholt of SRI for preparation of the window response computer program.

II INCIPIENT FAILURE LOAD PREDICTION

Discussion of Approach

This chapter was prepared to illustrate the approach taken in the development of a method for predicting the probability of glass failure in a window subjected to air blast loading caused by a nuclear explosion. Window parameters, namely glass size, thickness, and type, were assumed to be known. Loading parameters also assumed to be known were approximate weapon yield, ambient air pressure, speed of sound in undisturbed air, and clearing distance.

In work done by Schardin,[14] windows exposed to explosions were found to behave similarly to a simple oscillator. Therefore, the differential equation of motion for a single-degree-of-freedom system with no damping was selected for use in this investigation, as follows:

$$\frac{d^2x}{dt^2} = \frac{1}{m}\left[F(t) - R(x)\right] \tag{1}$$

where $F(t)$ = a time dependent forcing function and

$R(x)$ = a resistance-displacement function.

The first step in determining a resistance-displacement function for glass panes was to select an analytical approach. Window glass was considered in the literature as a flat plate with length and width corresponding to the exposed length and width of the pane and thickness equal to the pane thickness. Actual edge conditions are probably somewhere between simply supported and fixed; however, the frame offers little resistance to rotation[15] and lateral movement[15,16] during loading. Therefore, the assumption of simply supported edges is generally accepted in the literature. From static tests on glass panes,[11,15,16] central deflections at failure are reported to be from one to seven times the glass thickness. Deflections of this magnitude preclude the use of small deflection plate theory, which is invalid for deflections exceeding one-half of the thickness. Thus, it seemed appropriate that window glass should be analyzed as a simply supported, rectangular plate with large deflections. The development of the incipient failure prediction method herein was accomplished for square plates for reasons that are discussed in the last section of this chapter.

In small deflection plate analysis, it is assumed that applied loads are resisted by bending stresses alone. When analyzing thin plates with deflections equal to several thicknesses but still small relative to other plate dimensions, maximum stresses may still be within the elastic strength of the material. Under these conditions, the load carrying ability is greatly enhanced by the addition of direct tensile stresses to the bending stresses.[17] The direct tensile stresses are a result of stretching the middle plane of the plate. One step beyond this type of load resistance is membrane action in which the stresses developed by stretching the middle surface carry all of the load with no bending action present.

Timoshenko[18] provides the basic approach to large deflection plate theory, which includes the strain of the middle plane as a result of bending. The result is two nonlinear differential equations for which the solution in the general case is not known. As an alternative, he provides an approximate solution originally recommended by Föppl in which small deflection plate theory and membrane theory are combined to account for bending and direct tension, respectively. The approach is discussed in the next section of this chapter.

The next step in the analysis was to have been a development of the Föppl approach such that maximum stresses occurring in the plate could be compared with allowable stresses for glass panes. Attempts were made to establish such a procedure during this investigation but they were suspended for two reasons. First, available test data did not provide strain gage results near failure, thus an understanding of how bending and membrane stresses combine could not be obtained. Second, available breaking stress or strength data were found to be modulus of rupture data adequate for predicting probable failure of glass laths but not comparable to the stresses developed in a window pane. It was concluded that ultimate strength or breaking stress of glass panes was too elusive a quantity to be considered as a failure criterion. This conclusion is supported in the literature by Greene[19] who observed that the concept of glass strength as a material property has no real meaning or existence. Further support was derived from Mould[20] who concludes that a meaningful failure criterion for glass would be a complete theory of the kinetics of flaw behavior. (Glass strength as related to flaws was discussed in Chapter I.)

For the reasons stated above, window glass response was based on a load-deflection relationship rather than on an ultimate strength relationship. Because of the spread in glass test data, the loading with about a 50 percent probability of causing failure is reported. Sufficient test data were found to support the establishment of a load-deflection equation, the selection of a static failure load, and the estimation of a static to dynamic response transition. These subjects are discussed in subsequent sections of this chapter.

Development of a Static Resistance Function

The approximate solution to plate problems containing a combination of bending and membrane stresses has been discussed. That solution was used to derive the following load-central deflection relationship for $\nu = 0.25$:

$$\frac{q}{E}\left(\frac{s}{h}\right)^4 = 21.9\left(\frac{w_o}{h}\right) + 31.0\left(\frac{w_o}{h}\right)^3 \qquad (2)$$

where 21.9 w_o/h is the bending term and $31.0(w_o/h)^3$ is the membrane term.

Seaman[21] continued the same approach by first incorporating $\nu = 0.23$ for glass:

$$\frac{q}{E}\left(\frac{s}{h}\right)^4 = 21.7\left(\frac{w_o}{h}\right) + 28.6\left(\frac{w_o}{h}\right)^3. \qquad (3)$$

Then he corrected the membrane coefficient to allow for movable-edge rather than immovable-edge membrane action:

$$\frac{q}{E}\left(\frac{s}{h}\right)^4 = 21.7\left(\frac{w_o}{h}\right) + 12.8\left(\frac{w_o}{h}\right)^3. \qquad (4)$$

Equation 4 provides one possible form of a static load-central deflection relationship. Before accepting this equation derived from plate and membrane theory, actual test data were required for comparison and validation. Test data are limited; however, the work done by Bowles and Sugarman[16] was considered the best available because of the number of tests performed. Their failure tests, the results of which are presented in Table 3, were all performed on 40-in. square panes. Tests were designed such that failure occurred in approximately 30 seconds. The equation they derived to fit their test data is:

$$\frac{q}{E}\left(\frac{s}{h}\right)^4 = 21.9\left(\frac{w_o}{h}\right) + 2.72\left(\frac{w_o}{h}\right)^3. \qquad (5)$$

In an attempt to compare their equation with Equation 2, they suggest that "the difference in the membrane coefficient is partially due to lateral movement of the panel during loading." Table 4 contains more of their test results for loads far below failure.

The load-central deflection data for very large panes presented in Table 5 were taken from Orr.[15] Two shortcomings of these data are that

Table 3

LOAD - CENTRAL DEFLECTION FAILURE DATA FOR SQUARE PANES

Sample	Number of Panes Tested	Mean Thickness, h (in.)	$\frac{s}{h}$*	Mean Bursting Pressure (psi)	Mean Central Deflection, w_o (in.)	$\frac{q}{E}\left(\frac{s}{h}\right)^4$†	$\frac{w_o}{h}$
1/8-in. plate	40	0.122	328	0.754	0.760	871	6.23
3/16-in.plate	30	0.197	203	1.412	0.726	240	3.68
1/4-in. plate	30	‡	160	1.811	0.651	119	2.60
3/8-in. plate	30	0.373	107	3.625	0.610	47.9	1.64
24-oz sheet§	30	0.110	364	0.692	0.807	1210	7.34
32-oz sheet§	30	0.158	253	1.369	0.870	562	5.51
3/16-in. sheet	30	0.195	205	1.910	0.860	338	4.41

* s = 40 inches for all samples.
† $E = 10^7$ psi.
‡ Since no value was given, h = 0.250 in. was assumed.
§ This work was done in England where pane thicknesses differ slightly from the U.S. thicknesses shown in Table 1.

Source: Data from Reference 16 appear in columns 1, 2, 3, 5, and 6. Calculations based on the data (Reference 21) were added in columns 4, 7, and 8.

Table 4

STRESS DATA

Sample	Pressure (psi)	$\frac{w_o}{h}$	Measured Central Stress (psi) Upper Surface	Lower Surface	Bending Stress (psi)	Membrane Stress (psi)	$\frac{q}{E}\left(\frac{s}{h}\right)^{4}$*
1/8-in. plate	0.05	1.61	810	-380	595	215	57.8
	0.1	2.40	1210	-380	795	415	115.6
	0.15	2.98	1480	-320	900	580	173.3
	0.2	3.43	1700	-200	950	750	231.1
	0.25	3.78	2880				288.9
3/16-in. sheet	0.05	0.59	670	-485	577	93	8.8
	0.10	0.92	1150	-750	950	200	17.7
	0.15	1.19	1520	-925	1222	298	26.6
	0.2	1.41	1830	-1030	1430	400	35.4
	0.25	1.62	2120	-1070	1595	525	44.3
	0.3	1.81	2370	-1080	1725	645	53.1
	0.35	1.96	2580	-1075	1827	753	62.0
1/4-in. plate	0.1	0.42	710	-630	670	40	6.6
	0.2	0.70	1400	-1080	1240	160	13.1
	0.3	0.93	2000	-1410	1705	295	19.7
	0.4	1.13	2510	-1640	2075	435	26.2
	0.5	1.32	2930	-1805	2367	563	32.8
	0.6	1.48	3300	-1930	2615	685	39.3
	0.7	1.63	3640	-2010	2825	815	45.9
	0.8	1.76	3940	-2040	2990	950	52.4
3/8-in. plate	0.2	0.25	640	-550	595	45	2.6
	0.4	0.41	1270	-1070	1170	100	5.3
	0.6	0.57	1910	-1550	1730	180	7.9
	0.8	0.70	2540	-2000	2270	270	10.6
	1.0	0.81	3120	-2360	2740	380	13.2
	1.2	0.92	3690	-2650	3170	520	15.9
	1.4	1.03	4010				18.5
	1.6	1.12	4530				21.2
	1.8	1.21	5040				23.8
	2.0	1.30	5570				26.4
	2.20	1.38	6060				29.1

* Mean values of h presented in Table 3 were used since thickness values were not given with these data.

Source: Data from Reference 16 appear in columns 1 through 5. Calculations assuming elastic theory (Reference 21) appear in Columns 6, 7, and 8.

Table 5

FAILURE LOAD - CENTRAL DEFLECTION DATA FOR
LARGE PLATE GLASS PANES

Glass Size (in.)	Average Thickness, h (in.)	Pane Area (in^2)	$\frac{\sqrt{A}}{h}$ or $\frac{s}{h}$*	Failure Pressure (psi)	Maximum Deflection, w_o (psi)	$\frac{q}{E}\left(\frac{s}{h}\right)^4$	$\frac{w_o}{h}$
82 X 82	0.2373	6724	345.6	0.3628	1.200	517.3	5.06
	0.240	6724	341.7	0.3602	1.189	490.8	4.95
	0.303	6724	270.6	0.5601	1.200	300.4	3.96
	0.301	6724	272.4	0.3901	1.000	214.9	3.32
82 X 102	0.2344	8364	390.2	0.2726	1.300	631.7	5.55
	0.2453	8364	372.8	0.2501	1.200	483.2	4.89
	0.3045	8364	300.3	0.3756	1.200	305.6	3.94
	0.305	8364	299.8	0.3751	1.200	303.2	3.93
82 X 120	0.242	9840	409.9	0.2258	1.400	637.4	5.78
	0.239	9840	415.0	0.1638	1.200	486.1	5.02
	0.303	9840	327.4	0.3094	1.311	355.4	4.33
	0.304	9840	326.3	0.3056	1.300	346.4	4.28
	0.369	9840	268.8	0.3898	1.200	203.6	3.25
	0.372	9840	266.6	0.4017	1.200	203.1	3.23
72 X 120	0.114	8640	815.4	0.1161	1.400	5131.4	12.28

* All panes were analyzed as squares. In the case of a rectangular pane, s is the side of a square having an area, A, equal to the actual area of the rectangle.

Source: Data from Reference 15 appear in columns 1, 2, and 6. Original data reported in psf are presented in psi in column 5. Calculations using the data (Reference 21) appear in columns 3, 4, 7, and 8.

each value represents only a single test and that the panes were very slowly loaded with several 5- to 25-minute breaks in the loading for measurements to be taken. The tests were performed on rectangular and square plates with aspect ratios between 0.6:1 and 1:1.

Seaman[21] used the nondimensional load values, $(q/E)(s/h)^4$, and the nondimensional deflection values, w_o/h, of Tables 3, 4, and 5 to establish the following static load-central deflection relationship for square panes at rupture:

$$\frac{q}{E}\left(\frac{s}{h}\right)^4 = 21.7\left(\frac{w_o}{h}\right) + 2.80\left(\frac{w_o}{h}\right)^3. \tag{6}$$

Equation 6 and the data of Tables 3, 4, and 5 are shown in Figure 1. Unsuccessful attempts to obtain a better fit of the data were made in this investigation by allowing adjustment of the bending coefficient as well as the membrane coefficient. Also, curve fitting procedures were applied so that other equations fitting the data might be studied for validity. A better fit was hard to find. Also, it was futile to give meaning to the results of the curve fitting equations. Therefore, Equation 6 was adopted for use as the static resistance function since it displayed a direct relationship to accepted theory.

Static Failure Load Determination

Equation 6 provided a relationship between applied static load and central deflection for square panes of either plate or sheet glass. To use the equation, the static failure load (or deflection) for each specific case of area, thickness, and type of glass was required. Charts 1 and 4 of Reference 22 were selected for this purpose. The charts, with the following modifications, appear as Figures 2 and 3:

- A scale showing the load in psi was added

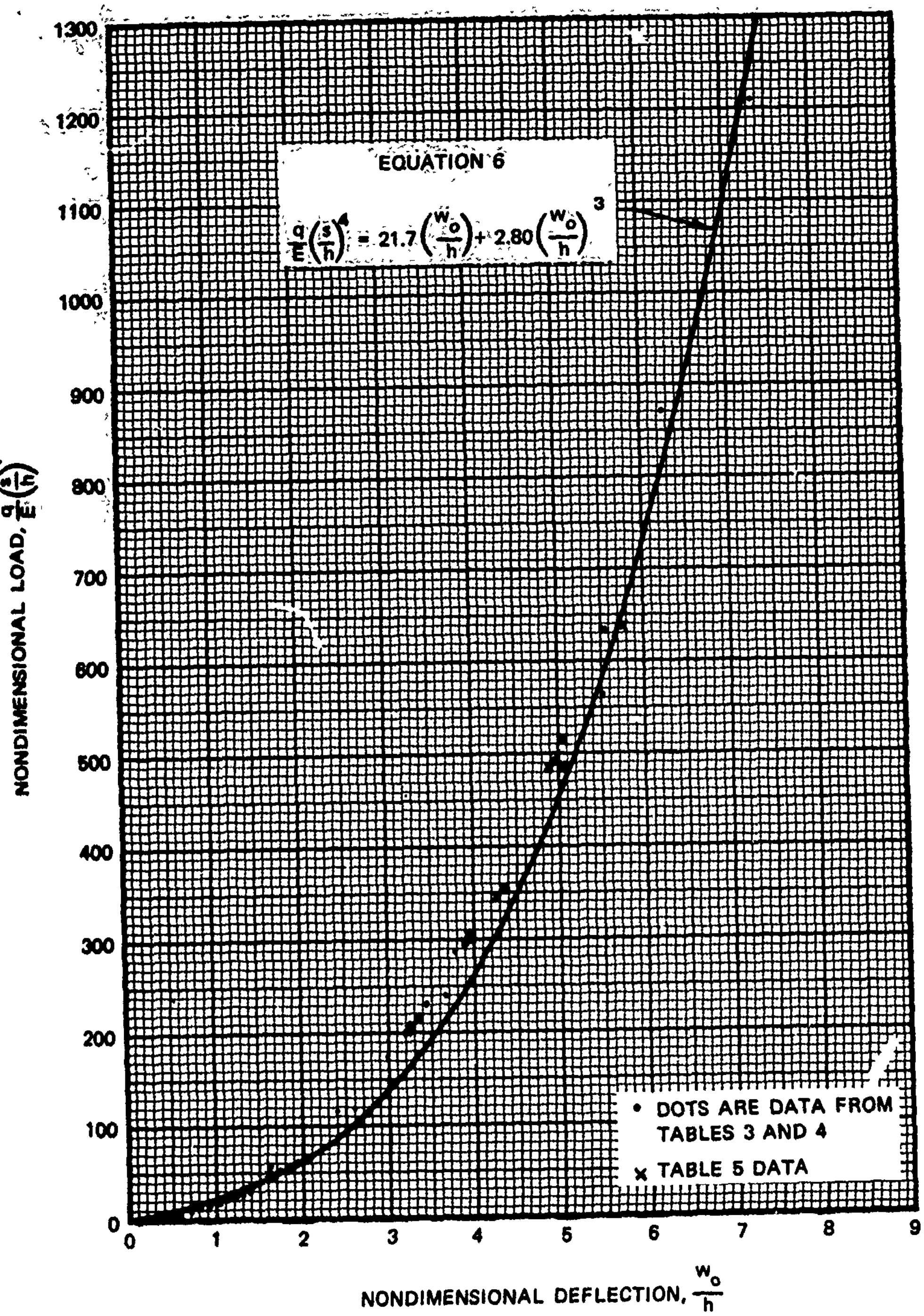

FIG. 1 STATIC LOAD VERSUS CENTRAL DEFLECTION FOR SQUARE PANES OF SHEET AND PLATE GLASS

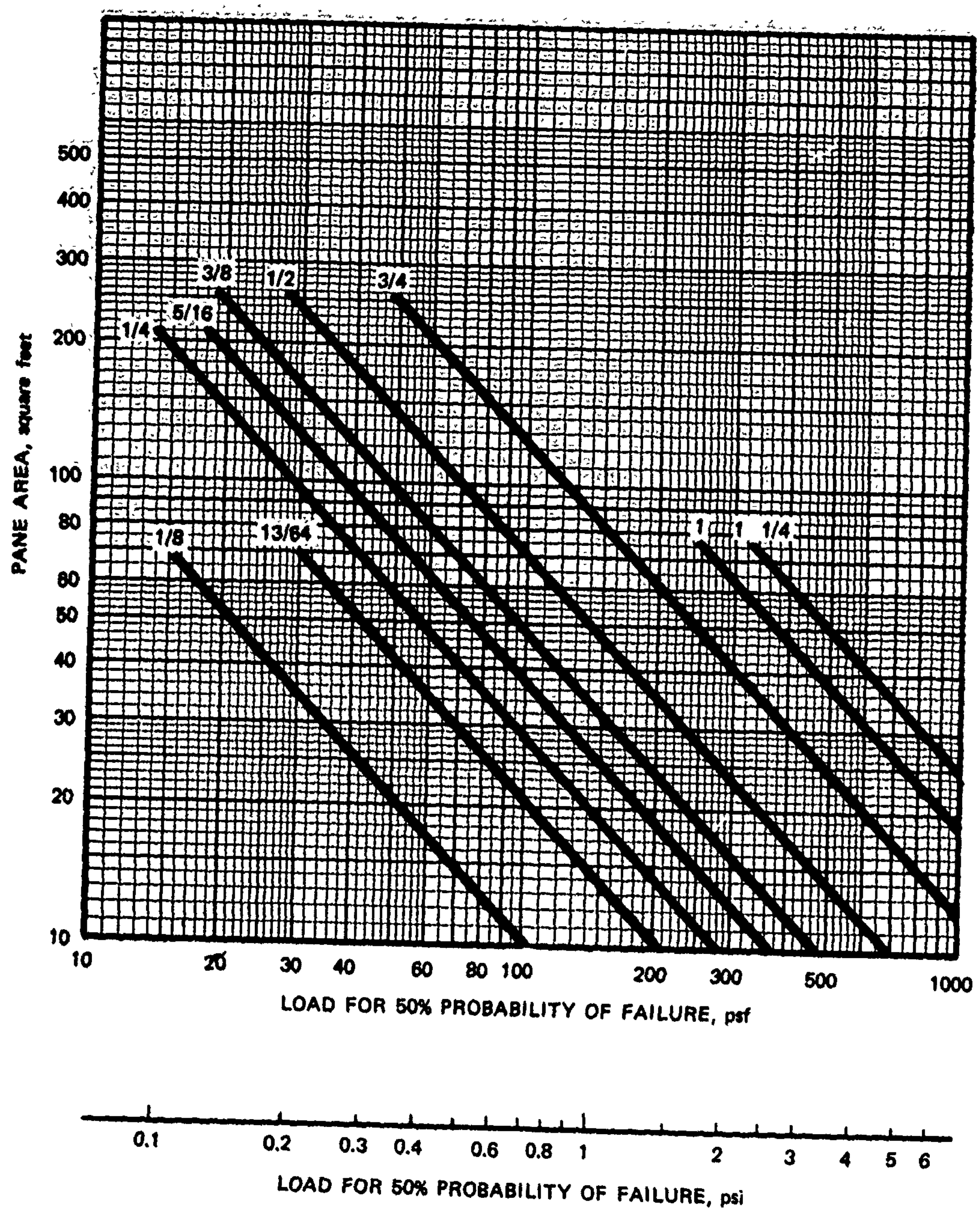

SOURCE: Adapted from Ref. 22.

FIG. 2 PLATE GLASS FAILURE LOADS FOR TIME TO FAILURE OF 60 SECONDS

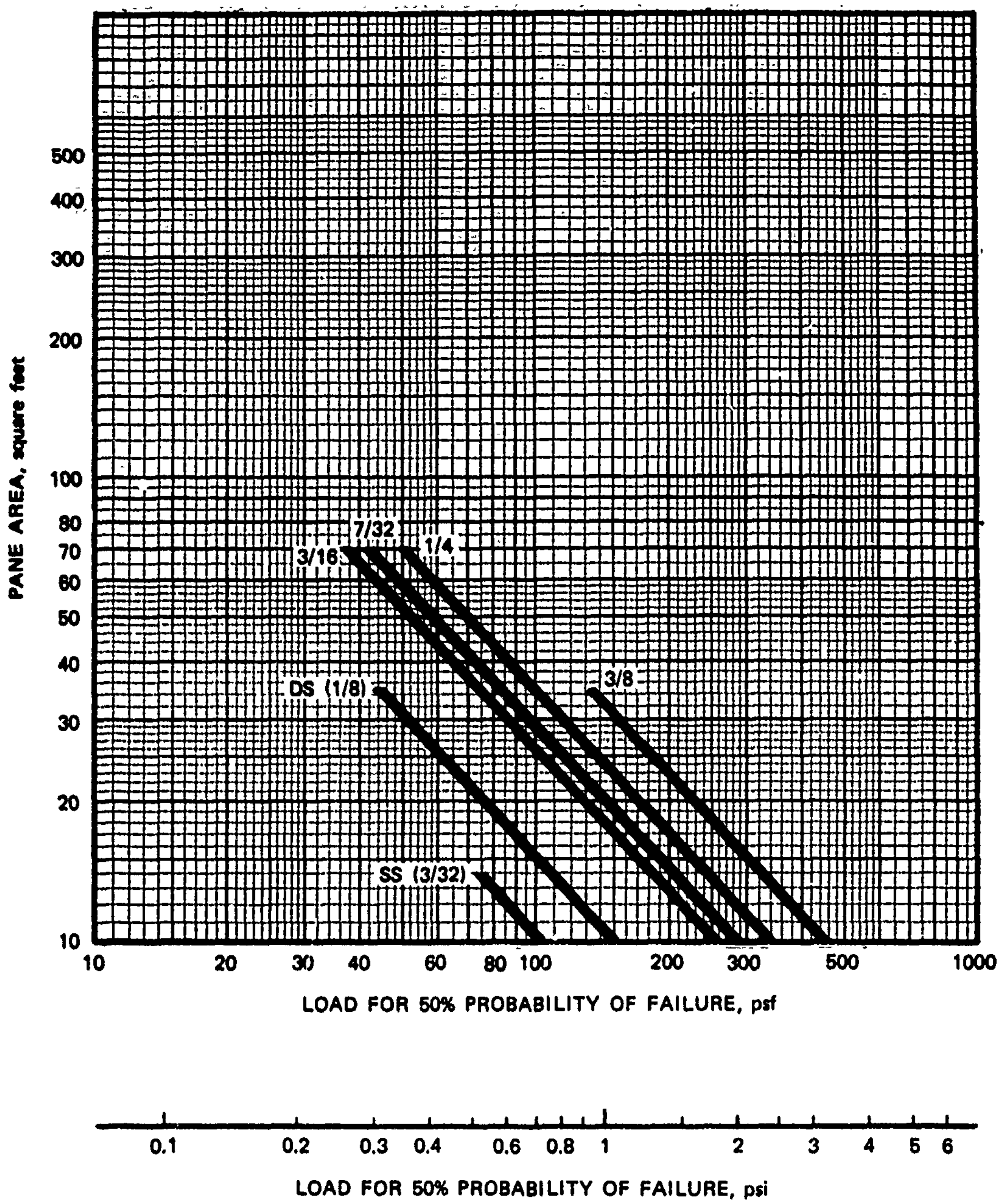

SOURCE: Adapted from Ref. 22.

FIG. 3 SHEET GLASS FAILURE LOADS FOR TIME TO FAILURE OF 60 SECONDS

- All load values were multiplied by 2.5 to remove the factor of safety, thus providing the load for 50 percent probability of failure

The figures in their original form were developed empirically to represent the behavior of plate and sheet glass as it exists in service. Orr's results were used for values in the size range above 10 square feet. U.S. Bureau of Standards' data (similar to those shown in Appendix C) were used for points associated with a glass area of 0.1 square foot. Data from the two sources with like thicknesses were connected by smooth curves and then "adjusted rationally to conform to data and to experience available in the intermediate area."[23]

Curve fitting procedures were applied in this study to obtain equations describing the information shown graphically in Figures 2 and 3. For plate glass (Figure 2)

$$q_{sf} = \frac{18,300}{A} h^{1.38} \qquad (7)^*$$

and for sheet glass (Figure 3)

$$q_{sf} = \frac{2.5}{A} (-336 + 8530\ h - 7710\ h^2). \qquad (8)^*$$

Equations 7 and 8 were used to predict the 50 percent probable static failure loads to be used in conjunction with the response curve shown in Figure 1.

Transition from Static to Dynamic Response

The fact that the ultimate tensile strength of glass is inversely proportional to the length of time that the load is acting has been

* The computer program routinely provided six significant figures that were used in subsequent and related calculations. After all such work was completed, values to be shown in the report were rounded to three significant figures, arbitrarily and not to imply any specific degree of accuracy in predicting glass pane behavior.

studied before.[24] The relationship developed between strength and time duration of load was based on tests[6] of 1/4-in. glass rods. In glass plates, ". . . a failure always originates at some form of imperfection on the surface or on the cut edge. The larger the plate, or the greater the area stressed, the greater the possibility of an imperfection being present and the lower the stress required to cause failure."[15] On this basis, it was decided that an extrapolation of 1/4-in. glass rod strength to glass pane strength was unwarranted for this study.

Data relating breaking stress to various loading rates[22] were used to develop Figure 4. The breaking stress values were normalized to the stress corresponding to a 60-second time to failure since Equations 7 and 8 were based on that time to failure. It was assumed that the relationship between load and stress is such that a factor selected from Figure 4 could be applied directly to Equations 7 and 8. Thus, the increased load carrying capacity of glass panes subjected to dynamic instead of static loads could be taken into consideration. The curve fitting equation of the six types tried that best fits the data was

$$\frac{\sigma}{\sigma_o} = 1.37\ t^{-0.0653} \qquad (9)$$

where σ_o indicates the stress with a time to failure of 60 seconds.

Use of the computer program described later in this chapter revealed a time to incipient failure of between 10 and 40 milliseconds for most windows. Very large panes with thicknesses greater than 1/4 in. had higher times to incipient failure. However, using 10 to 40 milliseconds as the predominant range of interest led to selection of 1.8 as the ratio of dynamic to static breaking strength for use in this study. Thus, Equation 7 for plate glass becomes

$$q_{df} = \frac{33,000}{A}\ h^{1.38} \qquad (10)^*$$

* The footnote appearing on page 18 applies to this equation also.

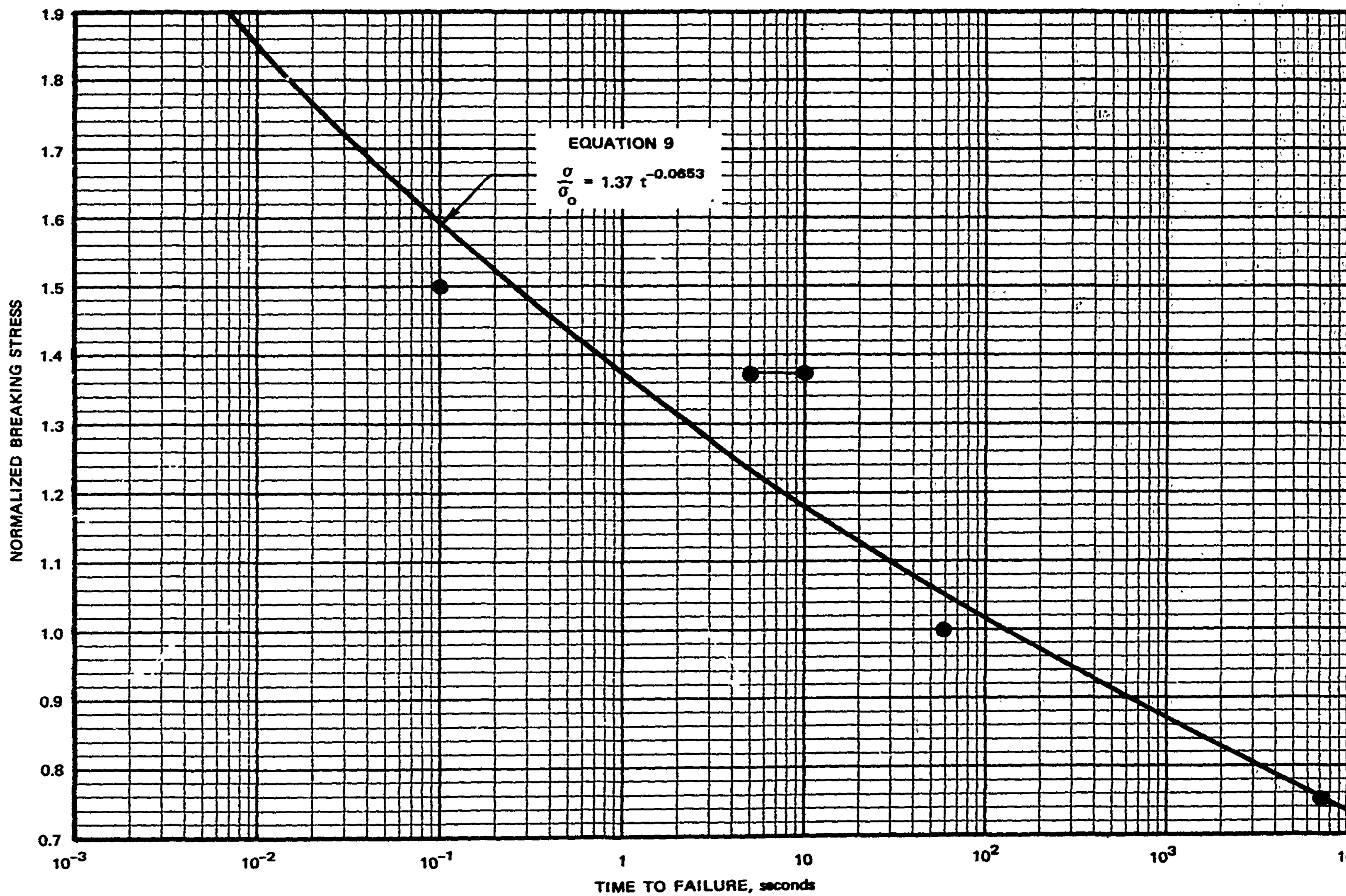

FIG. 4 EFFECT OF LOADING RATE ON NORMALIZED BREAKING STRESS

and Equation 8 for sheet glass becomes

$$q_{df} = \frac{4.5}{A} (-336 + 8530\,h - 7710\,h^2). \qquad (11)^*$$

It became possible at this point to describe the dynamic response of windows to air blast loading by using Equation 6 with the failure loads provided by Equations 10 and 11.

Air Blast Loading

The loading function selected was the pressure-time relationship shown in Figure 5, which describes the interaction of a nuclear blast wave with the front face of a closed rectangular structure. Even though windows are located randomly and overpressures vary with location on a wall, this average front-face loading was chosen as the pressure felt by any window in a wall facing an explosion. The equations describing front-face loading are:[25]

$$p_r = 2\,p_{so}\left(\frac{7\,P_o + 4\,p_{so}}{7\,P_o + p_{so}}\right) \qquad (12)$$

$$p_{do} = \frac{5}{2}\left(\frac{p_{so}^{\,2}}{7\,P_o + p_{so}}\right) \qquad (13)$$

$$p_s = p_{so}\left(1 - \frac{t}{t_o}\right) e^{-t/t_o} \qquad (14)$$

$$p_d = p_{do}\left(1 - \frac{t}{t_u}\right)^2 e^{-2t/t_u} \qquad (15)$$

$$U = c_o\left(1 + \frac{6\,p_{so}}{7\,P_o}\right)^{1/2} \qquad (16)$$

$$t_c = \frac{3\,S}{U} \qquad (17)$$

---

* The footnote appearing on page 18 applies to this equation also.

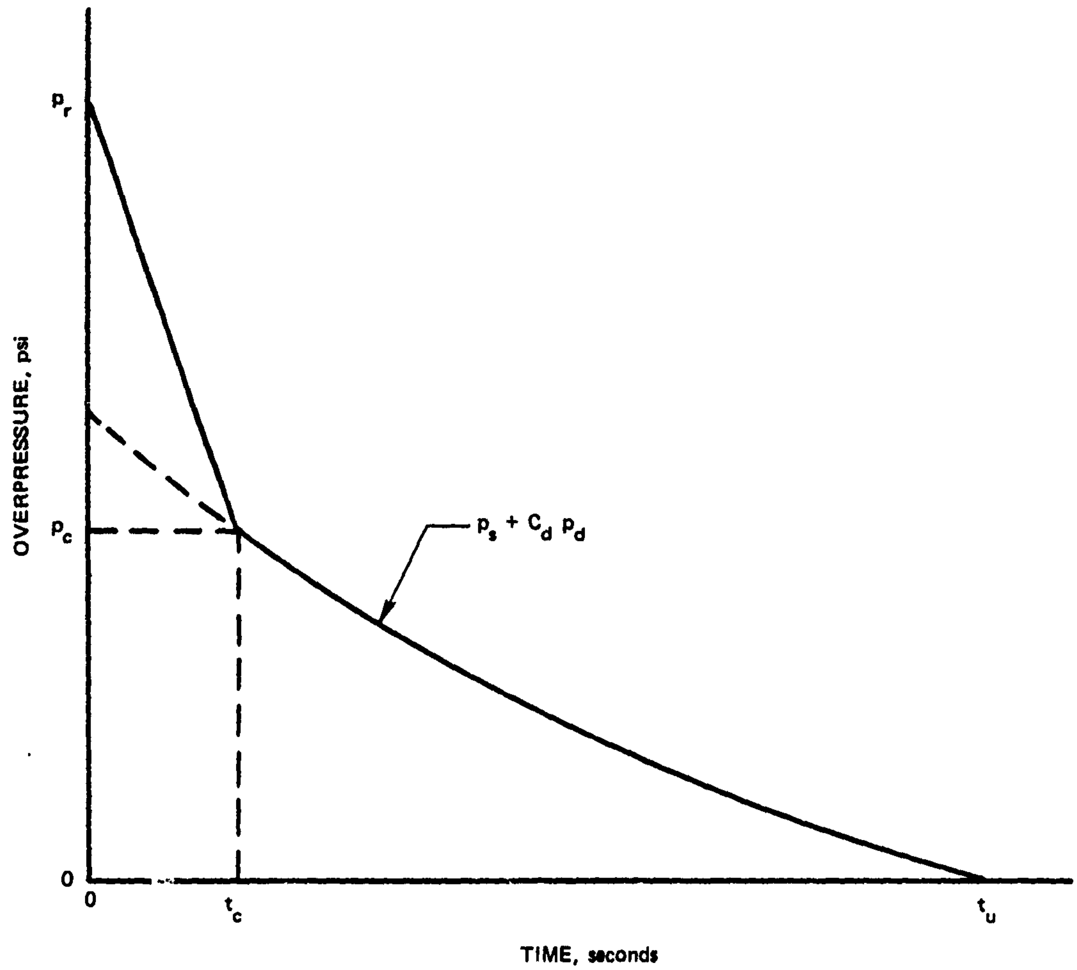

FIG. 5 FRONT-FACE AIR BLAST LOADING

$$p_c = p_s + C_d p_d \qquad (18)$$

$$t_o = \frac{W^{1/3}}{(2.2399 + 0.1886\ p_{so})} \ . \qquad (19)^*$$

The following assumptions were made concerning the loading:

- A linear decay from peak reflected pressure to stagnation pressure
- No back-face loading
- $t_u = t_o$
- $C_d = 1.0$

The equations describing the loading function shown in Figure 5 are:

$$p(t) = \frac{t_c - t}{t_c}(p_r - p_c) + p_c \qquad 0 \le t \le t_c \qquad (20)$$

$$p(t) = p_s + C_d p_d \qquad t_c \le t \le t_o \qquad (21)$$

$$p(t) = 0 \qquad t \ge t_o \ . \qquad (22)$$

The loading function for windows parallel to a blast wave (windows in side walls) was obtained by letting S = 0, leading to $t_c = 0$ (Equation 17), thus causing Equation 20 to be eliminated from any computations. Because of the negligible effect of the stagnation term, $C_d p_d$ (Equation 21), at very low overpressures, the drag coefficient, C_d, was not changed[25] from 1.0 to -0.4 in loading calculations for windows in side walls.

Window Pane Response to Nuclear Blast Wave Loading

A computer program was developed to solve Equation 1 for the incipient failure pressure of a square pane of either sheet or plate glass subjected to nuclear blast wave loading. A flow chart and the FORTRAN program

---

* Equation 19 was taken from Reference 26.

are presented in Figure 6 and Table 6, respectively.* The resistance-displacement subroutine combines Equation 6 with either Equation 10 or 11 depending on an input statement specifying glass type. Thus, the R(x) portion of Equation 1 is provided. The F(t) portion of Equation 1 is contained in the applied force-time subroutine for which Equations 12 through 22 were used to create a load-time function (Figure 5) given weapon yield, ambient pressure, speed of sound, and clearing distance.

Rather than attempting an exact solution, Equation 1 is solved numerically within the program by applying the Newmark β Method.[27] The method entails solving the differential equation in short time increments using the values at the end of one increment for the start of the next increment. The program was developed using a value for β that results in a linear variation of acceleration within each increment. The incipient failure pressure is found by an interval halving routine that narrows the size of the interval between a load that causes failure and one that does not.

Incipient Failure Prediction Results

A 1 Mt weapon was selected to determine the blast wave positive phase duration; however, pane incipient failure pressures were found to be insensitive to positive phase duration over an examined weapon yield range of 1 kt to 100 Mt. Other parameters fixed in solving for incipient failure pressures were an ambient atmospheric pressure of 14.7 psi and a speed of sound in undisturbed air of 1120 feet per second. A clearing

---

* The computer program was originally developed by a colleague, J. L. Bockholt, for another OCD project involving the analysis of walls. Program modifications for use herein were made by Bockholt.

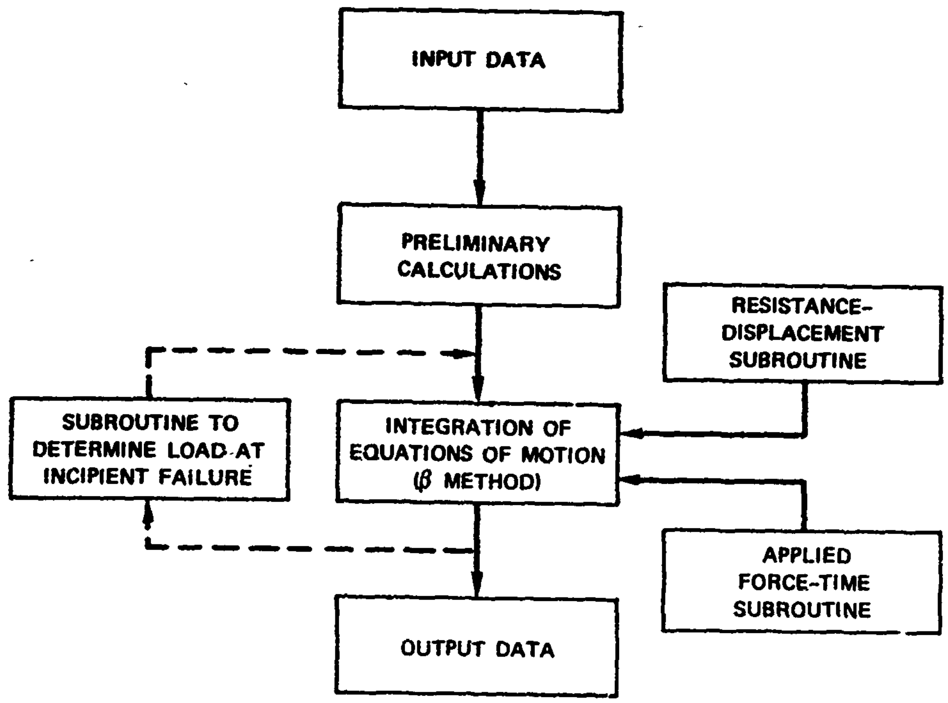

FIG. 6 COMPUTER PROGRAM FLOW CHART

Table 6

COMPUTER PROGRAM

```
* ANALYSIS ØF WINDØWS SUBJECTED TØ DYNAMIC LATERAL LØADS
*
60 FØRMAT("OINPUT SIDE,H,GLASSTYPE")
61 FØRMAT("OGLASSTYPE NØT RECØGNIZED -- RETYPE")
62 FØRMAT("OPRØPERTIES ØF THE WINDØW BEING ANALYZED ARE AS FØLLØWS:",
& /,5X,"LENGTH ØF SIDE =",F7.2," INCHES     THICKNESS =",F7.4,
& " INCHES",/,5X,"TYPE ØF GLASS =",2A4,11X,"STATIC STRENGTH =",
& F6.3," PSI")
65 FØRMAT(F6.3,F7.3,F12.2,F12.3,F14.5)
66 FØRMAT("OIS TIME HISTØRY ØF THE WINDØW DESIRED (YES=1,NØ=0)")
68 FØRMAT("OTHE TIME HISTØRY ØF THE WINDØW IS AS FØLLØWS:",//,
&" TIME   LØAD   ACCELERATIØN   VELØCITY   DISPLACEMENT")
70 FØRMAT("OIS SPECIFIC LØAD, INCLUDING PRESSURE, TØ BE GIVEN (INPUT
& 0)"/" ØR IS INCIPIENT CØLLAPSE PRESSURE TØ BE FØUND (INPUT 1)")
71 FØRMAT("OTHE VALUES ØF THE PARAMETERS AT THE FINAL TIME INTERVAL
& ARE:"/"  T =",F6.3," SECØNDS            P =",F7.3," LB/IN."
&       /"  A =",F9.2," IN./SEC/SEC     V =",F9.3," IN./SEC"
&      /"  Y =",F7.4," IN.")
72 FØRMAT(1H0,7("----------"))
73 FØRMAT("OWINDØW DID NØT FAIL - MAXIMUM DEFLECTIØN REACHED AT",
& F6.3," SECØNDS")
74 FØRMAT("OWINDØW FAILED AT",F7.3," SECØNDS")
*
CØMMØN YI,QT,ADH4,E,AREA,PF,TIME,P,L1
DIMENSIØN A(100),V(100),Y(100),T(100),PL(100)
REAL MASS
ALPHA GLASSTYPE,LETTER
*
*  INPUT DATA
5 PRINT 60
INPUT,SIDE,H,GLASSTYPE
PRINT 70
INPUT,L1
CALL FØRCE(2)
*
*  DETERMINE VALUES ØF ØFTEN USED VARIABLES
E=10000000.0
DELTA=0.001
AREA=SIDE*SIDE
MASS=0.09*AREA*H/386.07
ZKLM=0.67
PFMAX=0; PFMIN=0
ADH4=(SIDE/H)**4
13 IF(GLASSTYPE.EQ."HEET")GØTØ 10
IF(GLASSTYPE.EQ."LATE")GØTØ 9
PRINT 61; INPUT,GLASSTYPE; GØ TØ 13
```

Table 6 (Continued)

```
*
9 PFSTAT=18309.1*H**1.37849/AREA
LETTER="   P"; GØTØ 25
*
* PLATE GLASS
10 PFSTAT=2.5*(-336.532+8532.32*H-7706.59*H*H)/AREA
LETTER="   S"
25 PRINT 62,SIDE,H,LETTER,GLASSTYPE,PFSTAT
*  80% INCREASE IN DYNAMIC STRENGTH ØVER STATIC STRENGTH
PFDYN=1.8*PFSTAT
IF(L1.EQ.0)GØTØ 23
*  INITIAL VALUES FØR DETERMINING INCIPIENT CØLLAPSE PRESSURE
PF=PFDYN
GØ TØ 20
16 PF=(PFMAX+PFMIN)/2.0
20 CALL FØRCE(3)
*
*  INITIALIZE VALUES FØR BETA METHØD (BETA=1/6)
23 TIME=0
T(1)=0
I=1
DELTA=0.001
CALL FØRCE(1)
PL(1)=P
PT=P*AREA
Y(1)=0; V(1)=0
V(1)=0
A(1)=PT/(MASS*ZKLM)
*
*  PRØCEDURE FØR ALL SUBSEQUENT INTERVALS
1 I=I+1
TIME=TIME+DELTA
8 T(I)=TIME
11 KØUNT=0
A(I)=A(I-1)
Y(I)=Y(I-1)+DELTA*V(I-1)+DELTA*DELTA*A(I-1)/2.0
XI=Y(I)/H
CALL FØRCE (1)
PL(I)=P
PT=P*AREA
2 CALL RESIST
*
* SAFEGUARD TØ PRØTECT AGAINST ANY IRREGULARITIES IN PRØGRAM
KØUNT=KØUNT+1
IF(KØUNT.LE.10)GØTØ4
DELTA=DELTA/2.0
TIME=TIME-DELTA
```

Table 6 (Continued)

```
565 ICHECK=ICHECK+1
570 IF(ICHECK.GT.3)GØTØ 999
575 GØTØ 8
580*
585 4 ANEW=(PT-QT)/(MASS*ZKLM)
590 ADELTA=ANEW-A(I)
595 Y(I)=Y(I)+DELTA*DELTA*ADELTA/6.0
600 XI=Y(I)/H
605 A(I)=ANEW
610* CHECK TØ SEE IF ASSUMED VALUE ØF ACCELRATIØN IS WITHIN
615*  DESIRED ACCURACY ØF CALCULATED VALUE
620 IF(ABS(ADELTA/ANEW).GT.0.01)GØTØ 2
625 3 V(I)=V(I-1)+DELTA*(A(I)+A(I-1))/2.0
630* CHECK TØ DETERMINE IF MAXIMUM DEFLECTIØN HAS BEEN REACHED
635* IF SØ WALL DID NØT FAIL
640 15 IF(Y(I).LE.Y(I-1))GØTØ 6
645* CHECK TØ SEE IF WALL STILL HAS RESISTANCE- IF NØT,WALL FAILED
650 IF(PFDYN*AREA-QT)7,7,1
655*
660* INTERVAL HALVING PRØCEDURE TØ FIND LØAD CAUSING INCIPIENT FAILURE
665* WALL DID NØT FAIL - SET PFMIN TØ PF
670 6 IFAIL=0
675 IF(L1.EQ.0)GØTØ 18
680 PFMIN=PF
685 IF(PFMAX)19,19,17
690 19 PF=2.0*PF
695 GØTØ 20
700* WALL FAILED - SET PFMAX TØ PF
705 7 IFAIL=1
710 IF(L1.EQ.0)GØTØ 18
715 PFMAX=PF
720* CHECK TØ SEE IF INTERVAL IS WITHIN DESIRED ACCURACY
725 17 IF((PFMAX-PFMIN)/PFMAX.GT.0.01)GØTØ 16
730*
735* ØUTPUT DATA
740 18 CALL FØRCE(4)
745 IF(IFAIL.EQ.0)PRINT 73,TIME
750 IF(IFAIL.EQ.1)PRINT 74,TIME
755 PRINT 66
760 INPUT,M
765 IF(M)22,22,21
770 21 PRINT 68
775 PRINT 65,(T(J),PL(J),A(J),V(J),Y(J),J=1,I)
780 GØTØ 12
785 22 PRINT 71,T(I),PL(I),A(I),V(I),Y(I)
790 12 PRINT 72
```

Table 6 (Continued)

```
795 GØTØ 5
800 999 STØP; END
1000*
1005 SUBRØUTINE RESIST
1010*  THIS SUBRØUTINE DETERMINES THE DYNAMIC RESISTANCE ØF THE WINDØW
1015 CØMMØN XI,QT,ADH4,E,AREA,PR,TIME,P,L1
1020 QT=AREA*(E/ADH4)*(21.7*XI+2.8*XI**3)
1025 RETURN; END
1030*
2000 SUBRØUTINE FØRCE (IENTRY)
2005*  THIS SUBRØUTINE DETERMINES THE LØAD ACTING ØN THE WINDØW
2010 CØMMØN XI,QT,ADH4,E,AREA,PR,TIME,P,L1
2015 GØTØ(1,2,3,4),IENTRY
2020*
2025* DETERMINE LØAD ACTING ØN THE WALL
2030 1 IF(TIME-TC)101,102,102
2035 101 P=PC+(TC-TIME)*(PR-PC)/TC
2040 RETURN
2045 102 IF(TIME-TO)103,104,104
2050 103 P=PS0*(1-TIME/TO)*EXP(-TIME/TO)+PD0*(1-TIME/TO)**2
2055 &      *EXP(-2*TIME/TO)
2060 RETURN
2065 104 P=0
2070 RETURN
2075*
2080*  INPUT LØAD DATA
2085 2 PRINT 630
2090 IF(L1.EQ.0)GØTØ 205
2095 INPUT, W,P0,C0,S
2100 RETURN
2105 205 PRINT 655
2110 INPUT,W,P0,C0,S,PS0
2115 PR=2.0*PS0*(7.0*P0+4.0*PS0)/(7.0*P0+PS0)
2120 IF(S.EQ.0)PR=PS0
2125 GØTØ 305
2130*
2135*  DETERMINE LØAD PRØPERTIES FØR GIVEN PEAK PRESSURE
2140 3 PS0=(PR-14.0*P0+SQRT(196.0*P0*P0+196.0*P0*PR+PR*PR))/16.0
2145 302 IF(S.EQ.0)PS0=PR
2150 305 PD0=2.5*PS0*PS0/(7.0*P0+PS0)
2155 U=C0*SQRT(1.0+6.0*PS0/(7.0*P0))
2160 TC=3.0*S/U
2165 TO=W**0.3333/(2.2399+0.1886*PS0)
2170 PC=PS0*(1.0-TC/TO)*EXP(-TC/TO)+PD0*(1.0-TC/TO)**2*EXP(-2.0*TC/TO)
2175 RETURN
2180*
```

Table 6 (Concluded)

```
2185*  ØUTPUT LØAD DATA FØR LØAD ACTING ØN WALL
2190 4 IF(L1.EQ.0)GØTØ 390
2195 PRINT 660
2200 GØTØ 395
2205 390 PRINT 665
2210 395 CØNTINUE
2215 400 PRINT 600, W,PØ,CØ,S,U,TO,PR,PSØ,PDØ,TC
2220 RETURN
2225*
2230 600 FØRMAT(10X,"W =",F8.1," KT   PØ =",F6.2," PSI     CØ =",F6.1,
2235 &" FPS",/,10X,"S =",F6.1," FT      U =",F7.1," FPS    TO =",F6.3,
2240 &" SEC",/,9X,"PR =",F7.3," PSI  PSØ =",F7.3," PSI   PDØ =",F7.3,
2245 &" PSI",/,9X,"TC =",F7.4," SEC")
2250 630 FØRMAT(" INPUT W,PØ,CØ,S")
2255 655 FØRMAT("&,PSØ")
2260 660 FØRMAT("OLØAD CAUSING INCIPIENT FAILURE IS AS FØLLØWS:")
2265 65 FØRMAT("OPRØPERTIES ØF LØAD ACTING ØN WINDØW ARE AS FØLLØWS:")
2270 777 RETURN; END
```

distance of 20 feet was used in calculating front-face loading. That distance was established from a series of computer runs demonstrating that the incipient failure overpressure was influenced very little when the clearing distance exceeded 20 feet. Incipient failure predictions, using the above-mentioned parameters, are presented in Figures 7 and 8 for plate glass and Figures 9 and 10 for sheet glass. Figures 7 and 9 relate to side-wall loading and Figures 8 and 10 relate to front-face loading.

A statistically normal strength distribution and a coefficient of variation of 25 percent were assumed in Reference 22 from which Figures 2 and 3 were prepared. The 50 percent probability of failure stated in conjunction with those figures has been carried through to Figures 7 through 10. The maximum pane areas shown in Figures 7 through 10 were limited to those allowed by the Uniform Building Code[28] when designing for the least wind load, i.e., 15 pounds per square foot. More information on allowable pane sizes is found in Appendix A.

The development in this chapter leading to Figures 7 through 10 was for square panes. It is believed that use of the figures is valid for panes with aspect ratios as low as 1/3. The strongest argument in support of this statement is that the information used in preparing Figures 2 and 3 is valid for any pane with an aspect ratio exceeding 1/3. Furthermore, extensive development of an analytical method for rectangular panes did not seem warranted. The membrane term for square panes was shown to be significantly changed by applying test data to the analytical equations. Insufficient test data were available to make a similar comparison had the development herein been for rectangular panes. Finally, the data in Table 5, which include some rectangular pane data, plotted well in Figure 1.

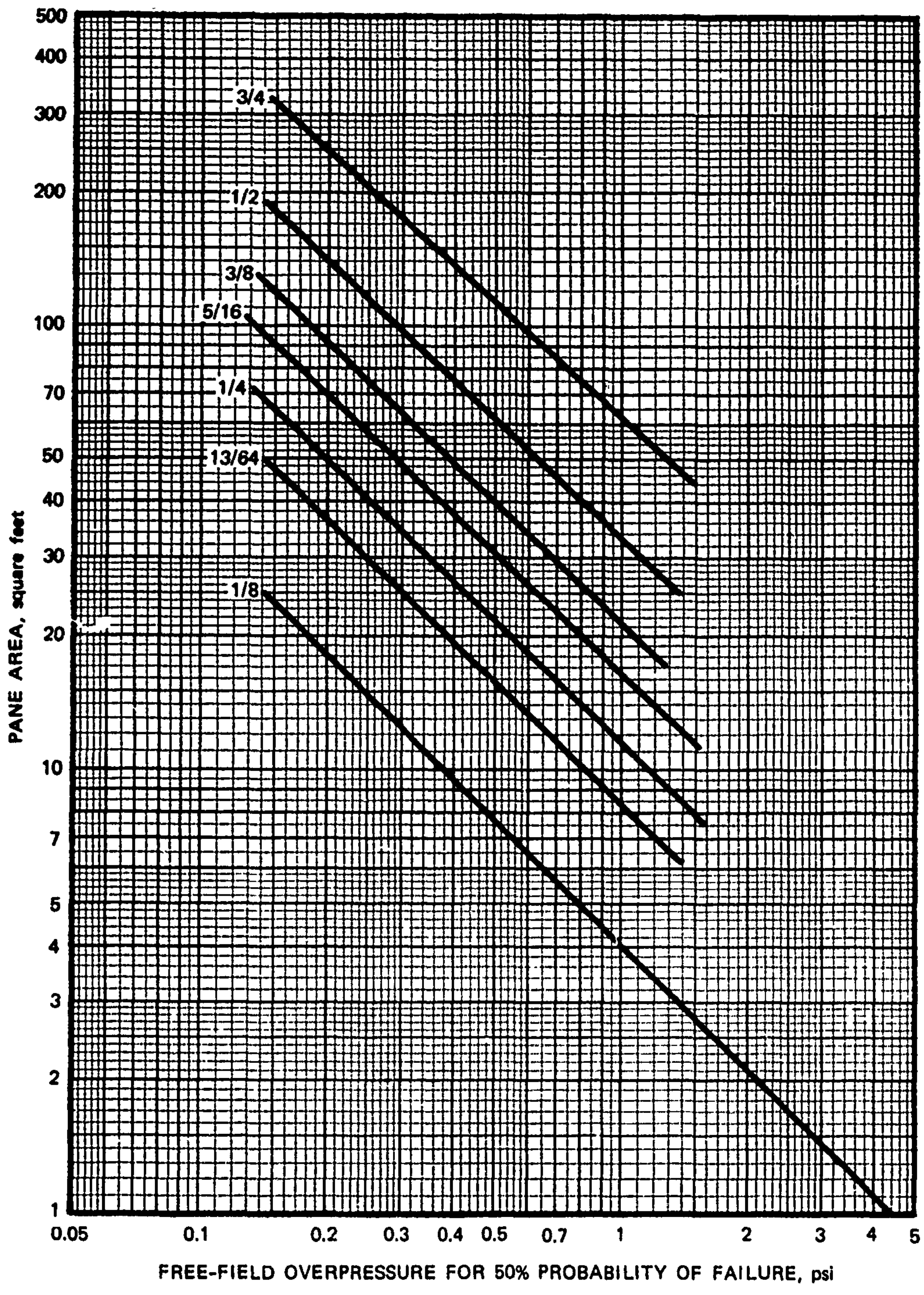

FIG. 7 PLATE GLASS INCIPIENT FAILURE PRESSURES FOR SIDE-WALL LOADING AS A FUNCTION OF PANE AREA AND THICKNESS

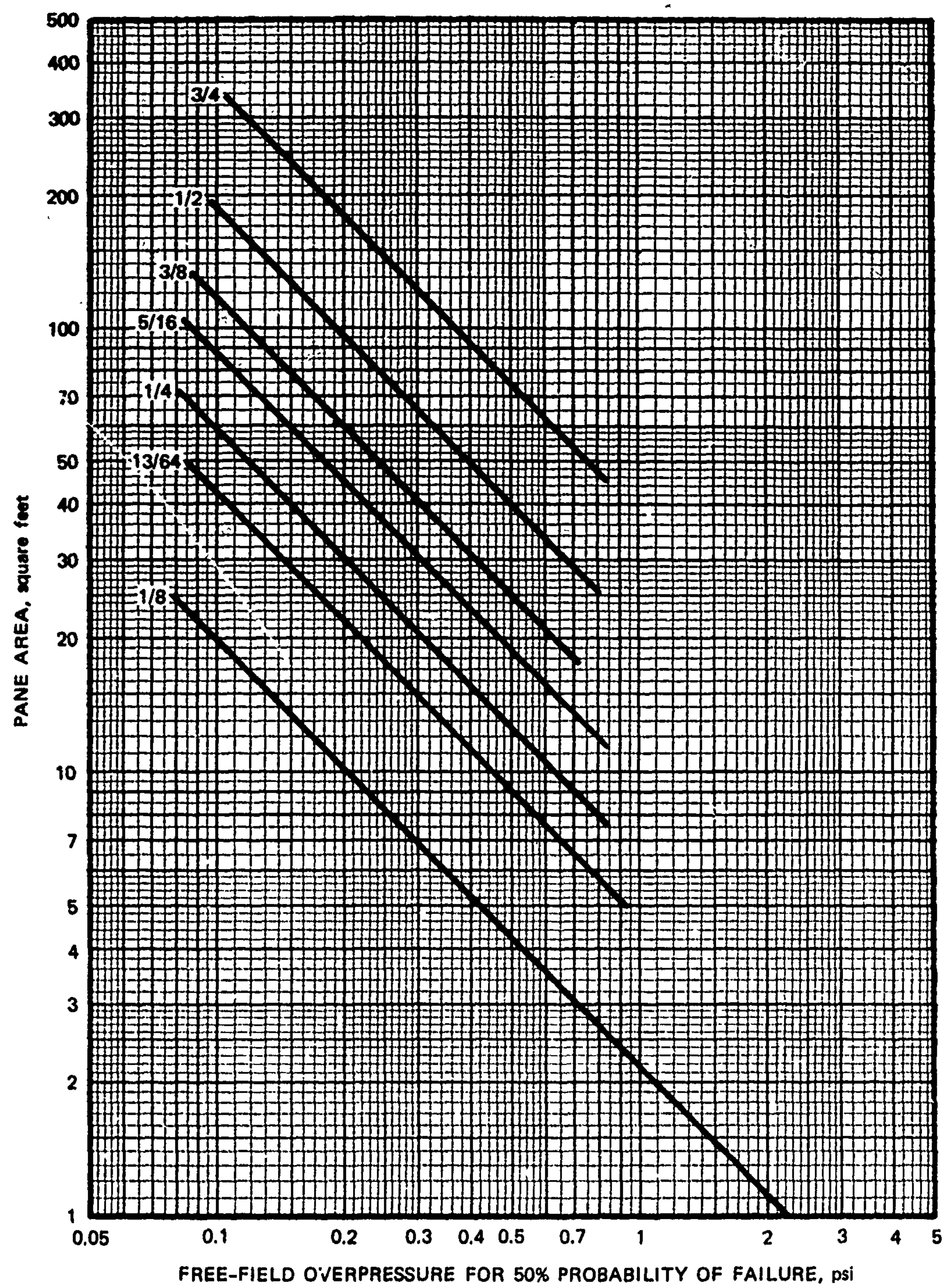

FIG. 8 PLATE GLASS INCIPIENT FAILURE PRESSURES FOR FRONT-FACE LOADING AS A FUNCTION OF PANE AREA AND THICKNESS

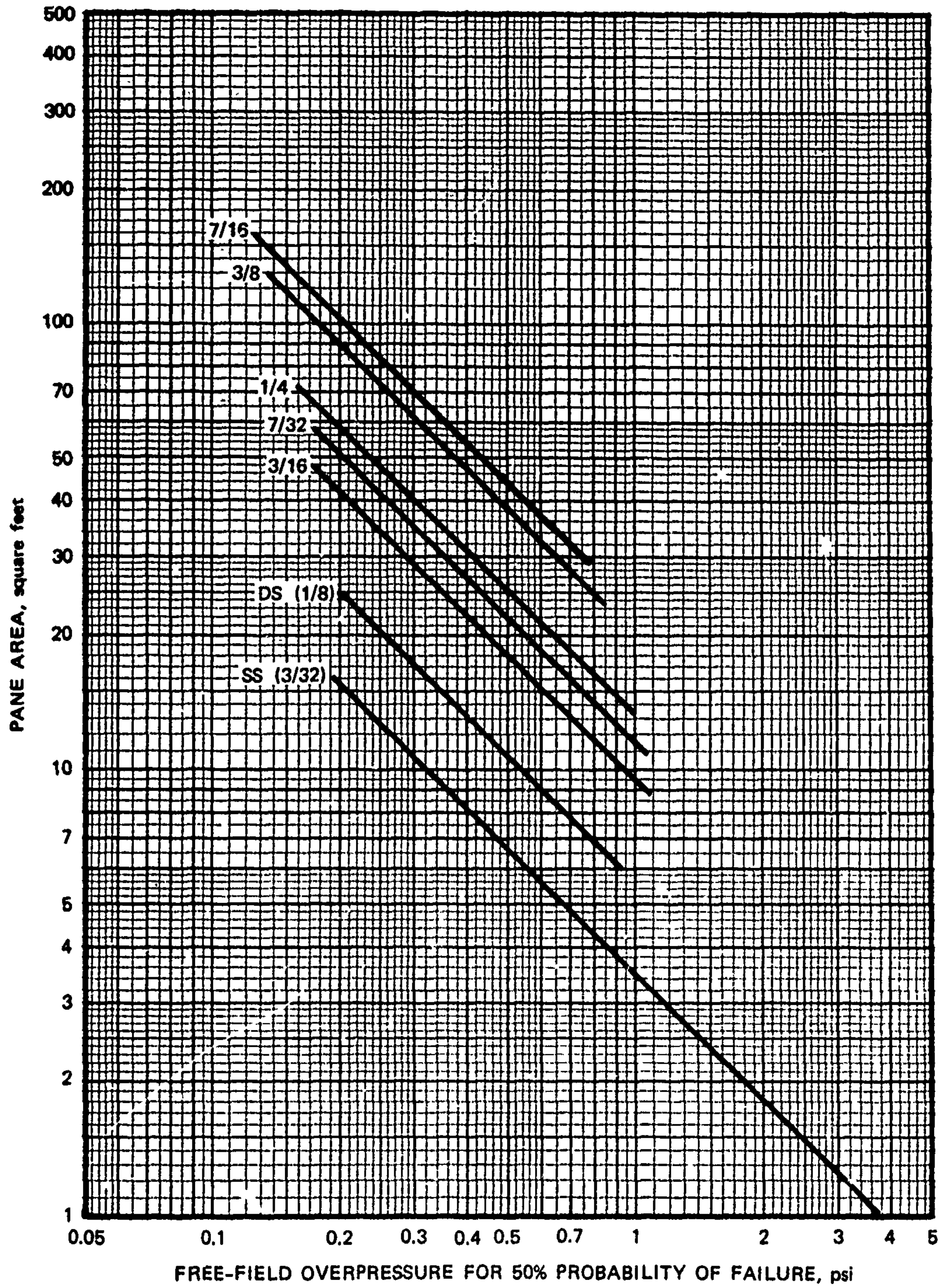

FIG. 9 SHEET GLASS INCIPIENT FAILURE PRESSURES FOR SIDE-WALL LOADING AS A FUNCTION OF PANE AREA AND THICKNESS

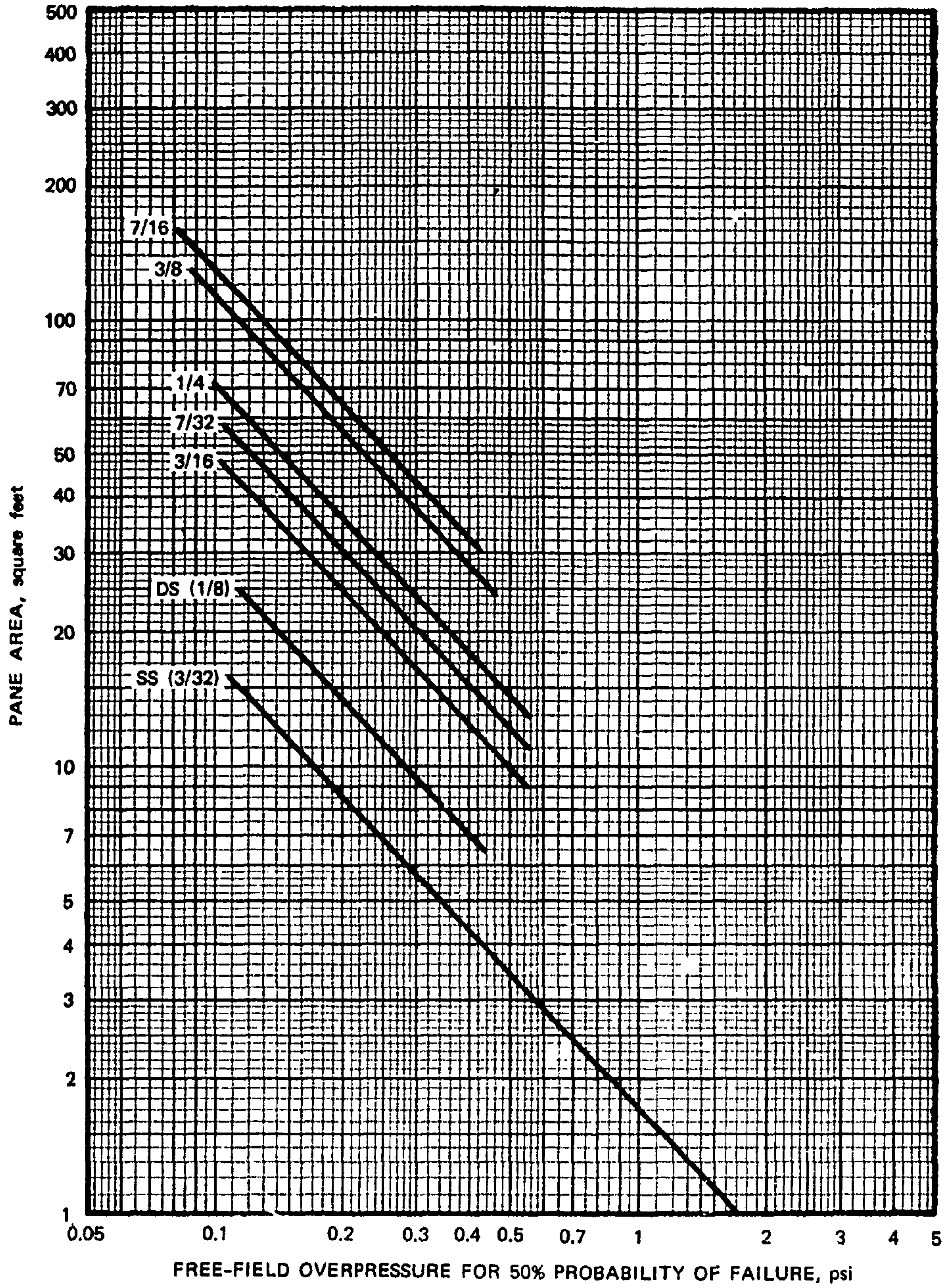

FIG. 10 SHEET GLASS INCIPIENT FAILURE PRESSURES FOR FRONT-FACE LOADING AS A FUNCTION OF PANE AREA AND THICKNESS

In multipane windows, the premature failure of muntins* too weak to withstand the pressures distributed to them by the glass panes was not analyzed in this investigation. However, to obtain an approximate incipient failure overpressure, it is suggested that all thin, weak muntins be ignored; thus the area within substantial frame members, considered as a pane area, is then used in the appropriate one of the Figures 7 through 10. For example, approximate results for the window types shown in Figure B-1 could be found as follows: type 1, two pane areas (upper and lower); types 2, 3, and 8, two pane areas each (right and left) with a third pane area for the vent in type 8; types 4 and 5, the greatest area (and thus the lowest incipient failure pressure) within substantial frame members is found by considering the entire movable portion as one pane area; types 6 and 7, four pane areas each; and type 9, one pane area equal to the area of the large, center pane (assuming all frame members are strong).

Some full scale test data concerning window response to dynamic loadings are contained in Appendix D. A shatter pressure prediction equation is given in Appendix D as Equation D-1. The table accompanying the equation indicates that the shatter pressure should be adjusted for various aspect ratios. For reasons stated previously in this section, application of the table to methods discussed in this chapter is not recommended.

The option of specifying an overpressure in the input data to the computer program was employed in developing figures indicating time to failure in Appendix E.

---

* A muntin is a thin member separating panes of glass within a window frame.

III WEIGHT, NUMBER, AND SPATIAL DENSITY OF GLASS FRAGMENTS

Introduction

Data on mass,* velocity, and spatial density of glass missiles resulting from window failure caused by a nuclear explosion were first taken during Operation Teapot.[29] Glass missiles emanating from multipane windows with either steel or wood frames were trapped in Styrofoam absorbers. The same data were analyzed further with consideration given to biological implications.[30] Then a model[31] that predicted the velocity of glass fragments was developed using drag characteristics determined in drop tests.[32] Further testing was done during Operation Plumbbob[33,34] with one of the objectives being a comparison of missile velocities predicted by the model and those measured in the field. A discussion of the translation model and its use in predicting the velocity of glass fragments is presented in Chapter IV. Since the test procedures, data collected, and discussions of results are already well documented, this chapter is limited to providing methods based on the Operation Teapot data for predicting the fragment weight distribution, the probable number of fragments, and the spatial distribution of fragments.

In the Teapot tests, houses were located at 4,700, 5,500, and 10,500 feet from a nuclear explosion with a yield of nearly 30 kt, which caused peak overpressures of 5.0, 3.8, and 1.9 psi, respectively, at the

---

* All nuclear test data consistently report mass in grams, using mass in the lay sense, i.e., synonymous with weight. The term weight is used in this report. Weights in grams found herein may be converted to the English system of weights by using 454 grams per pound.

three distances. Only data from windows facing ground zero and mounted in houses were selected for use in this chapter. Data from windows mounted in house side or rear walls with respect to ground zero and from windows mounted in the open were not used.

Fragment Weight

Data[29] from 13 traps located behind seven different house front windows are presented in Table 7. The data are grouped by overpressure and glass thickness. Both the geometric mean fragment weight and the average fragment weight are shown in the table. The former provides the best indication of the most probable fragment weight to expect since it is changed very little by the presence of a few heavy pieces. The latter is useful in calculations of the total number and spatial density of fragments. Values summarizing the data for each window were calculated and added to the tabulated field data.

Figure 11, prepared from information contained in Table 7, is presented as a means of predicting both average and geometric mean fragment weights. Because of the limited data found in the literature, predictions for single and double strength glass thicknesses only are given; however, these two thicknesses make up most of the glass installed in windows today.

An additional scale has been provided for use if the window in question is in a side wall with respect to ground zero. It was believed that reflected pressures cause window failures in front walls. Since no reflection occurs on side walls, the free-field overpressure for side walls must be approximately equal to the reflected pressure for front walls, so that the peak pressure load causing window failure will be nearly the same in each case. Thus, the front-face p_{so} values were placed on the lower scale, the corresponding p_r values were placed on the upper scale, and the upper scale was labeled as p_{so} for side windows. It was realized

Table 7

WINDOW GLASS FRAGMENT WEIGHT DATA*

Free-Field Overpressure, p_{so} (psi)	Trap Designation	Average Thickness of Panes h (in.)	Number of Fragments Caught in Traps†	Geometric Mean Weight, M_{50} (gm)	Average Weight, $\overline{M}$ (gm)	Distance from Window to Trap, x (ft)	Size of Individual Panes (in.)	Number of Panes per Window	Frame Material
5.0	2A	.092	254	.140	.226	8.83	12 × 12	16	Wood‡
5.0	2C	.096	423	.140	.282	13.50	12 × 16	20	Steel
5.0	$2D_1$	.094	247	.113	.307	9.00	12 × 16	12	Steel
5.0	$2D_2$	.089	231	.095	.140	9.00			
			478	.104	.226				
5.0	$2E_1$	.124	242	.153	.415	10.50	12 × 23.5	9	Steel§
5.0	$2E_2$	.122	732	.142	.241	10.50			
			974	.145	.284				
3.8	$3C_1$	.120	61	.810	1.275	7.00	12 × 12	16	Wood§
3.8	$3C_2$	.118	259	.540	.993	7.00			
			320	.580	1.047				
1.9	$4B_1$	.124	1	2.125	2.125	10.67	15 × 18	20	Steel‡
1.9	$4B_2$	.123	11	1.322	1.677	10.67			
1.9	$4B_3$	.124	5	1.596	1.704	10.67			
1.9	$4B_4$	.124	5	4.407	5.260	10.67			
			22	1.854	2.518				
1.9	4D	.088	15	.694	1.312	13.50	12 × 16	20	Steel‡

* All data were taken from 13 traps located behind 7 windows mounted in house walls that faced ground zero. In cases of more than one trap per window, data from traps have been combined to provide results for each window as well as each trap.

† The number of fragments given is limited to the number for which the velocity could be calculated.

‡ Window covered with venetian blinds.

§ Window covered with curtains.

Source: Reference 29.

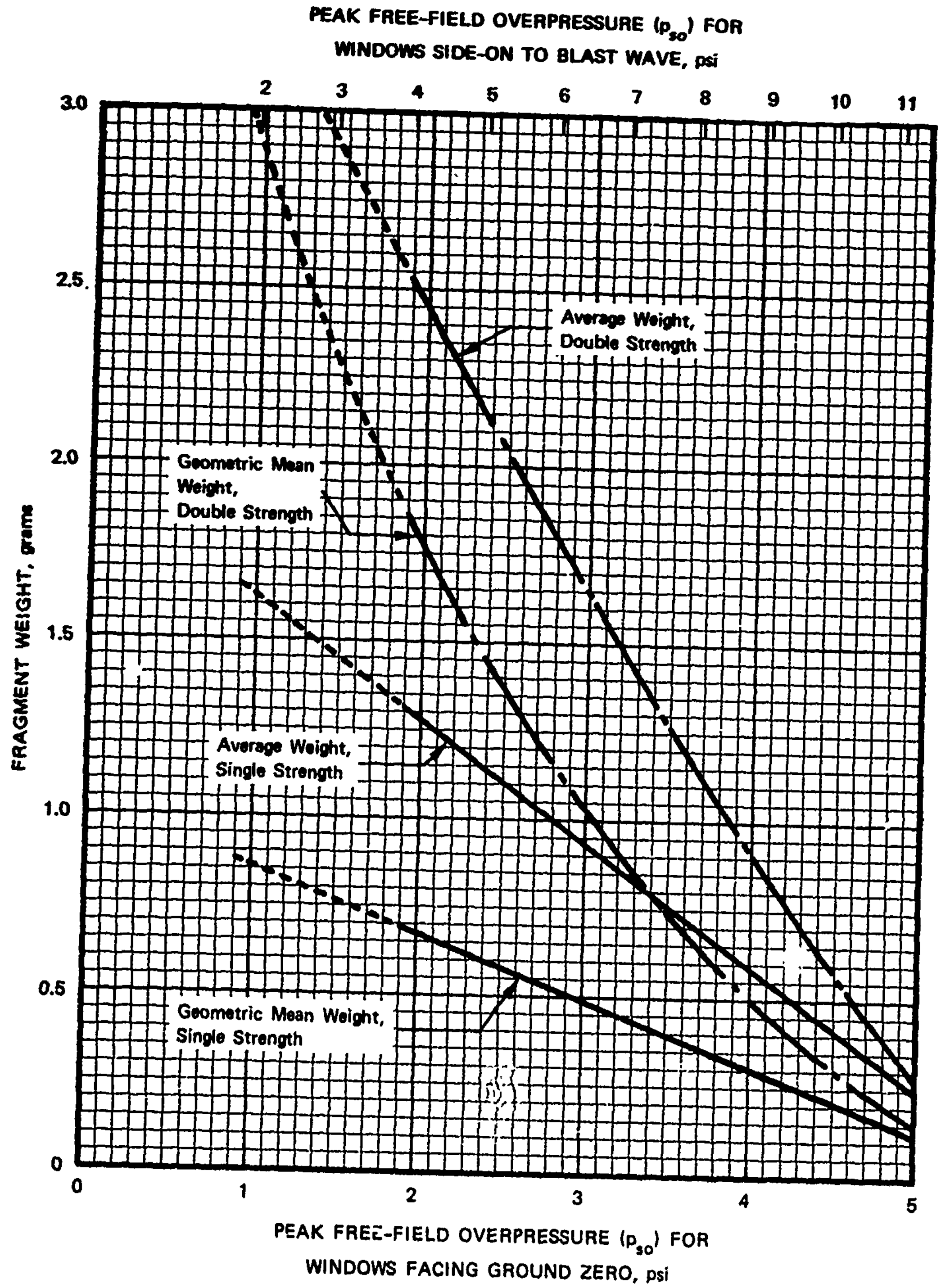

SOURCE: Based on data in Table 7.

FIG. 11 FRAGMENT WEIGHT PREDICTIONS

that drag loading for front and side walls is not the same; however, the differences introduced by accounting for drag loading at these low overpressures were neglected since they were so small.

Number of Fragments

The total number of glass fragments originating from a window can be estimated if it is assumed that the average weight of fragments caught in a trap or traps behind the window is indicative of the average weight of all of the fragments produced by the window.[29] Accepting that assumption, it follows that:

$$N = \frac{A h \gamma}{\overline{M}} \quad . \tag{23}$$

Equation 23 accounts for the fact that the number of fragments depends on overpressure as well as pane properties since $\overline{M}$ is taken from Figure 11.

Spatial Density of Fragments

The spatial density of fragments very close to a window can be estimated by dividing the total number of fragments by the window area:[29]

$$N_o = \frac{N}{A} = \frac{h\gamma}{\overline{M}} \quad . \tag{24}$$

Equation 2· was used in preparing Table 8.

The spatial density data presented in Table 8 were grouped only by overpressure. Further grouping by thickness as was done for the fragment weight data in Table 7 was not done here since:

- The spatial density versus overpressure curve reaches a maximum at 3.8 psi and no single strength data were available at that pressure

Table 8

WINDOW GLASS SPATIAL DENSITY DATA

Free-Field Overpressure, P_{so} (psi)	Trap Designation	Distance from Window to Trap, x (ft)	Average Spatial Density per Trap, N_x (fragments per sq ft)	Average N_x per Window (fragments per sq ft)	Average N_x per Window Times 2.5 (fragments per sq ft)	Average Spatial Density at Window, N_o (fragments per sq ft)	Percent of N_o Remaining After Approximately 10 Feet of Travel: $\frac{N_x}{N_o} \times 100\%$	Percent of N_o Remaining After Approximately 10 Feet of Travel: $\frac{2.5\ N_x}{N_o} \times 100\%$
5.0	2A	8.83	72.1	72.1	180	2393	3.0%	7.5%
5.0	2C	13.50	120.1	120.1	300	2001	6.0	15.0
5.0	$2D_1$	9.00	70.1	68.0	170	2380	2.8	7.1
5.0	$2D_2$	9.00	65.6					
5.0	$2E_1$	10.50	68.7	138.5	346	2546	5.4	13.6
5.0	$2E_2$	10.50	207.9					
			100.8	99.7	249	2330	4.3%	10.7%
3.8	$3C_1$	7.00	17.3	45.5	114	668	6.8	17.0
3.8	$3C_2$	7.00	73.6					
			45.5					
1.9	$4B_1$	10.67	0.3	1.56	3.9	289	0.5	1.4
1.9	$4B_2$	10.67	3.1					
1.9	$4B_3$	10.67	1.4					
1.9	$4B_4$	10.67	1.4					
1.9	4D	13.50	4.3	4.3	10.8	394	1.1	2.7
			2.1	2.93	7.35	342	0.8%	2.1%

Source: Columns 1-4 represent data found in Reference 29. The remaining columns represent calculations performed in this investigation using these data and the data in Table 7.

- The N_x values at 1.9 and 5.0 psi appear to be fairly insensitive to glass thickness

- It seemed desirable to maintain a correlation between this work and the biological considerations presented in Chapter V herein

Average spatial densities, N_x, in fragments per square foot, found by dividing the number of missiles in a trap by the surface area of the trap, are presented in the fourth column of Table 8. The N_x values

> . . . are based on the missiles whose velocities were computed. Judging from the appearance of the front of the first cells* of several traps, it was estimated that about 60 per cent of the missiles striking a trap arrived in such a way that their velocities could not be computed. Missiles striking the trap at low velocities failed to embed themselves in the Styrofoam. Other missiles entered holes already made by previous missiles, and some missiles were lost because their trajectories stopped at the boundary between cells. . . . the impact of large objects made gross deformations in the Styrofoam, making it impossible to evaluate the velocities for smaller glass missiles which were already present. . . . Consideration should be given to the fact that these traps were estimated to have an efficiency of about 40 per cent in catching missiles.[29]

The calculated values shown in Table 8 are plotted in Figure 12. Points were connected by straight lines since no intermediate values were available to suggest a different curve. The curves are based on multipane, single or double strength windows with total glass areas of between 2,300 and 5,400 sq in. The upper curve accounts for the 40 percent efficiency of the traps while the lower curve is representative of the actual number of missiles caught.

The upper curve in Figure 12 is recommended for use in predicting fragment spatial density approximately 10 feet behind a window. N_{10} can

---

* Several layers of Styrofoam were used in each trap, each thickness being referred to as a cell.

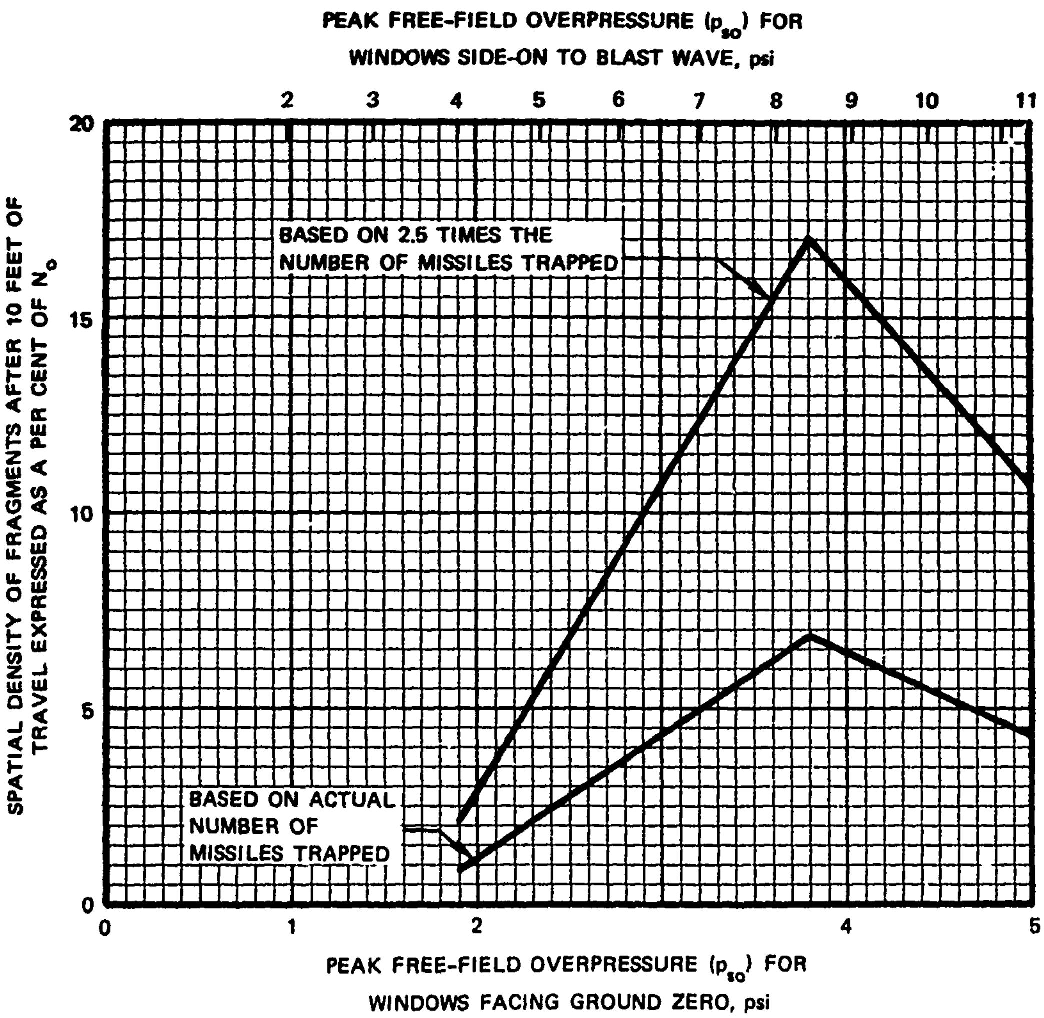

SOURCE: Based on data in Table 8.

FIG. 12 SPATIAL DENSITY PREDICTIONS AFTER 10 FEET OF TRAVEL AS A FUNCTION OF OVERPRESSURE be found by multiplying the percentage obtained from Figure 12 by N_0, which is found by using Equation 24. Since no other data were found, it is suggested that Figure 12 serve as a rough guide to spatial densities for windows both larger and smaller than the size range tested.

It was believed that spatial density depended on the pressure causing window failure, which is reflected pressure for front windows and free-field overpressure for side windows. Therefore, an additional overpressure scale for side windows has been provided across the top of Figure 12 following the same procedure described previously in this chapter for the scale at the top of Figure 11.

IV FRAGMENT TRANSLATION MODEL

Bowen's translation model[31] is an available method for estimating distance, velocity, and acceleration data at various times for glass missiles. The model is applicable to a classical blast wave ". . . not appreciably modified by terrain effects and possessing a well-defined shock front." Five assumptions were made in creating the model:

1. No surface friction existed. Glass fragment translation through air satisfies this assumption perfectly.

2. No energy gain or loss resulted from ". . . moving with or against gravity. The kinetic energy that is lost during lofting would be regained as the object fell to its original elevation, thus mitigating somewhat the error in the predicted motion."

3. ". . . only the propelling force of the wind was considered." This assumption means that the initial velocity of a fragment was taken as zero, i.e., a fragment is treated as though it is suspended motionless in space and then operated on by the blast winds only. The validity of this assumption pertaining to glass fragments is questionable.

4. ". . . the properties of an object which governed acceleration (area presented to the wind, drag coefficient, and mass) . . ." were assumed constant throughout acceleration.

5. ". . . no allowance was made for the fact that a displaced object may be moved to a lower overpressure region and thus be acted upon by correspondingly weaker blast winds."

Table 9 is a presentation of the results obtained by Bowen based on the foregoing discussion. Five blast wave parameters are needed to use the model, namely, P_o, c_o, p_{so}, t_o, and t_u. Values for t_o for standard conditions can be found with sufficient accuracy using Equation 19. Values for t_u can be found by multiplying t_o by an appropriate factor selected from Figure 13. A fragment acceleration coefficient, which accounts for the fragment area presented to the wind, the weight, and the drag coefficient of the fragment, is also required:*

$$\alpha = \frac{A_f}{m} C_d . \tag{25}$$

The results of tests[32] performed to determine α for pieces of 0.125-in. thick window glass and 0.225-in. thick plate glass, dropped both flat and edge first, are presented in Figure 14.

The above blast and fragment parameters are combined into the following nondimensional terms for use in Table 9:

$$P = p_{so}/P_o \tag{26}$$

$$A = \alpha P_o t_u g / c_o \tag{27}$$

$$T = t/t_o \tag{28}$$

$$V(n) = (v/c_o) \times 10^n \tag{29}$$

$$D(n) = (x/t_u c_o) \times 10^n \tag{30}$$

$$\dot{V}(n) = (\dot{v} t_u / c_o) \times 10^n . \tag{31}$$

The decimal point location is indicated in Table 9 by the letter n. For example, if P = 0.10, A = 1000, and T = 0.120, V(6) is found to be 55677,

---

* α is defined[31,32] as the presented area divided by the fragment mass and then reported in ft^2/lb. On the basis of the footnote on page 36, α is considered herein as area/unit weight, retaining the units ft^2/lb in all usages.

Table 9

COMPUTED MOTION PARAMETERS FOR OBJECTS DISPLACED BY CLASSICAL BLAST WAVES

P	A	T:	0	.002	.004	.008	.015	.030	.060	.120	.250	.500	.750	1.000	Final	T_{final}
		V (7):	0	88	175	345	635	1218	2253	3912	6333	8820	9941	10296	10312	
.068	3	D (8):	0	1	3	12	44	169	641	2327	8439	25850	47142	70020	78517	1.092
		V̇ (7):	49066	48500	47950	46860	45040	41460	35410	26640	16090	7350	2990	450	0	
		V (7):	0	293	582	1149	2109	4038	7433	12801	20435	27852	30821		31449	
	10	D (7):	0		1	4	14	56	212	766	2750	8303	14963		22561	1.020
		V̇ (6):	16355	16155	15958	15573	14930	13670	11560	8541	4970	2080	693		0	
		V (7):	0	877	1741	3433	6278	11930	21674	36500	56161	72687	77374		77687	
	30	D (7):	0	1	3	12	43	167	625	2219	7761	22595	39619		49734	0.895
		V̇ (6):	49066	48359	47666	46319	44085	39766	32709	22998	12132	3979	645		0	
		V (6):	0	291	576	1127	2037	3777	6578	10369	14477	16736			16896	
	100	D (7):	0	3	10	41	141	537	1952	6613	21514	57390			84057	0.676
		V̇ (5):	16355	15998	15651	14987	13915	11942	8989	5442	2159	293			0	
		V (6):	0	864	1692	3245	5674	9907	15714	21879	26410				27340	
	300	D (7):	0	8	31	120	403	1468	4990	15361	44252				94925	0.458
		V̇ (5):	49066	46971	45000	41392	35994	27296	16832	7547	1650				0	
		V (6):	0	2776	5253	9478	15143	22942	30579	35809	37497				37500	
	1000	D (7):	0	25	98	356	1151	3772	11148	29385	72750				79332	0.270
		V̇ (4):	16355	14546	13015	10583	7675	4336	1807	466	5				0	
		V (6):	0	7549	13179	20999	28954	36776	41926	43909					43993	
	3000	D (7):	0	71	259	884	2484	7005	17782	41155					56458	0.159
		V̇ (4):	49066	35858	27310	17282	9279	3569	948	75					0	
		V (6):	0	17670	26508	35305	41625	46042	47903						48084	
	9000	D (7):	0	175	579	1712	4167	10150	22914						36728	0.092
		V̇ (3):	14720	6565	3687	1618	621	164	20						0	
		V (7):	0	186	370	732	1346	2586	4797	8373	13662	19090	21447	22143	22172	
.10	3	D (7):	0		1	3	9	35	134	488	1780	5484	10009	14854	16451	1.081
		V̇ (6):	10563	10446	10331	10105	9727	8981	7720	5874	3592	1607	617	79	0	
		V (7):	0	619	1231	2433	4466	8550	15748	27142	43334	58605	64117		65030	
	10	D (7):	0	1	2	9	30	117	442	1596	5735	17274	30974		44789	0.991
		V̇ (6):	35211	34780	34357	33530	32151	29451	24934	18455	10662	4157	1159		0	
		V (6):	0	186	368	725	1324	2507	4527	7550	11421	14366	14980		14990	
	30	D (7).	0	2	7	26	90	345	1288	4545	15714	44931	77637		87959	0.828
		V̇ (5):	10563	10400	10240	9930	9418	8437	6853	4713	2352	630	40		0	
		V (6):	0	615	1214	2364	4238	7745	13170	20056	26737	29507			29549	
	100	D (6):	0	1	2	9	29	109	391	1291	4051	10392			12684	0.588
		V̇ (5):	35211	34274	33371	31661	28948	24111	17254	9631	3229	166			0	
		V (6):	0	1815	3527	6674	11421	19217	28969	38092	43502				44039	
	300	D (6):	0	2	6	25	81	287	940	2759	7546				12672	0.382
		V̇ (4):	10563	9957	9398	8408	7002	4921	2717	1042	148				0	
		V (6):	0	5730	10604	18439	28080	39911	49951	55677					56779	
	1000	D (7):	0	52	197	717	2179	6786	18945	47387					97492	0.220
		V (4):	35211	29769	25479	19234	12654	6243	2219	430					0	
		V (6):	0	14926	24836	37145	48177	57673	63035	64483					64485	
	3000	D (7):	0	140	496	1613	4298	11440	27641	61685					66790	0.129
		V̇ (3):	10563	6740	4663	2596	1225	408	88	1					0	
		V (6):	0	32061	44935	56140	63298	67740	69201						69239	
	9000	D (7):	0	323	1015	2836	6574	15342	33599						42608	0.075
		V̇ (3):	31690	10438	5105	1957	672	153	9						0	
		V (7):	0	137	273	540	994	1916	3574	6298	10428	14752	16649	17259	17290	
.15	1	D (7):	0			2	7	26	98	360	1330	4146	7613	11338	13067	1.114
		V̇ (7):	76671	77860	77070	75510	72890	57720	58890	45730	28730	13000	5130	970	0	
		V (7):	0	411	817	1617	2976	5727	10648	18654	30564	42539	47360	48571	48610	
	3	D (7):	0		1	6	20	77	294	1072	3927	12109	22033	32571	35280	1.064
		V (6):	23601	23347	23097	22607	21787	20168	17418	13352	8165	3461	1188	93	0	
		V (6):	0	137	272	537	985	1885	3466	5954	9430	12492	13406		13491	
	10	D (7):	0	1	5	19	66	255	963	3469	12410	36978	65553		87180	0.934
		V (6):	78671	77685	76716	74829	71681	65535	55283	40583	22700	7722	1498		0	
		V (6):	0	409	812	1595	2903	5459	9741	15930	23339	28069			28614	
	30	D (6):	0		1	6	19	75	276	962	3251	9009			14907	0.737
		V (5):	23601	23188	22784	22005	20728	18311	14505	9531	4283	787			0	
		V (6):	0	1353	2659	5140	9097	16235	26597	38527	48331				50886	
	100	D (6):	0	1	5	18	62	230	802	2548	7610				18291	0.493
		V (5):	78671	75942	73342	68503	61051	48440	32022	15799	4053				0	
		V (6):	0	3959	7601	14071	23308	37233	52609	64838	70129				70248	
	300	D (6):	0	4	14	52	167	572	1776	4920	12715				16408	0.310
		V̇ (4):	23601	21681	19979	17107	13344	8421	4021	1251	71				0	
		V (6):	0	12152	21747	35909	51461	68068	80049	85424					85866	
	1000	D (6):	0	11	41	143	415	1215	3191	7580					11803	0.176
		V̇ (4).	78671	61322	49088	33388	19384	8167	2417	287					0	

Source: Ref. 31.

Table 9 (Continued)

P	A	T:	0	.002	.004	.008	.015	.030	.060	.120	.250	.500	.750	1.000	Final	T_{final}
		V (6):	0	29712	46419	64522	78639	89205	94174						94913	
.15	3000	D (7):	0	281	957	2937	7384	18539	42794						78423	0.103
		V̇ (3):	23601	12265	7478	3581	1471	422	67						0	
		V (5):	0	5724	7468	8791	9543	9952							10040	
	9000	D (7):	0	594	1768	4656	10315	23180							49210	0.060
		V̇ (3):	70804	15437	6494	2178	671	124							0	
		V (8):	0	709	1412	2797	5159	9972	18694	33219	55666	79530	90144	93841	94326	
.20	.3	D (8):	0	1	2	10	34	131	501	1847	6879	21660	39963	59715	75430	1.195
		V̇ (7):	41667	41270	40880	40120	38830	36280	31870	25160	16130	7380	3000	750	0	
		V (7):	0	236	470	932	1718	3318	6211	11005	18345	25994	29258	30281	30336	
	1	D (7):	0		1	3	11	44	167	613	2275	7125	13085	19477	22777	1.127
		V̇ (6):	13889	13754	13620	13360	12921	12050	10551	8277	5237	2321	886	169	0	
		V (7):	0	709	1410	2791	5140	9905	18458	32445	53308	73877	81694	83460	83509	
	3	D (7):	0	1	2	10	33	130	497	1818	6679	20600	37382	55103	59218	1.058
		V̇ (6):	41667	41233	40806	39970	38568	35793	31048	23932	14589	5913	1872	108	0	
		V (6):	0	236	469	926	1699	3246	5958	10200	16013	20819	22032		22099	
	10	D (6):	0		1	3	11	43	162	582	2072	6108	10725		13452	0.894
		V̇ (5):	13889	13711	13537	13198	12632	11527	9687	7043	3807	1145	156		0	
		V (6):	0	706	1397	2741	4971	9290	16389	26321	37483	43582			43974	
	30	D (6):	0	1	2	9	33	125	458	1573	5210	14074			20710	0.677
		V̇ (5):	41667	40854	40063	38542	36066	31440	24313	15301	6234	784			0	
		V (6):	0	2324	4550	8730	15269	26672	42325	58939	70827				72901	
	100	D (6):	0	2	8	31	103	375	1277	3931	11310				22876	0.437
		V̇ (4):	13889	13299	12743	11726	10203	7746	4781	2129	430				0	
		V (6):	0	6744	12803	23233	37417	57327	77289	91341	95988				95997	
	300	D (6):	0	6	23	85	266	888	2651	7054	17590				19256	0.270
		V̇ (4):	41667	37336	33631	27665	20384	11787	5046	1336	14				0	
		V (5):	0	2017	3504	5549	7607	9598	10884	11356					11371	
	1000	D (6):	0	18	66	223	623	1747	4410	10160					13346	0.153
		V̇ (3):	13889	10028	7569	4729	2501	946	245	16					0	
		V (5):	0	4669	6954	9200	10795	11887	12336						12373	
	3000	D (7):	0	441	1452	4268	10327	25025	56278						87144	0.089
		V̇ (3):	41667	18053	9993	4311	1624	423	49						0	
		V (5):	0	8302	10362	11795	12545	12921							12976	
	9000	D (7):	0	867	2491	6329	13659	30061							54150	0.052
		V̇ (2):	12500	1959	745	230	67	10							0	
		V (7):	0	108	215	427	788	1526	2869	5122	8633	12351	13974	14533	14611	
.25	.3	D (7):	0			1	5	20	75	279	1044	3299	6089	9095	11534	1.199
		V̇ (7):	64655	64070	63500	62370	60480	56690	50100	39890	25720	11590	4620	1170	0	
		V (7):	0	360	717	1422	2623	5074	9522	16940	28356	40143	45027	46504	46632	
	1	D (7):	0		1	5	17	65	250	925	3445	10810	19837	29489	34777	1.135
		V̇ (6):	21552	21351	21154	20767	20114	18813	16556	13078	8287	3585	1321	244	0	
		V (6):	0	108	215	426	784	1513	2823	4971	8168	11245	12346	12566	12571	
	3	D (7):	0	1	4	14	50	195	745	2733	10052	30943	55942	82193	86992	1.045
		V̇ (6):	64655	63999	63352	62086	59957	55734	48467	37432	22617	8734	2533	91	0	
		V (6):	0	360	715	1411	2586	4935	9034	15389	23897	30479	31872		31910	
	10	D (6):	0		1	5	17	64	242	866	3061	8918	15513		18373	0.857
		V̇ (5):	21552	21268	20990	20448	19546	17787	14861	10662	5542	1469	126		0	
		V (6):	0	1074	2126	4161	7520	13956	24332	38369	53178	60127			60345	
	30	D (6):	0	1	4	14	49	185	674	2284	7414	19566			26056	0.628
		V̇ (5):	64655	63256	61899	59300	55100	47358	35710	21496	7949	638			0	
		V (6):	0	3528	6880	13102	22646	38751	59733	80440	93498				95022	
	100	D (6):	0	3	12	45	151	544	1809	5419	15118				26728	0.396
		V̇ (4):	21552	20464	19452	17631	14981	10901	6316	2564	406				0	
		V (5):	0	1015	1906	3393	5326	7874	10230	11727					12110	
	300	D (6):	0	9	33	123	383	1231	3559	9182					21572	0.243
		V̇ (4):	64655	56495	49759	39389	27546	14769	5777	1323					0	
		V (5):	0	2959	5005	7645	10121	12330	13642	14043					14045	
	1000	D (6):	0	26	94	310	841	2279	5591	12612					14590	0.137
		V̇ (3):	21552	14433	10322	5995	2938	1026	238	6					0	
		V (5):	0	6521	9346	11921	13615	14711	15106						15123	
	3000	D (7):	0	617	1974	5614	13207	31215	68967						94176	0.080
		V̇ (3):	64655	23671	12102	4817	1713	409	32						0	
		V (5):	0	10886	13173	14661	15394	15735							15768	
	9000	D (7):	0	1144	3200	7928	16810	36491							58110	0.046
		V̇ (2):	19397	2292	807	234	65	8							0	
		V (7):	0	152	302	600	1108	2150	4054	7268	12307	17623	19908	20690	20804	
.30	.3	D (7):	0			2	7	27	104	388	1457	4617	8524	12729	16174	1.201
		V̇ (6):	9247	9168	9090	8937	8678	8160	7249	5814	3762	1673	657	170	0	
		V (7):	0	506	1008	1998	3690	7146	13443	23996	40294	56964	63694	65668	65841	
	1	D (7):	0		2	7	23	90	347	1283	4797	15073	27633	41028	48756	1.142
		V̇ (6):	30822	30548	30277	29746	28849	27054	23912	18990	12031	5091	1819	328	0	
		V (6):	0	152	302	598	1103	2128	3975	7008	11505	15732	17162		17414	
	3	D (6):	0			2	7	27	103	378	1391	4272	7695		11771	1.035
		V̇ (6):	92446	91547	90641	88868	85880	79935	69639	53809	32177	11873	3175		0	
		V (6):	0	505	1003	1980	3627	6911	12616	21374	32820	41136	42616		42633	
	10	D (6):	0		2	7	23	88	332	1186	4162	11986	20680		23309	0.825
		V̇ (5):	30822	30404	29994	29196	27868	25283	20989	14847	7420	1741	84		0	

Table 9 (Continued)

P	A	T:	0	.002	.004	.008	.015	.030	.060	.120	.250	.500	.750	1.000	Final	T_{final}
		V (6):	0	1507	2979	5820	10481	19319	33295	51603	69808	77210			77317	
.30	30	D (6):	0	1	5	20	67	253	913	3055	9739	25202			30955	0.590
		V̇ (5):	92466	90267	88139	84084	77580	65751	48368	27908	9431	450			0	
		V (5):	0	493	959	1812	3097	5199	7811	10227	11592				11700	
	100	D (6):	0	4	16	62	205	726	2369	6931	18862				30043	0.366
		V̇ (4):	30822	29024	27372	24446	20304	14203	7778	2916	362				0	
		V (5):	0	1408	2615	4574	7018	10069	12707	14243					14554	
	300	D (6):	0	12	45	165	505	1584	4456	11223					23530	0.223
		V̇ (4):	92466	78821	67944	51892	34628	17406	6319	1269					0	
		V (5):	0	4007	6614	9801	12613	14977	16288	16622					16623	
	1000	D (6).	0	35	124	400	1057	2791	6701	14888					15638	0.125
		V̇ (3):	30822	19210	13089	7141	3298	1080	227	1					0	
		V (5):	0	8452	11745	14572	16324	17411	17755						17762	
	3000	D (6):	0	80	250	692	1593	3697	8066						10009	0.073
		V̇ (3).	92466	29055	13911	5196	1770	393	19						0	
		V (5):	0	13411	15882	17400	18113	18421							18440	
	9000	D (7):	0	1523	3982	9527	19826	42498							61565	0.043
		V (2):	27740	2584	852	236	63	6							0	
		V (7):	0	200	399	792	1465	2845	5380	9689	16489	23665	26730	27787	27954	
.35	.3	D (7):	0		1	3	9	35	135	503	1898	6037	11155	16664	21476	1.214
		V̇ (6):	12500	12399	12300	12104	11773	11105	9919	8014	5213	2304	902	244	0	
		V (7):	0	668	1330	2638	4874	9455	17828	31936	53819	76087	84941	87520	87766	
	1	D (7):	0	1	2	9	30	117	448	1662	6236	19633	35989	53412	64400	1.156
		V (6):	41667	41314	40965	40280	39119	36786	32661	26086	16555	6909	2433	451	0	
		V (6):	0	200	399	790	1456	2812	5259	9284	15239	20735	22522		22817	
	3	D (6):	0		1	3	9	35	133	488	1798	5512	9904		15059	1.032
		V̇ (5).	12500	12379	12260	12026	11631	10842	9465	7321	4343	1549	392		0	
		V (6):	0	666	1323	2610	4778	9094	16560	27922	42468	52503	54045		54051	
	10	D (6).	0	1	2	8	29	114	426	1517	5291	15092	25877		28159	0.802
		V (5):	41667	41088	40520	39416	37577	34002	28070	19607	9475	2010	54		0	
		V (6):	0	1986	3922	7647	13727	25146	42895	65500	86877	94593			94626	
	30	D (6):	0	2	6	25	86	322	1156	3827	12011	30607			35439	0.563
		V (4):	12500	12178	11867	11278	10338	8651	6225	3462	1084	29			0	
		V (5):	0	648	1255	2356	3986	6582	9678	12393	13795				13873	
	100	D (6).	0	5	21	79	259	908	2912	8356	22309				32959	0.345
		V̇ (4):	41667	38931	36446	32114	26131	17658	9221	3240	321				0	
		V (5):	0	1836	3376	5812	8748	12247	15113	16674					16934	
	300	D (6):	0	15	57	207	623	1917	5281	13059					25233	0.210
		V̇ (3):	12500	10412	8801	6512	4174	1991	683	123					0	
		V (5):	0	5110	8261	11945	15031	17522	18828						19114	
	1000	D (6):	0	44	153	485	1257	3251	7681						16550	0.118
		V (3):	41667	24324	15896	8237	3639	1133	220						0	
		V (5):	0	10385	14091	17125	18918	19993	20302						20305	
	3000	D (6):	0	97	298	809	1834	4200	9082						10523	0.069
		V (2)·	12500	3439	1561	555	183	39	1						0	
		V (5):	0	15854	18478	20011	20716	20998							21011	
	9000	D (7):	0	1799	4610	10861	22381	47630							64499	0.040
		V̇ (2):	37500	2863	897	242	61	5							0	
		V (7)·	0	85	170	338	625	1216	2308	4176	7152	10315	11679	12169	12276	
.40	.1	D (8):	0	1	3	11	38	147	569	2126	8072	25810	47818	71554	99719	1.290
		V (6):	5405	5365	5324	5245	5110	4837	4346	3542	2326	1035	413	124	0	
		V (7):	0	256	510	1013	1874	3646	6909	12481	21305	30570	34470	35803	36019	
	.3	D (7):	0		1	3	11	44	170	636	2410	7679	14187	21181	27648	1.227
		V̇ (6):	16216	16092	15969	15727	15315	14481	12986	10544	6866	2996	1157	314	0	
		V (6):	0	85	170	337	624	1211	2287	4107	6931	9775	10879	11191	11220	
	1	D (7):	0	1	3	11	37	147	565	2102	7902	24880	45545	67506	81618	1.159
		V (6):	54054	53613	53177	52320	50864	47924	42680	34193	21638	8843	3026	542	0	
		V (6).	0	256	509	1009	1861	3596	6730	11882	19456	26282	28390		28705	
	3	D (6):	0		1	3	11	44	167	615	2265	6918	12385		18505	1.020
		V (5).	16216	16062	15909	15609	15102	14087	12304	9501	5565	1900	445		0	
		V (6):	0	851	1690	3332	6095	11580	21018	35224	52969	64529	66013		66017	
	10	D (6):	0	1	3	11	37	143	534	1893	6554	18495	31501		32888	0.776
		V̇ (5):	54054	53278	52516	51035	48573	43790	35884	24677	11475	2164	17		0	
		V (5):	0	254	500	973	1740	3167	5343	8033	10449	11215			11216	
	30	D (6):	0	2	8	31	107	402	1429	4678	14454	36285			39581	0.537
		V̇ (4):	16216	15763	15327	14503	13201	10894	7656	4095	1183	13			0	
		V (5):	0	825	1591	2966	4966	8064	11617	14573	15964				16015	
	100	D (6)	0	7	26	99	321	1109	3499	9858	25862				35565	0.326
		V̇ (4).	54054	50090	46531	40426	32208	21021	10478	3453	261				0	
		V (5)	0	2318	4220	7151	10567	14457	17496	19044					19255	
	300	D (6).	0	19	71	254	753	2271	6139	14938					26743	0.198
		V (3):	16216	13187	10925	7832	4828	2196	713	114					0	
		V (5)·	0	6310	9999	14135	17440	20014	21289						21529	
	1000	D (6).	0	54	185	576	1465	3724	8678						17359	0.111
		V (3)	54054	29529	18538	9154	3887	1155	207						0	
		V (5):	0	12379	16446	19635	21444	22492	22762						22763	
	3000	D (6):	0	116	349	930	2080	4709	10108						10979	0.065
		V̇ (2)	16216	3921	1695	576	185	37							0	

Table 9 (Continued)

P	A	T:	0	.002	.004	.008	.015	.030	.060	.120	.250	.500	.750	1.000	Final	T_{final}
		V (5):	0	18272	21013	22542	23232	23486							23493	
.40	9000	D (7):	0	2086	5253	12216	24965	52810							67114	0.038
		$\dot{V}$ (2):	48649	3081	919	243	59	3							0	
		V (7):	0	126	252	500	926	1808	3445	6279	10842	15700	17784	18546	18737	
.50	.1	D (7):	0			2	5	21	81	305	1166	3750	6962	10427	14825	1.310
		$\dot{V}$ (6):	8333	8277	8222	8112	7925	7541	6835	5637	3733	1652	660	209	0	
		V (7):	0	379	755	1499	2777	5416	10310	18748	32238	46383	52281	54316	54742	
	.3	D (7):	0		1	5	16	63	243	912	3477	11134	20596	30763	42156	1.274
		$\dot{V}$ (6):	25000	24828	24657	24321	23745	22564	20403	16744	10974	4744	1823	521	0	
		V (6):	0	126	251	499	924	1797	3407	6149	10422	14680	16291	16739	16786	
	1	D (6):	0			2	5	21	81	301	1135	3582	6551	9702	11991	1.180
		$\dot{V}$ (6):	83333	82710	82092	80874	78794	74546	66825	53929	34108	13611	4542	837	0	
		V (6):	0	378	753	1492	2754	5325	9979	17633	28792	38517	41321		41691	
	3	D (6):	0		1	5	16	62	238	875	3219	9784	17431		25665	1.010
		$\dot{V}$ (5):	25000	24770	24543	24096	23338	21806	19081	14709	8459	2720	577		0	
		V (6):	0	1257	2495	4916	8978	17010	30702	50930	75199	89664			91114	
	10	D (6):	0	1	4	15	52	201	751	2643	9037	25084			41899	0.744
		$\dot{V}$ (5):	83333	82071	80833	78427	74431	66692	53969	36155	15816	2500			0	
		V (5):	0	374	736	1426	2536	4560	7550	11068	13977				14736	
	30	D (6):	0	3	11	44	150	559	1962	6299	18986				46961	0.503
		$\dot{V}$ (4):	25000	24203	23440	22011	19783	15935	10756	5400	1377				0	
		V (5):	0	1210	2316	4266	7015	11082	15453	18806	20176				20198	
	100	D (6):	0	9	36	137	440	1491	4579	12540	32074				40074	0.302
		$\dot{V}$ (4):	83333	76067	69685	59047	45357	27936	12931	3867	175				0	
		V (5):	0	3350	5992	9889	14180	18740	22055	23584					23731	
	300	D (6):	0	26	98	343	993	2907	7632	18145					29349	0.182
		$\dot{V}$ (3):	25000	19466	15572	10581	6127	2588	775	101					0	
		V (5):	0	8772	13461	18387	22041	24735	25977						26158	
	1000	D (6):	0	73	245	739	1829	4528	10350						18758	0.102
		$\dot{V}$ (3):	83333	40540	23831	10903	4371	1220	191						0	
		V (5):	0	16256	20959	24368	26234	27243							27462	
	3000	D (6):	0	156	445	1144	2500	5564							11778	0.060
		$\dot{V}$ (2):	25000	4890	1951	629	191	35							0	
		V (5):	0	22867	25819	27343	28009	28228							28230	
	9000	D (7):	0	2584	6340	14474	29240	61350							71606	0.035
		$\dot{V}$ (2):	75000	3527	973	249	57	2							0	
		V (7):	0	175	348	693	1285	2512	4805	8800	15268	22113	25002	26050	26325	
.60	.1	D (7):	0		1	2	7	28	110	415	1594	5139	9539	14279	20689	1.330
		$\dot{V}$ (6):	11842	11770	11699	11557	11314	10807	9858	8189	5434	2368	933	299	0	
		V (7):	0	524	1045	2077	3852	7525	14372	26250	45311	65121	73208	75953	76552	
	.3	D (7):	0		2	6	22	85	329	1239	4746	15223	28139	41990	58498	1.292
		$\dot{V}$ (6):	35526	35304	35082	34643	33888	32322	29394	24275	15905	6741	2536	724	0	
		V (6):	0	175	348	691	1280	2495	4741	8580	14555	20398	22528	23091	23148	
	1	D (6):	0		1	2	7	28	109	408	1543	4861	8868	13102	16217	1.182
		$\dot{V}$ (5):	11842	11759	11677	11514	11235	10659	9593	7763	4872	1879	600	104	0	
		V (6):	0	523	1042	2065	3812	7374	13817	24382	39565	52265	55616		55989	
	3	D (6):	0		2	6	21	84	321	1179	4325	13048	23105		32969	0.988
		$\dot{V}$ (5):	35526	35205	34887	34260	33192	31022	27119	20772	11645	3485	649		0	
		V (5):	0	174	345	679	1238	2336	4187	6863	9934	11600			11724	
	10	D (6):	0	1	5	20	70	270	1002	3497	11793	32183			50288	0.709
		$\dot{V}$ (4):	11842	11651	11463	11098	10495	9331	7435	4832	1979	255			0	
		V (5):	0	516	1014	1957	3456	6138	9973	14261	17542				18240	
	30	D (6):	0	4	15	59	200	739	2558	8057	23730				53438	0.472
		$\dot{V}$ (4):	35526	34242	33021	30752	27269	21412	13869	6545	1468				0	
		V (5):	0	1661	3157	5741	9278	14280	19338	22955	24240				24247	
	100	D (6):	0	12	48	181	575	1907	5716	15274	38258				43920	0.282
		$\dot{V}$ (3):	11842	10641	9609	7939	5883	3430	1487	406	9				0	
		V (5):	0	4532	7966	12826	17890	22992	26456	27914					28011	
	300	D (6):	0	35	128	441	1250	3562	9130	21309					31570	0.170
		$\dot{V}$ (3):	35526	26463	20454	13213	7247	2864	801	84					0	
		V (5):	0	11430	17048	22631	26516	29252	30426						30558	
	1000	D (6):	0	94	308	907	2196	5324	11988						19952	0.095
		$\dot{V}$ (2):	11842	5146	2850	1219	466	123	17						0	
		V (5):	0	20161	25382	28914	30780	31741							31917	
	3000	D (6):	0	194	538	1353	2909	6393							12456	0.056
		$\dot{V}$ (2):	35526	5718	2124	656	192	32							0	
		V (5):	0	27313	30406	31899	32525	32714							32714	
	9000	D (7):	0	3083	7414	16684	33410	69669							75464	0.032
		V (1):	10658	384	99	25	5								0	
		V (7):	0	228	455	905	1678	3280	6264	11447	19774	28472	32092	33402	33790	
.70	.1	D (7):	0		1	3	9	36	140	526	20.4	6467	11968	17885	27204	1.384
		$\dot{V}$ (6):	15909	15810	15711	15516	15179	14481	13175	10889	7151	3065	1196	388	0	
		V (7):	0	685	1366	2714	5030	9821	18729	34116	58594	83649	93707	97100	97878	
	.3	D (7):	0		2	8	27	108	418	1570	5992	19123	35233	52470	74779	1.317
		$\dot{V}$ (6):	47727	47418	47111	46502	45455	43288	39247	32221	20859	8669	3220	930	0	
		V (6):	0	228	455	903	1672	3254	6169	11118	18726	26006	28589	29257	29325	
	1	D (6):	0		1	3	9	36	138	515	1941	6073	11030	16253	20284	1.191
		$\dot{V}$ (5):	15909	15793	15677	15449	15057	14252	12767	10242	6318	2366	736	127	0	

Table 9 (Ccntinued)

P	A	T:	0	.002	.004	.008	.015	.030	.060	.120	.250	.500	.750	1.000	Final	T_{final}
		V (6):	0	684	1361	2696	4970	9593	17900	31353	50269	65532	69320		69708	
.70	3	D (6):	0		2	8	27	106	405	1483	5392	16090	28317		39757	0.978
		V̇ (5):	47727	47265	46807	45907	44377	41283	35773	26965	14672	4164	718		0	
		V (5):	0	227	500	884	1607	3016	5352	8641	12259	14091			14200	
	10	D (6):	0	2	7	26	89	340	1254	4332	14375	38619			57995	0.690
		V̇ (4):	15909	15624	15344	14805	13917	12228	9544	5997	2323	259			0	
		V (5):	0	673	1319	2534	4441	7786	12411	17350	20895				21555	
	30	D (6):	0	5	19	75	252	920	3142	9713	28030				59489	0.454
		V̇ (4):	47727	45771	43925	40531	35415	27071	16841	7529	1538				0	
		V (5):	0	2154	4065	7302	11612	17452	23080	26882	28088				28091	
	100	D (6):	0	16	61	226	709	2309	6775	17747	43749				47593	0.269
		V̇ (3):	15909	14071	12528	10101	7237	4024	1650	420	4				0	
		V (5):	0	5796	10027	15800	21532	27050	30624	32019					32087	
	300	D (6):	0	44	159	537	1494	4166	10478	24117					33687	0.161
		V̇ (3):	47727	34077	25521	15762	8262	3105	822	71					0	
		V (5):	0	14136	20600	26691	30787	33526	34651						34753	
	1000	D (6):	0	114	369	1064	2529	6035	13437						21070	0.091
		V̇ (2):	15909	6241	3284	1339	489	125	15						0	
		V (5):	0	23956	29627	33241	35085	36019							36162	
	3000	D (6):	0	230	624	1540	3271	7126							13080	0.053
		V̇ (2):	47727	6498	2269	678	195	30							0	
		V (5):	0	31560	34768	36223	36821								36985	
	9000	D (7):	0	3537	8371	18637	37083								79003	0.031
		V̇ (1):	14318.	412	100	25	5								0	
		V (7):	0	290	579	1150	2132	4163	7939	14462	24841	35480	39802	41337	41793	
.80	.1	D (7):	0		1	3	11	45	175	656	2505	7995	14738	21965	33526	1.391
		V̇ (6):	20513	20380	20248	19987	19538	18608	16872	13853	8970	3748	1429	458	0	
		V (6):	0	87	174	345	639	1246	2372	4306	7349	10399	11590	11982	12070	
	.3	D (7):	0	1	2	10	34	135	522	1959	7443	23602	43295	64289	92126	1.325
		V̇ (6):	61538	61124	60712	59896	58494	55596	50212	40913	26071	10530	3806	1075	0	
		V (6):	0	290	578	1147	2122	4125	7801	13991	23363	32088	35065	35794	35862	
	1	D (6):	0		1	3	11	45	173	642	2402	7453	13464	19772	24478	1.185
		V̇ (5):	20513	20355	20198	19889	19359	18271	16277	12921	7802	2810	835	133	0	
		V (6):	0	869	1730	3423	6303	12133	22531	39141	61924	79544	83588		83939	
	3	D (6):	0	1	2	10	34	133	505	1836	6612	19496	34073		46544	0.959
		V̇ (5):	61538	60897	60263	59017	56907	52663	45184	33452	17594	4678	714		0	
		V (5):	0	288	571	1120	2029	3784	6644	10560	14678	16607			16697	
	10	D (6):	0	2	8	32	111	423	1547	5281	17241	45592			65299	0.666
		V̇ (4):	20513	20105	19708	18943	17694	15350	11719	7106	2594	242			0	
		V (5):	0	853	1668	3189	5547	9594	15004	20524	24235				24822	
	30	D (6):	0	6	24	93	312	1129	3798	11531	32641				65051	0.435
		V̇ (4):	61538	58697	56037	51202	44050	32749	19558	8281	1524				0	
		V (5):	0	2716	5086	9024	14120	20743	26829	30720					31823	
	100	D (6):	0	20	75	278	860	2754	7921	20371					50915	0.256
		V̇ (3):	20513	17840	15650	12305	8522	4524	1762	418					0	
		V (5):	0	7202	12261	18922	25237	31069	34673	35976					36017	
	300	D (6):	0	54	194	645	1760	4812	11900	27053					35593	0.153
		V̇ (3):	61538	42031	30491	18019	9051	3245	815	55					0	
		V (5):	0	16984	24234	30726	34938	37657	38709						38782	
	1000	D (6):	0	141	440	1235	2885	6784	14955						22077	0.086
		V̇ (2):	20513	7263	3636	1418	500	123	13						0	
		V (5):	0	27759	33804	37438	39233	40117							40233	
	3000	D (6):	0	268	715	1736	3651	7891							13640	0.050
		V̇ (2):	61538	7122	2340	678	192	27							0	
		V (5):	0	35709	38955	40364	40940								41077	
	9000	D (7):	0	4015	9374	20681	40924								82115	0.02
		V̇ (1):	18462	428	99	24	5								0	
		V (7):	0	420	838	1665	3085	6019	11460	20815	35558	50433	56385	58504	59207	
1.00	.1	D (7):	0		1	5	16	62	240	900	3421	10863	19957	29685	47541	1.448
		V̇ (6):	31250	31041	30833	30421	29714	28251	25530	20826	13312	5454	2063	679	0	
		V (6):	0	126	251	499	924	1801	3422	6188	10491	14723	16345	16876	17013	
	.3	D (6):	0			1	5	19	72	268	1015	3197	5842	8654	12941	1.374
		V̇ (6):	93750	93091	92437	91141	88918	84333	75847	61310	38463	15169	5416	1571	0	
		V (6):	0	420	837	1660	3068	5953	11219	20000	33058	44873	48773	49711	49804	
	1	D (6):	0		1	5	16	62	236	876	3254	10002	17968	26300	33134	1.203
		V̇ (5):	31250	30994	30740	30238	29381	27629	24443	19154	11289	3917	1133	185	0	
		V (5):	0	126	250	495	909	1743	3215	5520	8579	10830	11315		11352	
	3	D (6):	0	1	3	13	47	182	688	2482	8821	25618	44422		59773	0.950
		V̇ (5):	93750	92669	91602	89512	85987	78958	66779	48217	24295	6047	837		0	
		V (5):	0	417	824	1612	2905	5365	9265	14384	19458	21628			21702	
	10	D (6):	0	3	11	44	151	573	2075	6959	22201	57530			78883	0.646
		V̇ (4):	31250	30529	29830	28495	26343	22397	16526	9523	3219	244			0	
		V (5):	0	1230	2394	4540	7798	13202	20060	26600	30664				31195	
	30	D (6):	0	8	33	127	421	1499	4933	14586	40217				75037	0.416
		V̇ (4):	93750	88601	83847	75368	63215	44977	25272	9954	1610				0	
		V (5):	0	3876	7170	12466	19001	27025	33893	37976					38982	
	100	D (6):	0	27	102	370	1124	3501	9784	24539					56771	0.243
		V̇ (3):	31250	26410	22601	17060	11219	5553	2014	437					0	

Table 9 (Concluded)

P	A	T:	0	.002	.004	.006	.015	.030	.060	.120	.250	.500	.750	1.000	Final	T_{final}
		V (5):	0	10033	16653	24913	32218	38567	42263	43476					43498	
1.00	300	D (6):	0	72	254	827	2198	5839	14111	31574					38927	0.145
		V̇ (3):	93750	59448	40990	22619	10682	3599	846	39					0	
		V (5):	0	22441	31088	38257	42633	45389	46370						46418	
	1000	D (6):	0	182	551	1504	3435	7925	17252						23839	0.081
		V̇ (2):	31250	9401	4355	1595	543	126	10						0	
		V (5):	0	34854	41589	45220	47022	47849							47935	
	3000	D (6):	0	331	857	2038	4227	9043							14623	0.047
		V̇ (2):	93750	8471	2520	721	194	25							0	
		V (5):	0	43453	46703	48152	48703								48810	
	9000	D (7):	0	4754	10898	23754	46671								87711	0.027
		V̇ (1):	28125	467	109	25	5								0	
		V (7):	0	644	1283	2545	4706	9143	17279	31000	52023	72550	80561	83400	84435	
1.3	.1	D (7):	0		2	6	23	89	342	1272	4768	14907	27164	40221	68159	1.523
		V̇ (6):	50904	50500	50100	49312	47968	45231	40280	32103	19851	7861	2931	981	0	
		V (6):	0	193	385	763	1410	2735	5153	9199	15302	21098	23258	23963	24163	
	.3	D (6):	0			2	7	27	102	379	1411	4374	7924	11684	18340	1.435
		V̇ (5):	15271	15144	15017	14769	14345	13486	11940	9413	5699	2166	761	226	0	
		V (6):	0	643	1280	2536	4673	9018	16831	29538	47752	63543	68549	69768	69898	
	1	D (6):	0		2	6	23	88	336	1230	4492	13551	24115	35121	45333	1.230
		V̇ (5):	50904	50404	49910	48940	47297	43997	38182	29020	16374	5421	1540	261	0	
		V (5):	0	193	382	754	1381	2626	4774	8022	12117	14960	15538		15578	
	3	D (6):	0	1	5	19	67	259	970	3446	11967	33980	58322		78039	0.949
		V̇ (4):	15271	15057	14847	14438	13757	12428	10219	7064	3353	781	101		0	
		V (5):	0	637	1256	2443	4367	7936	13367	20085	26277	28703			28770	
	10	D (6):	0	4	16	63	215	807	2867	9372	28995	73370			97398	0.632
		V̇ (4):	50904	49455	48062	45435	41294	33999	23848	12837	3991	253			0	
		V (5):	0	1872	3618	6780	11439	18807	27541	35259	39647				40132	
	30	D (6):	0	12	47	180	588	2052	6556	18764	50225				88643	0.401
		V̇ (3):	15271	14232	13292	11664	9434	6324	3294	1194	170				0	
		V (5):	0	5816	10573	17897	26386	36110	438'7	48061					48968	
	100	D (6):	0	38	143	510	1509	4547	122'1	30002					64662	0.232
		V̇ (3):	50904	41285	34139	24405	15046	6869	2306	455					0	
		V (5):	0	14564	23417	33709	42203	49042	52783	53889					53899	
	300	D (6):	0	99	345	1085	2797	7203	16988	37403					43367	0.137
		V̇ (2):	15271	8748	5652	2880	1262	399	88	2					0	
		V (5):	0	30518	40988	48842	53364	56088	56984						57012	
	1000	D (6):	0	240	705	1863	4153	9398	20201						26147	0.076
		V̇ (2):	50904	12461	5223	1787	583	128	8						0	
		V (5):	0	44930	52201	56004	57781	58541							58603	
	3000	D (6):	0	416	1044	2429	4966	10518							15899	0.044
		V̇ (1):	15271	1017	285	76	20	2							0	
		V (5):	0	54258	57460	58925	59432								59514	
	9000	D (7):	0	5716	12862	27692	54027								94835	0.026
		V̇ (1):	45813	504	117	25	4								0	
		V (6):	0	97	193	382	705	1364	2561	4546	7516	10345	11436	11827	11989	
1.7	.1	D (7):	0	1	2	9	31	122	469	1731	6412	19799	35857	52921	97502	1.638
		V̇ (6):	83046	82300	81562	80112	77653	72698	63917	49918	30033	11642	4342	1502	0	
		V (6):	0	290	577	1144	2110	4076	7628	13462	22037	29966	32887	33854	34170	
	.3	D (6):	0		1	3	9	37	140	515	1893	5791	10424	15318	25785	1.525
		V̇ (5):	24914	24677	24443	23984	23206	21645	18899	14575	8565	3181	1119	348	0	
		V (6):	0	966	1921	3800	6986	13412	24807	42926	68075	89200	95776	97464	97673	
	1	D (6):	0	1	2	9	31	121	459	1664	5981	17764	31384	45548	61411	1.278
		V̇ (5):	83046	82106	81179	79366	76320	70283	59924	44304	24092	7753	2232	419	0	
		V (5):	0	289	573	1128	2056	3880	6958	11460	16885	20496	21221		21279	
	3	D (5):	0		1	3	9	35	132	460	1565	4361	7427		10100	0.965
		V̇ (4):	24914	24503	24101	23324	22044	19599	15682	10413	4703	1062	145		0	
		V (5):	0	955	1677	3630	6431	11499	18903	27570	35083	37881			37957	
	10	D (5):	0	1	2	9	29	109	380	1213	3652	9067			11948	0.630
		V (4)·	83046	80201	77493	72452	64688	51545	34415	17426	5090	305			0	
		V (5):	0	2792	5357	9908	16414	26200	37099	46108	50917				51407	
	30	D (5):	0	2	6	24	79	269	836	2324	6071				10426	0.395
		V̇ (3):	24914	22860	21046	17997	14017	8867	4309	1461	193				0	
		V (5):	0	8537	15235	25108	35862	47424	55988	60447					61316	
	100	D (6):	0	52	192	672	1940	5667	14882	35525					73475	0.226
		V (3):	83046	64348	51304	34681	20100	8534	2695	498					0	
		V (5):	0	20626	32179	44690	54292	61727	65583	66639					66643	
	300	D (6):	0	134	449	1367	3424	8581	19838	43129					48278	0.133
		V̇ (2):	24914	12805	7748	3670	1526	454	95	2					0	
		V (5):	0	40614	53232	61542	66335	69064	69913						69930	
	1000	D (6):	0	305	866	2225	4863	10833	23058						28706	0.074
		V̇ (2):	83046	16580	6232	2076	643	137	7						0	
		V (5):	0	57276	64994	69046	70809	71537							71587	
	3000	D (6):	0	503	1230	2810	5681	11938							17324	0.043
		V (1):	24914	1224	333	83	21	2							0	
		V (5):	0	67375	70525	71957	72458								72529	
	9000	D (6):	0	666	1476	3148	6108								10285	0.025
		V̇ (1):	74741	543	126	27	4								0	

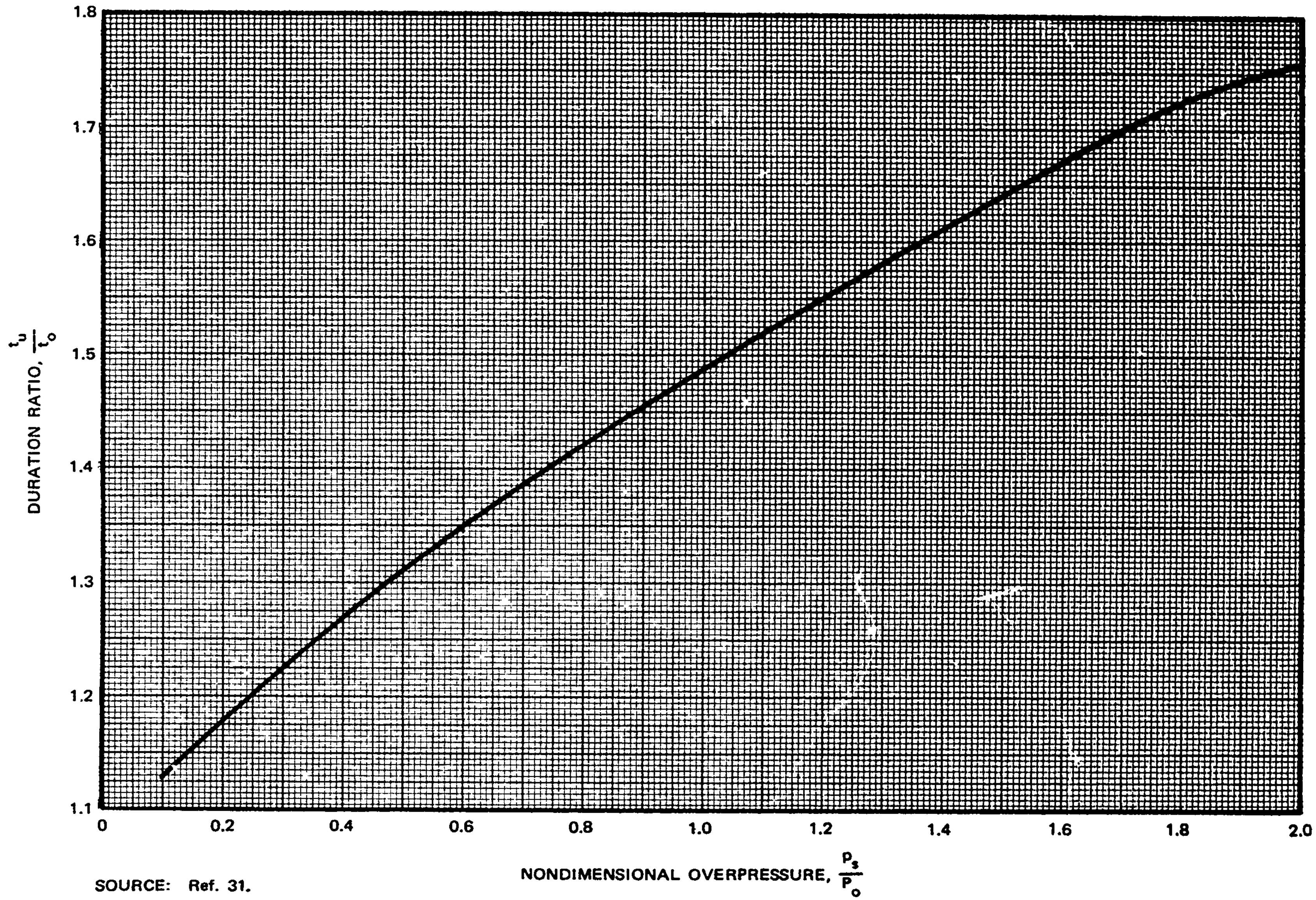

SOURCE: Ref. 31.

FIG. 13 RATIO OF DURATION OF WIND TO POSITIVE PHASE DURATION AS A FUNCTION OF OVERPRESSURE

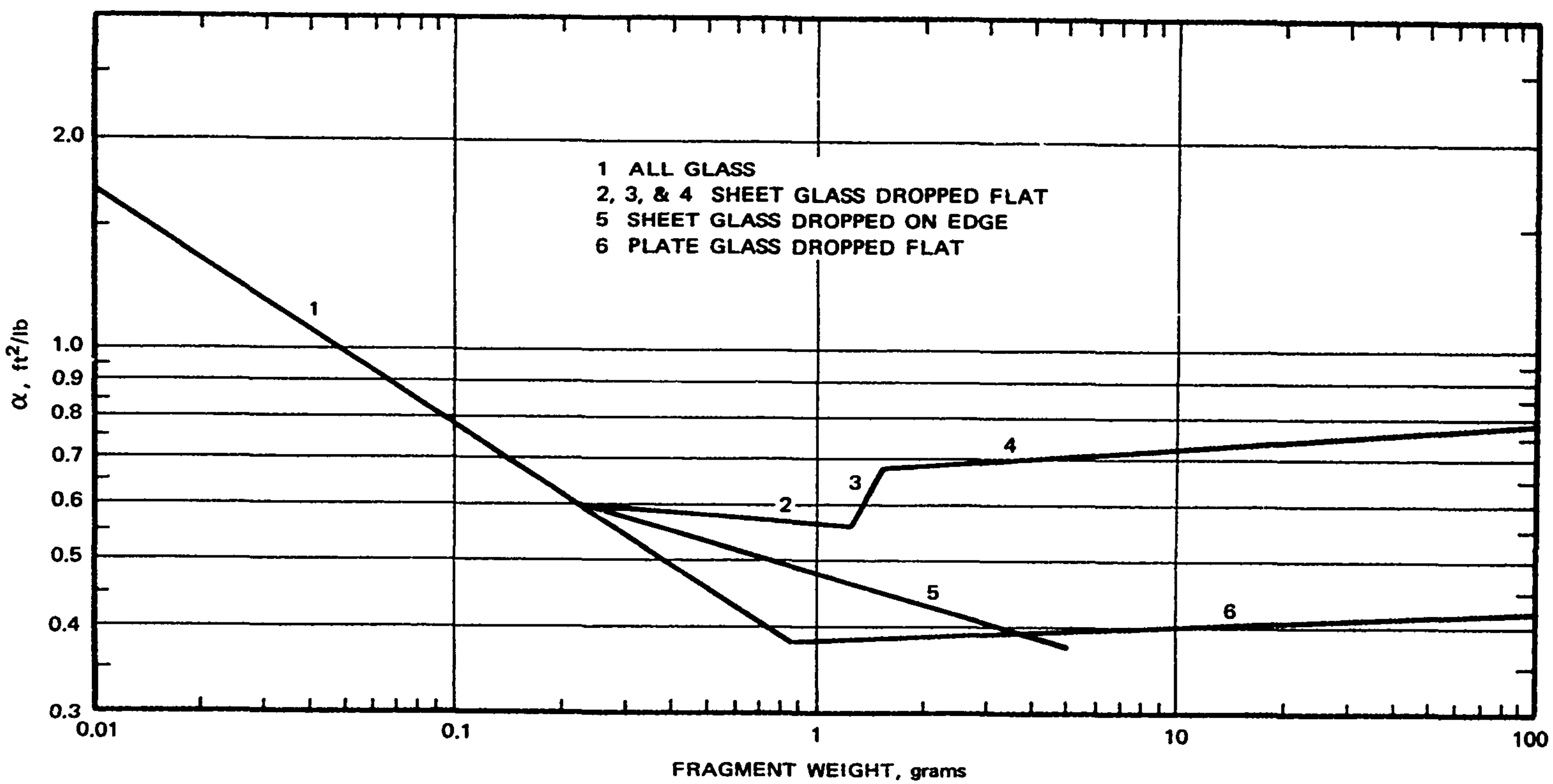

SOURCE: Ref. 32.

FIG. 14 SUMMARY OF ACCELERATION COEFFICIENT DATA FOR GLASS FRAGMENTS which means that the decimal point has been moved six places to the right. Thus, V is actually 0.055677. T_{final} in Table 9 is the time when the missile velocity and the wind velocity become equal.

Figures 15 through 20 were prepared[31] using Table 9. The figures provide maximum velocity and the corresponding travel distance as a function of α for W = 1, 20, and 1,000 kilotons.

To check the validity of the model, glass missiles emanating from windows in house walls that faced ground zero were trapped during the Operation Plumbbob test series. In general, the model predicted velocities lower than those measured in the field. The results of the tests are discussed in the following extracts from the test report.

> Velocities predicted for glass fragments on the basis of a free-field blast wave ignored any possible modification of the wave . . . by the structure containing the window in the case of the house installations. In some instances . . . the modification noted (as signified by missile velocities) was great enough to suggest that velocities also be computed for a blast wave with a duration the same as that for the free-field wave and with a maximum overpressure equal to the reflected overpressure assuming normal incidence of the free-field blast wave. Although this procedure cannot be rigorously defended by theory, its usefulness as an empirical guide in the prediction of missile velocities is apparent, provided, of course, that it conforms with the experimental evidence available.

It also seems possible that the discrepancies between predicted velocity and measured velocity might be a result of the assumption of zero initial velocity.

> It was observed that the steel window frames used in houses . . . were usually slightly bent in the direction of the blast wave. One frame in a house was actually blown free of its mount. . . . It is doubtful that the frames would have been bent if they had not contained glass. Thus one might suppose that defractive (sic) loading contributed not only to fragmentation of the glass but also to the acquisition of an initial velocity by the window panes before fragmentation was complete. . . .

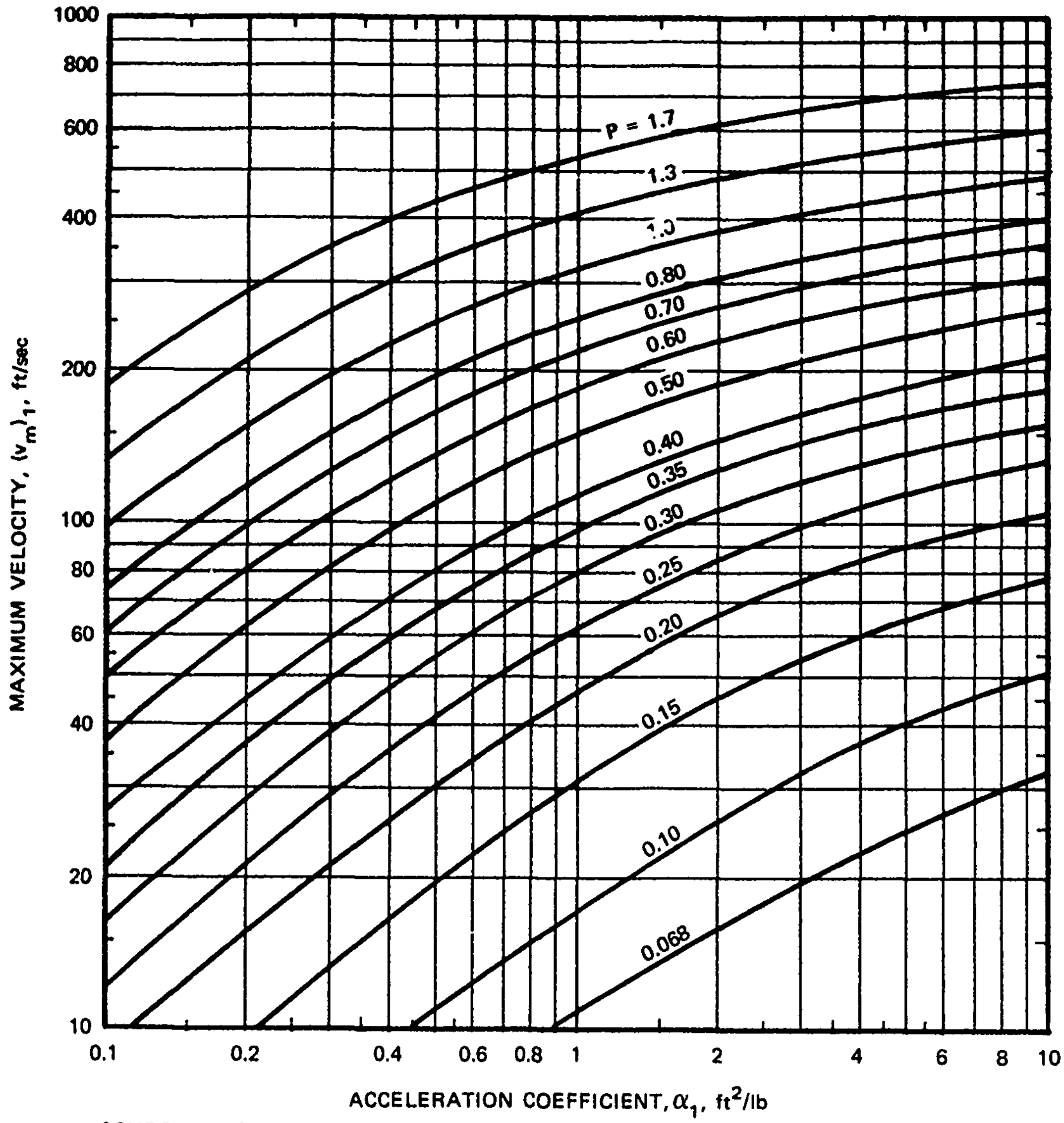

SOURCE: Ref. 31.

FIG. 15 PREDICTED MAXIMUM VELOCITY AS A FUNCTION OF ACCELERATION COEFFICIENT AND NONDIMENSIONAL PEAK OVERPRESSURE

Computed for W = 1 kt, P_o = 14.7 psi, and c_o = 1117 ft/sec

For other conditions, use:

$$\alpha_1 = \alpha\left(\frac{1117}{c_o}\right)^2\left(\frac{P_o}{14.7}\right)^{2/3} W^{1/3}$$

$$v_m = (v_m)_1\left(\frac{c_o}{1117}\right)$$

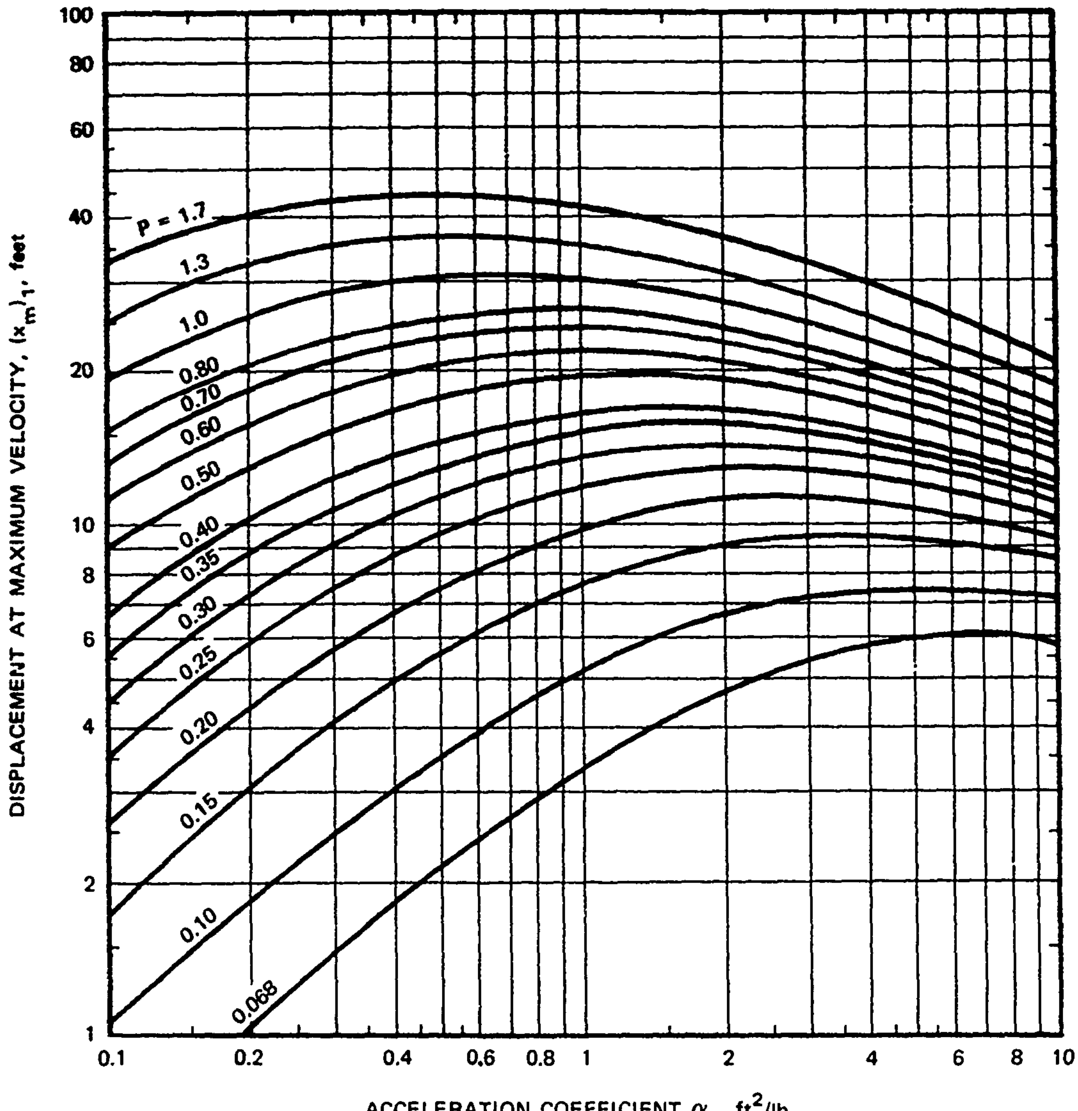

SOURCE: Ref. 31.

FIG. 16 PREDICTED DISPLACEMENT AT MAXIMUM VELOCITY AS A FUNCTION OF ACCELERATION COEFFICIENT AND NONDIMENSIONAL PEAK OVERPRESSURE
Computed for W = 1 kt, P_o = 14.7 psi, and c_o = 1117 ft/sec
For other conditions, use:

$$\alpha_1 = \alpha \left(\frac{1117}{c_o}\right)^2 \left(\frac{P_o}{14.7}\right)^{2/3} W^{1/3}$$

$$x_m = (x_m)_1 \left(\frac{14.7W}{P_o}\right)^{1/3}$$

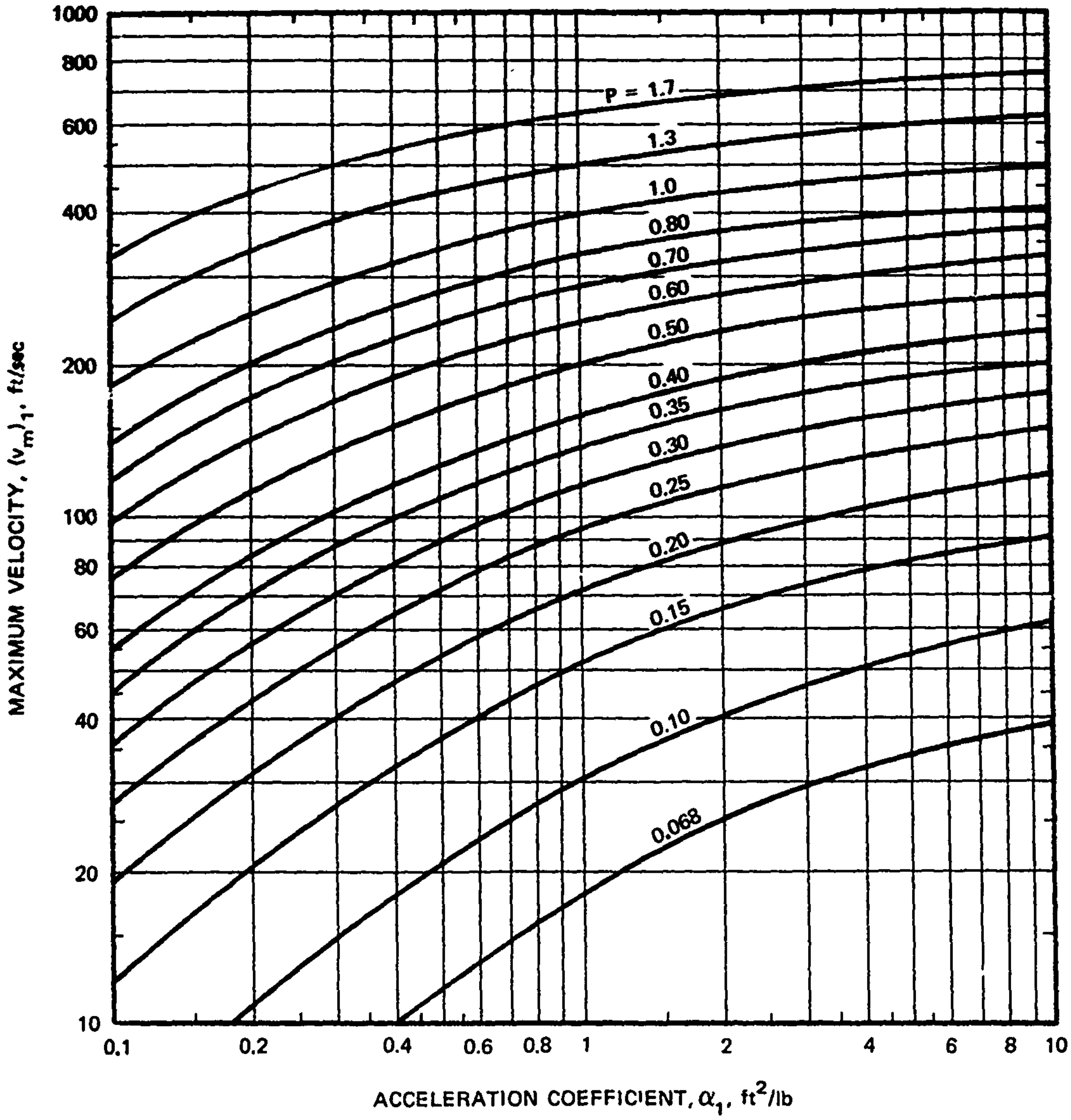

SOURCE: Ref. 31.

FIG. 17 PREDICTED MAXIMUM VELOCITY AS A FUNCTION OF ACCELERATION COEFFICIENT AND NONDIMENSIONAL PEAK OVERPRESSURE

Computed for W = 20 kt, P_o = 14.7 psi, c_o = 1117 ft/sec.

For other conditions, use:

$$\alpha_1 = \alpha\left(\frac{1117}{c_o}\right)^2\left(\frac{P_o}{14.7}\right)^{2/3}\left(\frac{W}{20}\right)^{1/3}$$

$$v_m = (v_m)_1\left(\frac{c_o}{1117}\right)$$

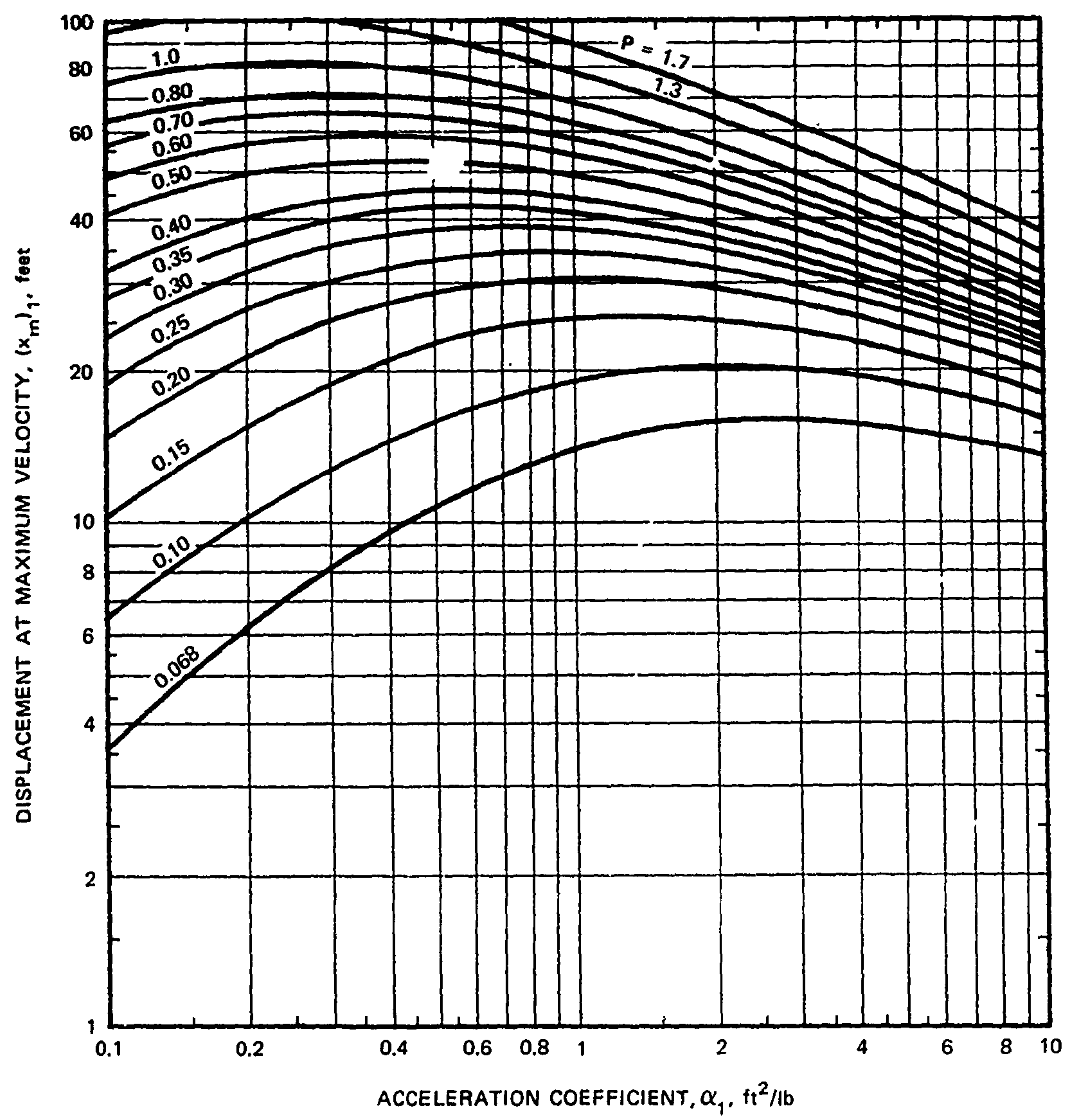

SOURCE: Ref. 31.

FIG. 18 PREDICTED DISPLACEMENT AT MAXIMUM VELOCITY AS A FUNCTION OF ACCELERATION COEFFICIENT AND NONDIMENSIONAL PEAK OVERPRESSURE

Computed for W = 20 kt, P_o = 14.7 psi, and c_o = 1117 ft/sec.

For other conditions, use:

$$\alpha_1 = \alpha\left(\frac{1117}{c_o}\right)^2\left(\frac{P_o}{14.7}\right)^{2/3}\left(\frac{W}{20}\right)^{1/3}$$

$$x_m = (x_m)_1\left(\frac{14.7W}{P_o 20}\right)^{1/3}$$

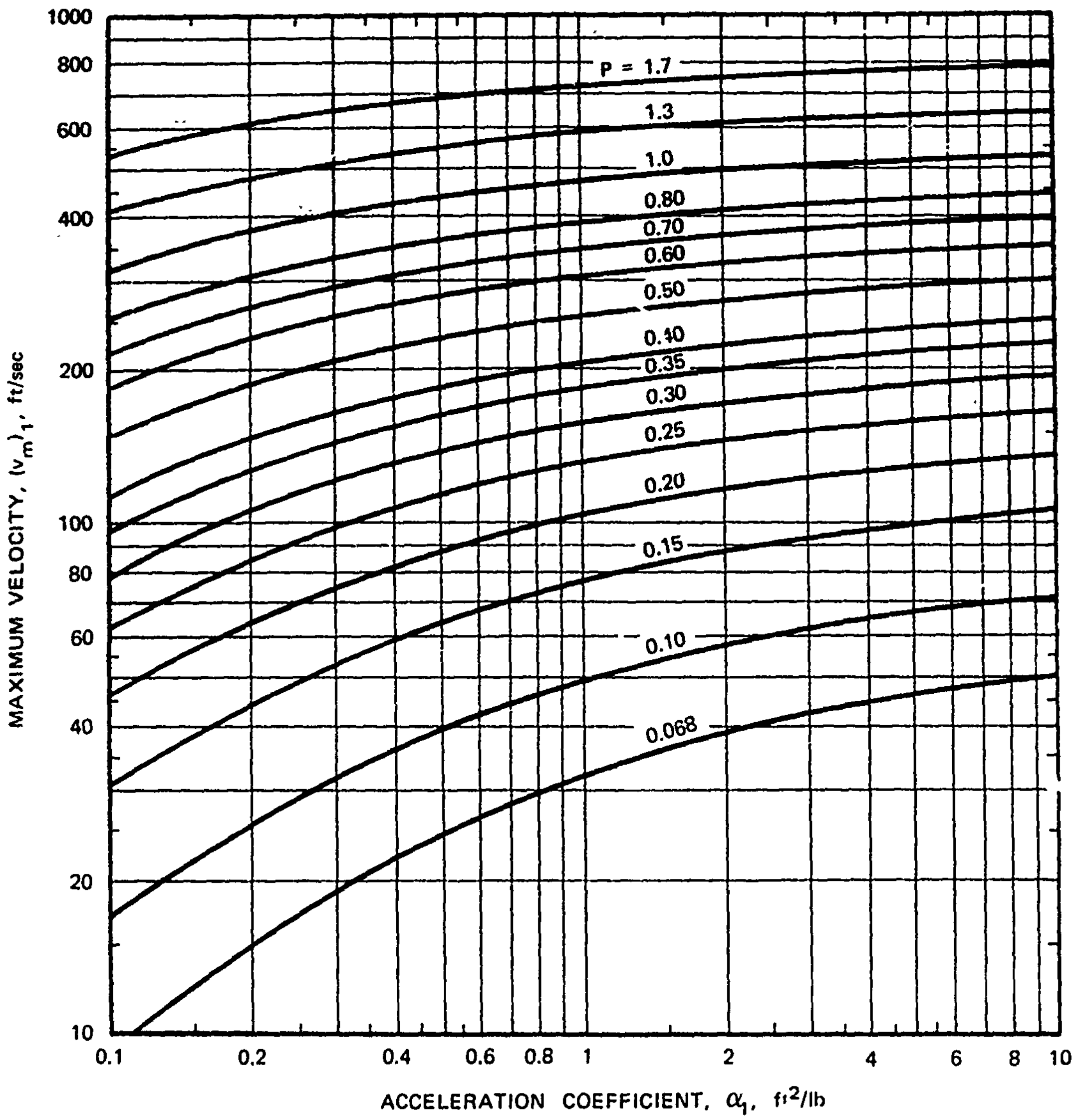

SOURCE: Ref. 31.

FIG. 19 PREDICTED MAXIMUM VELOCITY AS A FUNCTION OF ACCELERATION COEFFICIENT AND NONDIMENSIONAL PEAK OVERPRESSURE

Computed for W = 1 Mt, P_o = 14.7 psi, and c_o = 1117 ft/sec.
For other conditions, use:

$$\alpha_1 = \alpha\left(\frac{1117}{c_o}\right)^2\left(\frac{P_o}{14.7}\right)^{2/3}\left(\frac{W}{1000}\right)^{1/3}$$

$$v_m = (v_m)_1\left(\frac{c_o}{1117}\right)$$

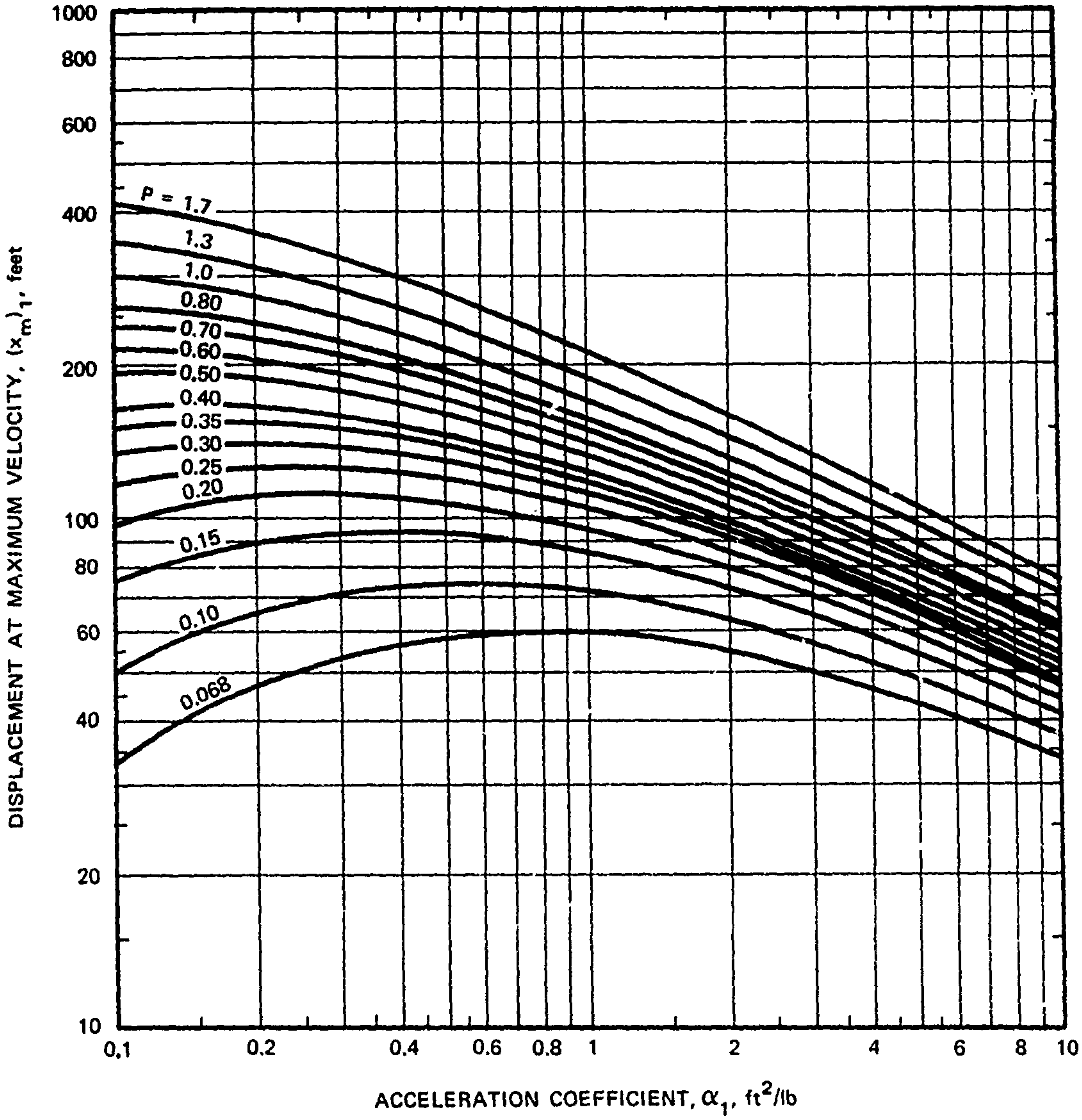

SOURCE: Ref. 31.

FIG. 20 PREDICTED DISPLACEMENT AT MAXIMUM VELOCITY AS A FUNCTION OF ACCELERATION COEFFICIENT AND NONDIMENSIONAL PEAK OVERPRESSURE

Computed for W = 1 Mt, P_o = 14.7 psi, and c_o = 1117 ft/sec

For other conditions, use:

$$\alpha_1 = \alpha\left(\frac{1117}{c_o}\right)^2\left(\frac{P_o}{14.7}\right)^{2/3}\left(\frac{W}{1000}\right)^{1/3}$$

$$x_m = (x_m)_1\left(\frac{14.7W}{P_o\,1000}\right)^{1/3}$$

If a pane supported along its edges is bent, a certain amount of potential and kinetic energy is stored in the pane before actual breakage occurs. Fragments near the center of the pane possessing the greater part of this energy would "pop out" at higher velocities than those near the perimeter. It should be pointed out that the energy thus temporarily stored in each pane is not necessarily derived from the blast winds but is due principally to the sudden increase in pressure existing at the leading edge of a classical blast wave. The defractive (sic) loading effect described above would be enhanced by the process of reflection but would be mitigated provided the blast wave arrived on the lee side of the pane before it shattered. Also, if shattering occurred before appreciable bending had taken place, as might be the case for a relatively strong blast wave, then the defractive (sic) effect would be minimal since the pressure difference between the front and rear of the pane would quickly vanish when the glass is broken.

Further general comments from the test report concerning the glass-fragment data follow:

In comparing the glass-fragment data obtained at all stations, a correspondence was noted between the geometric mean mass of the fragments caught in a trap and the geometric mean velocity. The samples containing the smaller fragments generally were the ones with the higher mean velocities. The variation of acceleration coefficient between small and large glass fragments is not large enough to explain the effect noted. An explanation is quite simple, however, if it is assumed that a relatively strong blast wave not only accelerates the fragments to higher velocities but also fragments the window glass into smaller pieces. . . .

. . . none of the fragments caught in houses impacted with the flat surface against the absorber. . . . Several factors could influence the rotation of a fragment during its travel from the window to the trap. One is missile size - larger fragments have higher moments of inertia and therefore greater resistance to forces tending to cause rotation. Another phenomenon inducing rotation is turbulence of the wind, which is likely to be more pronounced inside houses than in open areas. Still another, but more subtle, phenomenon is the mechanism of breakage of window glass. Results obtained from another study for low (marginal) blast pressures indicate that fragments from the center of the pane break free before those from the perimeter and therefore acquire correspondingly higher velocities. This sequence of events would not only result in an initial torque tending to cause rotation of many of the fragments but would also help explain the rather large variation in velocities measured in individual samples.

The data discussed above are presented in Figure 21. There were four windows, all with 11.5 in. X 23.5 in. panes of double strength glass mounted in steel frames. Three traps were placed behind each of the two windows that contained nine panes each. Four traps were placed behind each of the other two windows, which contained 20 panes each. These data were taken during Shot Galileo at a distance of 4,700 feet where p_{so} was approximately 3.8 psi. The model, using p_{so}, appears to have provided a lower bound for the data; using p_r, but retaining the duration calculation for p_{so}, it appears nearly to have established an upper bound for the data.

It might be noted that the geometric mean weight of the 2,523 fragments trapped was 0.321 grams, while the predicted weight using the data in Figure 11 was 0.580 grams. This difference is considered within the accuracy ranges encountered in this research.

Data were also collected from windows mounted in the open during Operation Plumbbob; however, such data were not considered indicative of glass entering a room and are not presented herein.

In tests conducted since Teapot and Plumbbob,[35] windows in a two-story house were subjected to a 1.2 psi blast wave caused by exploding five tons of TNT. The translation model again predicted velccities lower than those measured. Apparently, the initial velocity of the fragments must be taken into account to increase the accuracy of the model. A modification of the model to predict velocities more accurately at low overpressures is being considered.[35]

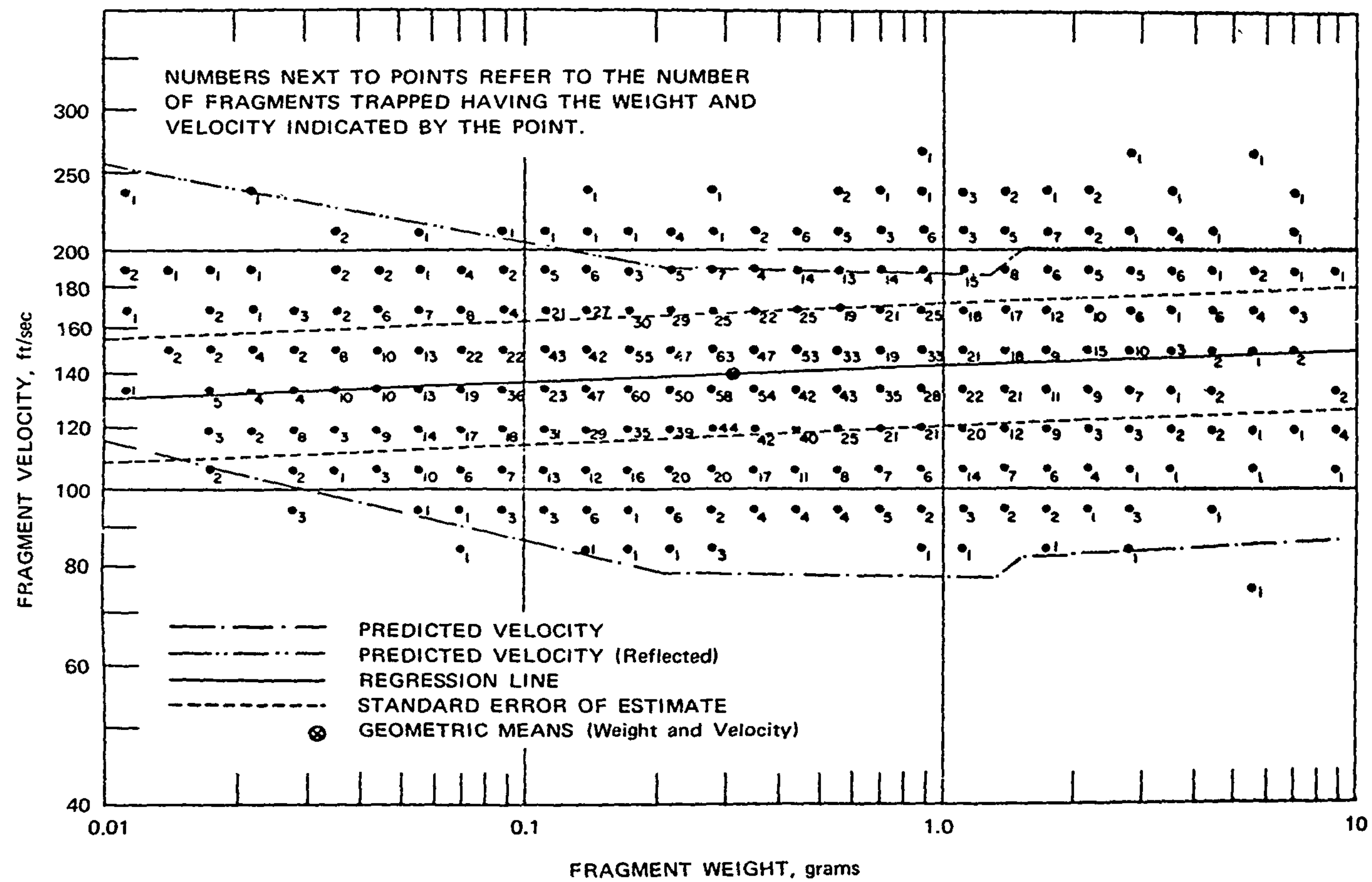

SOURCE: Ref. 33.

FIG. 21 OPERATION PLUMBBOB: ANALYSIS OF WINDOW GLASS FRAGMENTS FROM 14 TRAPS*

*Additional information: windows in house walls which faced ground zero, p_{so} = 3.8 psi, x (average) = 10.3 ft, N = 2523, geometric mean weight = 0.321 grams, geometric mean velocity = 140 ft/sec, all data from two windows with nine 11.5" x 23.5" panes and two windows with twenty 11.5" x 23.5" panes, double strength glass and steel frames.

The following procedure is recommended for estimating fragment velocity:

1. Establish P_o, c_o, p_{so}, p_r, W, t_o, and t_u.

2. Select a fragment weight; M_{50} predicted by Figure 11 is a logical first try.

3. Determine α from Figure 14. The lines depicting window or plate glass dropped flat are recommended.

4. Calculate A using Equation 27.

5. Solve for D(n) using Equation 30 by substituting the desired value for the fragment travel distance, x.

6. If the window is side-on to the blast wave, solve Equation 26 as shown. If the window is facing ground zero, substitute p_r for p_{so} in Equation 26.

7. Enter Table 9 with P, A, and D(n).

8. Read the corresponding V(n).

9. Solve for v using Equation 29.

V BIOLOGICAL CONSIDERATIONS

The effects of glass fragments on people have been observed at Nagasaki, Hiroshima, and at some accidental, nonnuclear explosions in the United States. The purpose of this chapter is to summarize previously accomplished work concerned with predicting the degree of injury to humans exposed to various glass missile situations. Data found in the literature for predicting injury to humans are based on tests conducted during Operations Teapot and Plumbbob[29,33,34] and subsequent work.[30-32] Injury prediction[30] is based on the penetration of glass missiles fired into the abdominal walls of anesthetized dogs. A word of caution was offered: "The authors are unaware of any reliable data which allows the penetration data obtained on dogs to be applied to the human case. However, the use of the penetration criteria for experimental animals to attempt to predict injury to the civilian and military population will underestimate the damaging potential of glass fragments."[30] Nonetheless, these data are presented in Figure 22 and suggested for use until modified by further research.

The weight and velocity data required to use Figure 22 are derived by methods described in Chapters III and IV. Unfortunately, a precise breakdown of deaths or degree of injuries was not found in the literature; however, Figure 22 delineates the probability of serious injuries. ". . . entry of one of the serous cavities of the body or penetration of the eye can be regarded as a serious wound at least because infections almost always occur. . ."[36] A serious wound has also been defined as "a laceration penetrating the skin wherein the missile either was stopped by bone or passed into the tissues to a depth of 10 mm or more."[34]

Preceding page blank

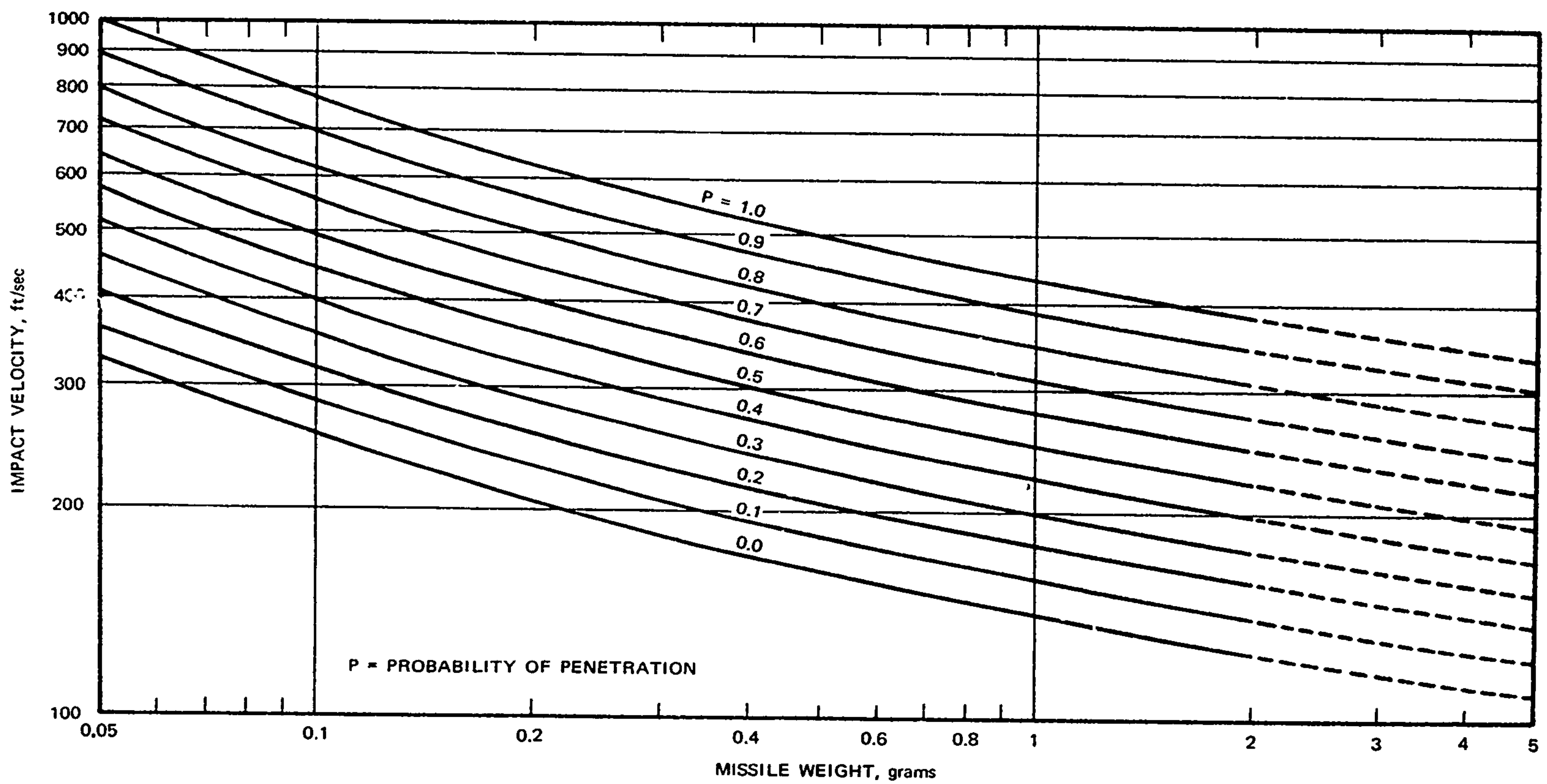

SOURCE: Ref. 30.

FIG. 22 PROBABILITY OF PENETRATION OF GLASS FRAGMENTS INTO THE ABDOMEN OF A DOG AS A FUNCTION OF MISSILE WEIGHT AND IMPACT VELOCITY

The latter quote applies to data taken from full scale field tests in which dogs were stationed approximately 10 feet behind windows exposed to a nuclear explosion.

The number of serious wounds is probably best estimated by using Figure 23. Again from the full scale field test data: ". . . on the average, for every 12 wounds suffered by an animal there was one potentially serious insult . . ."; ". . . in terms of area of the biological target, there were averages of 13.4 total injuries per square foot; the serious injuries numbered about 1.2 per square foot of presented surface area. Assuming a presented area, face-on, for a 160-lb lightly clothed human to be near 6 sq ft in a similar exposure, the above figures might represent a hazard from window glass involving 80 total wounds, of which 7 could be potentially dangerous to life without early surgical care."[34] The preceding quote applies to windows in building walls that faced ground zero, exposed to a free-field overpressure of approximately 2 to 4 psi.

One further set of data,[30,34] widely publicized in the literature, is given in Table 10. The table provides predictions for a 10-gram fragment after ten feet of travel. These data do not seem directly helpful since very few 10-gram fragments were noted in studying the data used to prepare this report.

Table 10

TENTATIVE CRITERIA FOR SECONDARY BLAST EFFECTS

Injury	Impact Velocity (ft/sec)
Skin laceration (threshold)	50
Serious wound	
Threshold	100
50% probability	180
Near 100% probability	300

Source: Reference 36.

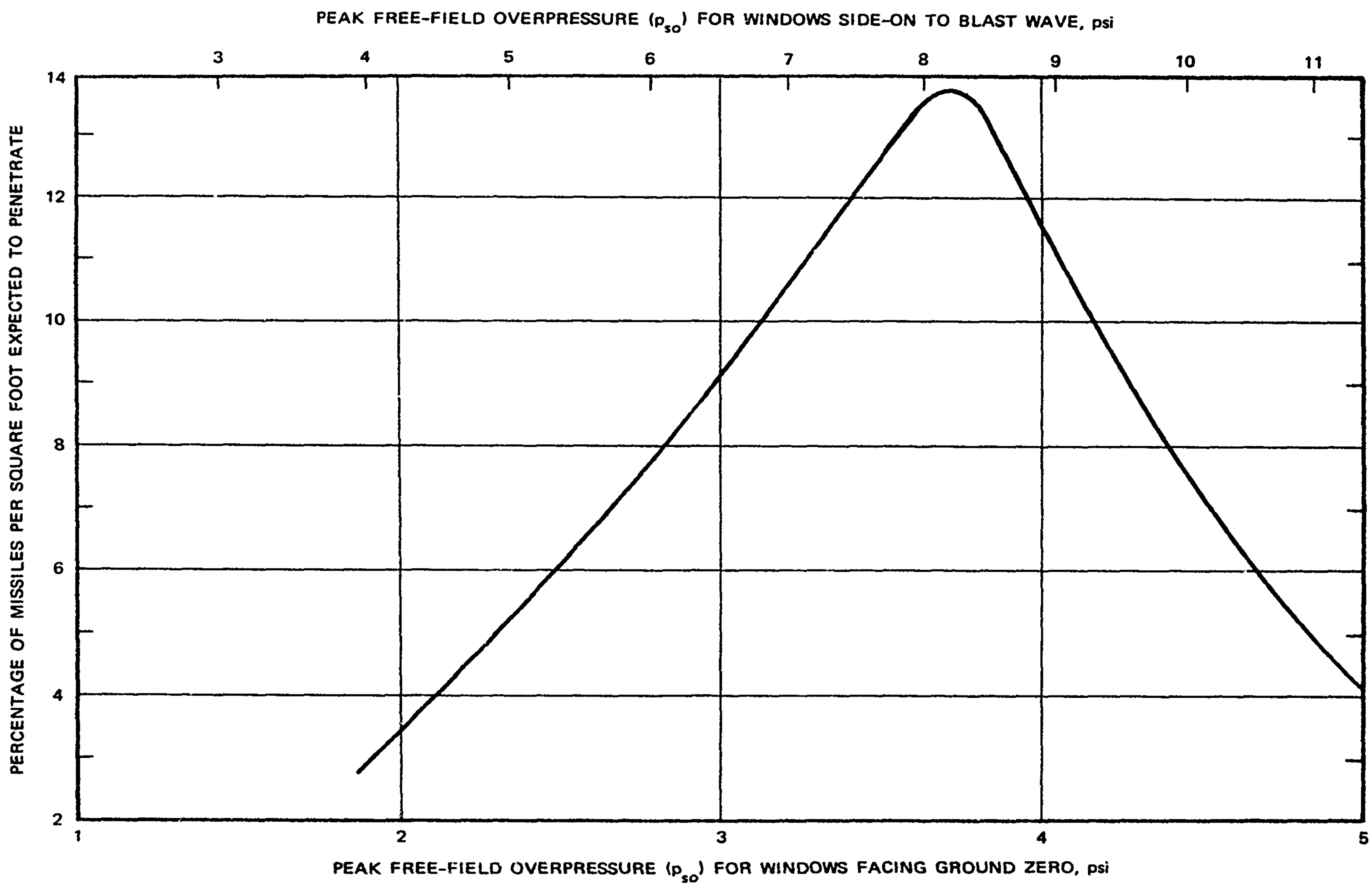

SOURCE: Adapted from Ref. 30.

FIG. 23 EXPECTED FREQUENCY OF PENETRATION AS A FUNCTION OF PEAK OVERPRESSURE*

* Computed for glass missiles occurring about 10 feet behind windows in house walls facing blast. Penetration criterion derived from dog abdomen studies.

The limited information provided by this chapter is intended only to be illustrative, since the subject is beyond the study scope as finally prescribed.

VI RECOMMENDED ADDITIONAL STUDY

Because modulus of rupture testing of glass laths is apparently not an indication of glass pane response to blast loading, further lath testing does not seem beneficial. However, tests conducted on windows in the shock tunnel operated by URS Corporation at Fort Cronkhite, for example, would be extremely helpful. Meaningful velocity, weight, and spatial density data could possibly be obtained by closing the tunnel with a wall containing a window. A second wall completely covered with the same type of Styrofoam used by Lovelace Foundation in its missile traps could be made movable so that the distance between walls could be varied. In the interest of economy, the same tests could be used to study room-filling phenomena. Also, as a better understanding of room-filling is obtained through work currently being done by a colleague, J. R. Rempel, it appears possible that application of the new knowledge to glass fragment translation might be an improvement over the current approach, which involves translation by the winds associated with a "classical" free-field blast wave.

The failure prediction approach presented in Chapter II is based on membrane and bending action at the center of a square plate. Possibly more attention should be given to determining the amount of error inherent in considering rectangular panes as square panes of the same area. This would not be possible without laboratory testing of rectangular panes in the same manner as the tests made by Bowles and Sugarman[16] on square panes. Another reason for further testing including stress-strain testing all the way to failure is that Orr[15] found that the greatest stress was not at the center. Rather it was some distance away along a diagonal,

Preceding page blank

and the membrane action was so pronounced in some cases that both surfaces were placed in tension. Further study of the reports by IITRI[37,38] might also be beneficial. IITRI's method of dividing a panel into a grid system allows for checks of failure stresses at locations other than the center. Tests were performed on hydrostone panels to substantiate this work.

As mentioned previously, the computer program presented in Chapter II is already capable of accepting a peak free-field overpressure as input. The results obtained include values for the velocity of the equivalent single-degree-of-freedom system through to failure. It seems possible that this information could be coordinated with Bowen's translation model to provide better estimates of fragment velocity.

VII APPLICATIONS

The purpose of this chapter is to demonstrate the type of information that can be obtained through the use of procedures presented in this report. Windows to be examined were selected from the 55 structures in the Research Triangle Institute (RTI) San Jose sample[39] of NFSS buildings. Buildings selected for analysis were limited to those with windows in shelter areas on floors above grade. If there were interior walls between windows and designated shelter areas, the windows were excluded from consideration. Buildings with windows meeting these criteria were chosen by studying the RTI report, copies of the original Phase II NFSS Data Collection Forms, and copies of the shelter location sketches required for each shelter space in the NFSS.

Out of the buildings that met the criteria, 14 were chosen for use in this chapter. The data collected for one window from each of the 14 buildings are presented in Table 11. Opening and pane sizes were determined from actual measurements or by scaling from photographs of the buildings. Pane thicknesses were determined by the method described in the footnote on page A-2 of this report.

Predictions of incipient failure overpressures are presented in Table 12 for each of the 14 windows. All of the glass in the 14 windows was found to be sheet glass, thus predictions were made using Figures 9 and 10. The pane area used to predict the incipient failure overpressure for a multipane window was determined from the apparent strength of the window frame. If a frame appeared strong, the area of the largest pane in the window was chosen since the largest pane among panes of equal thickness would fail at the lowest overpressure. If a frame seemed

Table 11

WINDOW FIELD DATA

RTI Bldg. Number*	Building Name and Address	Wall†	Floor	Opening Size, Width × Height (in.)‡	Window Frame Type and Material	Number of Panes per Window	Total Glass Area per Window (ft^2)	Pane Thickness (in.)§	Number of Similar Windows on this Floor and Wall
1	S.C. County Welfare Building 55 West Younger Ave. San Jose	C	2	30 × 74	Fixed glass, aluminum	1	12.4	3/16	61
8	De Anza Hotel 233 West Santa Clara St. San Jose	A	3	46 × 72	Double-hung wood	2	15.7	SS	10
10	S.C. County Court House 161 North 1st Street San Jose	D	1	54 × 114	Double-hung wood	2	32.9	1/4	8
12	San Jose State Library 4th & San Fernando San Jose	B	1	32.5 × 71	Projected aluminum	3	12.3	DS	39
15	San Jose Medical & Dental Bldg. 6th & Santa Clara San Jose	A	8	38.5 × 72	Double-hung wood	2	15.3	SS	13
16	Commercial Building 18-28 North 1st Street San Jose	A	2	39 × 72	Double-hung wood	2	14.4	SS	12
27	McLaughlin Hall University of Santa Clara Santa Clara	C	1	72 × 64	Casement, outswing, fixed center panes, steel	15	26.1	DS	15
28	Men's Residence Hall University of Santa Clara Santa Clara	A	2	71 × 62	Fixed center pane, 2 projected panes, movable vent, aluminum	9	17.7	DS	12

Table 11 (concluded)

RTI Bldg. Number*	Building Name and Address	Wall†	Floor	Opening Size, Width × Height (in.)	Window Frame Type and Material	Number of Panes per Window	Total Glass Area per Window (ft^2)	Pane Thickness (in.)§	Number of Similar Windows on this Floor and Wall
35	Stern Hall Unit #5 Stanford University Palo Alto	D	2	57 × 75	Projected steel	6	24.3	DS	11
38	Stauffer Building (Organic Chemistry Research) Stanford University, Palo Alto	C	1	118 × 90	Fixed steel	5	65.0	3/16	12
39	Escondido Village, Bldg #135 Stanford University, Palo Alto	C	6	64 × 96	Fixed aluminum	2	36.2	DS	4
43	Bldg #5A, Admissions & Treatment V.A. Hospital Palo Alto	D	2	42 × 74	Double-hung steel	2	17.5	DS	11
44	Stern Hall Unit #8 Stanford University, Palo Alto	B	2	57 × 75	Projected steel	6	24.3	DS	11
48	Law School Library Stanford University, Palo Alto	A	1	55.5 × 108	Double-hung wood	2	31.3	DS	16

* Numbers from one to 55 were assigned to selected NFSS buildings in the RTI survey.

† Letters, A, B, C, and D are used as in the NFSS to designate the four sides of a building: A is the address side; B, C, and D continue clockwise from A.

‡ If more than one size window was found in a wall, only the size occurring most often was reported.

§ SS was used for single strength and DS for double strength.

Table 12

INCIPIENT FAILURE OVERPRESSURE PREDICTIONS

RTI Bldg. Number	Wall	Floor	Incipient Failure, Free-Field Overpressure (psi) Front Facing*	Side Facing*	Remarks
1	C	2	0.4	0.7	Pane area of 12.4 ft^2 was used.
8	A	3	0.2	0.4	Pane area of 7.8 ft^2 was used.
10	D	1	0.4	0.8	Pane area of 16.4 ft^2 was used.
12	B	1	0.4	0.8	Frame appeared adequate; area of largest pane, 6.9 ft^2, was used.
15	A	8	0.2	0.4	Pane area of 7.6 ft^2 was used.
16	A	2	0.2	0.5	Pane area of 7.2 ft^2 was used.
27	C	1	0.3	0.6	Horizontal frame members considered weak; center 5 panes were treated as one 9.5 ft^2 pane.
28	A	2	0.4	0.7	Frame appeared adequate; area of largest pane, 7.3 ft^2, was used.
35	D	2	0.2	0.3	Cross members in projected portion considered weak; the 4 panes in the projected portion were considered as one 16.0 ft^2 pane.
38	C	1	0.2	0.3	Frame appeared adequate; area of largest pane, 29.2 ft^2, was used.
39	C	6	0.2	0.3	Pane area of 18.1 ft^2 was used.
43	D	2	0.3	0.6	Pane area of 8.7 ft^2 was used.
44	B	2	0.2	0.3	Cross members in projected portion considered weak; the 4 panes in the projected portion were considered as one 16.0 ft^2 pane.
48	A	1	0.2	0.3	Pane area of 15.7 ft^2 was used.

* Front facing refers to windows in a wall facing an approaching air blast wave; side facing refers to windows in a wall side-on to an approaching air blast wave.

weak, the areas of small panes adjacent to the weak members were added. This approach may be an overcompensation for the contribution to failure provided by the flexibility of thin muntins. Nevertheless, this approach is recommended until tests are performed that indicate a better method for obtaining the degree of strength reduction resulting from weak frame members.

Three peak overpressures, 2.0, 3.0, and 5.0 psi, which are within the range of available nuclear test data on glass, were selected to demonstrate the estimation of the following fragment characteristics: geometric mean weight, average weight, velocity, number produced, and spatial density.

The nuclear test data presented in Chapter III led to predictions of fragment weights for single and double strength window glass. Since three of the 14 windows are thicker than double strength glass, an extrapolation procedure was required. First, fragment weights for single and double strength glass were recorded in Table 13 using information obtained from Figure 11. It was noted that fragment weights appeared insensitive to thickness at p_{so} = 5.0 psi; therefore, the average and geometric mean fragment weights for double strength glass were used for both 3/16-in. and 1/4-in. thicknesses. Second, at 2.0 psi, the geometric mean fragment weight increased by a factor of 2.76 and the average fragment weight increased by a factor of 1.91 from single to double strength. Because direct use of these factors would have led to an inconsistent situation of geometric mean fragment weight larger than average fragment weight, a single value of 2.3 (the average of the 2.76 and 1.91 factors) was adopted for use in scaling up both geometric mean and average fragment weights. The 2.3 factor was applied in equal steps to thicknesses greater than double strength, because the progression of thickness ratios is so nearly constant, namely double strength to single strength, or 1/8 to 3/32 (ratio 1.33), 3/16 to 1/8 (ratio 1.5), and 1/4 to 3/16 (ratio 1.33):

Table 13

FRAGMENT WEIGHT AND VELOCITY PREDICTIONS
FOR OVERPRESSURES ABOVE INCIPIENT FAILURE

	Free-Field Overpressure (psi)		Geometric Mean Fragment Weight	Average Fragment Weight	Velocity of Geometric Mean Weight Fragment After
	Front Facing	Side Facing	M_{50}, (gm)	$\overline{M}$, (gm)	10 Feet of Travel (fps)*
Single strength	2.0	4.2	0.67	1.27	87
	3.0	6.5	0.48	0.93	132
	5.0	11.4	0.12	0.24	238
Double strength	2.0	4.2	1.85	2.43	92
	3.0	6.5	1.07	1.63	130
	5.0	11.4	0.14	0.28	234
3/16-in. sheet	2.0	4.2	4.3	5.6	93
	3.0	6.5	2.1	3.3	138
	5.0	11.4	0.14	0.28	234
1/4-in. sheet	2.0	4.2	9.8	13.0	94
	3.0	6.5	4.2	6.6	139
	5.0	11.4	0.14	0.28	234

* Velocities are given for a weapon yield of 1 Mt, ambient atmospheric pressures of 14.7 psi, speed of sound in undisturbed air of 1,126 fps, and α based on "dropped flat" curve in Figure 14. Linear interpolation was used in Table 9.

M_{50} for 3/16" = 1.85 grams X 2.3 = 4.3 grams

M_{50} for 1/4" = 1.85 grams X 2.3 X 2.3 = 9.8 grams

$\bar{M}$ for 3/16" = 2.43 grams X 2.3 = 5.6 grams

$\bar{M}$ for 1/4" = 2.43 grams X 2.3 X 2.3 = 13 grams.

An identical procedure, resulting in an average multiplying factor of 2.0, was used for the fragment weights at 3.0 psi. The results are recorded in Table 13. No nuclear test data were available to substantiate the above procedure; however, the procedure is suggested for use until test data become available.

The results of velocity calculations, which are recorded in Table 13, were based on the geometric mean fragment weight since that weight is the most likely to occur. Each velocity was calculated assuming the fragment had traveled 10 feet from the window; however, any distance could have been selected. Other assumptions are shown in the footnote accompanying Table 13. An example of a velocity calculation using the single strength glass data at p_{so} = 2.0 psi and following the steps at the end of Chapter IV, is:

1. The velocity was calculated first for a front-facing window with P_o = 14.7 psi, c_o = 1,126 fps, p_{so} = 2.0 psi, p_r = 4.2 psi (Equation 12), W = 1 Mt = 1,000 kt, and t_o = 3.821 sec (Equation 19). A value of t_u/t_o = 1.145 was obtained by entering Figure 13 with p_{so}/P_o = 2.0/14.7 = 0.136; hence t_u = 4.375 sec.

2. The fragment weight used was M_{50} = 0.67 grams (Table 13).

3. A value of α = 0.57 ft^2/lb was obtained by entering Figure 14 with the selected fragment weight.

4. Using Equation 27,

$$A = \frac{\alpha P_o t_u g}{c_o} = \left(0.57\ \frac{ft^2}{lb}\right)\left(14.7\ \frac{lb}{in^2}\right)(4.375\ sec)$$

$$\left(386\ \frac{in}{sec^2}\right)\left(\frac{1}{1126}\ \frac{sec}{ft}\right)\left(12\ \frac{in}{ft}\right)$$

$$A = 151$$

5. A value of n = 6 was chosen because D(6) is given in Table 9 for values of interest in this example:

$$D(6) = \frac{10\ ft}{4.375\ sec \times 1126\ ft/sec} \times 10^6 = 2030\ .$$

6. Since the window is facing ground zero,

$$P = \frac{p_r}{P_o} = \frac{4.2\ psi}{14.7\ psi} = 0.286\ .$$

7. From Table 9 using linear interpolation when required:

	P	A	D(6)	V(6)	Interpolating Between
a	0.25	100	1809	59,733	
b	"	"	5419	80,440	
c	"	"	2030	61,001	a & b
d	"	300	1231	78,740	
e	"	"	3559	102,300	
f	"	"	2030	86,826	d & e
g	0.30	100	726	51,990	
h	"	"	2369	78,110	
i	"	"	2030	72,721	g & h
j	"	300	1584	100,690	
k	"	"	4456	127,070	
l	"	"	2030	104,787	j & k
m	0.286	100	"	69,439	c & i
n	"	300	"	99,758	f & l
o	"	151	"	77,170	m & n

8. V(6) = 77,170 from step 7.

9. Using Equation 29, $v = 77{,}170 \times 1126\ fps \times 10^{-6} = 87\ fps$.

The above procedure was repeated for a side-facing window with p_{so} = 4.2 psi. Only values that changed from the previous example are shown below.

1. p_{so} = 4.2 psi, p_r is not applicable, and t_o = 3.298 sec (Equation 19). A value of t_u/t_o = 1.220 was obtained by entering Figure 13 with p_{so}/P_o = 4.2/14.7 = 0.286; hence t_u = 4.024 sec.

2. Same as front facing.

3. Same as front facing.

4. A = 139 (slight difference due to change in t_u).

5. D(6) = 2207 (slight difference due to change in t_u).

6. Since window is side-facing,

$$P = \frac{p_{so}}{P_o} = \frac{4.2 \text{ psi}}{14.7 \text{ psi}} = 0.286 \ .$$

   Note that the numerical result is the same as for the front-facing example.

7. Again a linear interpolation solution similar to the one given above for the front-facing example was used.

8. V(6) = 77,537 from step 7.

9. v = 87 fps, using Equation 29.

The above calculations demonstrate that velocity is insensitive to small changes in the duration of the winds (t_u). This conclusion was found to be true for the other velocities reported in Table 13 as well.

The spatial density of fragments at the window (N_0) was calculated for each of the 14 windows using Equation 24. Figure 12 was used to obtain the spatial density 10 feet from each window (N_{10}). These values are presented in Table 14.

Table 14

PREDICTIONS OF SPATIAL DENSITY AND NUMBER OF FRAGMENTS FOR OVERPRESSURES ABOVE INCIPIENT FAILURE

RTI Bldg. Number	Wall	Floor	Free-Field Overpressure (psi)		Number of Fragments Produced, N	Spatial Density of Fragments (fragments/ft^2)	
			Front Facing	Side Facing		At Window, N_0	10 Feet from Window, N_{10}
1	C	2	2.0	4.2	2,440	197	5.91
			3.0	6.5	4,140	334	35.7
			5.0	11.4	48,800	3,940	422
8	A	3	2.0	4.2	6,750	430	12.9
			3.0	6.5	9,230	588	62.9
			5.0	11.4	35,800	2,280	244
10	D	1	2.0	4.2	3,720	113	3.39
			3.0	6.5	7,340	223	23.9
			5.0	11.4	173,000	5,250	562
12	B	1	2.0	4.2	3,710	302	9.07
			3.0	6.5	5,550	451	48.2
			5.0	11.4	32,200	2,620	281
15	A	8	2.0	4.2	6,580	430	12.9
			3.0	6.5	9,000	588	62.9
			5.0	11.4	34,900	2,280	244
16	A	2	2.0	4.2	6,190	430	12.9
			3.0	6.5	8,470	588	62.9
			5.0	11.4	32,800	2,280	244
27	C	1	2.0	4.2	7,880	302	9.07
			3.0	6.5	11,800	451	48.2
			5.0	11.4	68,400	2,620	281
28	A	2	2.0	4.2	5,340	302	9.07
			3.0	6.5	7,980	451	48.2
			5.0	11.4	46,400	2,620	281

Table 14 (concluded)

RTI Bldg. Number	Wall	Floor	Free-Field Overpressure (psi) Front Facing	Side Facing	Number of Fragments Produced, N	Spatial Density of Fragments (fragments/ft^2) At Window, N_0	10 Feet from Window, N_{10}
35	D	2	2.0	4.2	7,340	302	9.07
			3.0	6.5	11,000	451	48.2
			5.0	11.4	63,700	2,620	281
38	C	1	2.0	4.2	12,800	197	5.91
			3.0	6.5	21,700	334	35.7
			5.0	11.4	256,000	3,940	422
39	C	6	2.0	4.2	10,900	302	9.07
			3.0	6.5	16,300	451	48.2
			5.0	11.4	94,800	2,620	281
43	D	2	2.0	4.2	5,280	302	9.07
			3.0	6.5	7,890	451	48.2
			5.0	11.4	45,800	2,620	281
44	B	2	2.0	4.2	7,340	302	9.07
			3.0	6.5	11,000	451	48.2
			5.0	11.4	63,700	2,620	281
48	A	1	2.0	4.2	9,450	302	9.07
			3.0	6.5	14,100	451	48.2
			5.0	11.4	82,000	2,620	281

The total number of fragments (N) emanating from each window, calculated by multiplying N_0 by the total glass area of a window, is also given in Table 14.

Appendix A

GLASS SELECTION PROCEDURE

Appendix A

GLASS SELECTION PROCEDURE

The usual situation in design would be a knowledge of the size, a X b, of the glass required and the location of the building. Building codes take over at this point and dictate the minimum thickness of glass required. Sheet glass is selected where surface quality is not paramount while plate glass is used where high surface quality is desired, such as for display windows.

Figure A-1 is used in the first design step to determine the resultant wind pressure for the particular locality. This information is used to enter Table A-1 to obtain the wind pressure in the height zone of the window above grade. The required thickness of either sheet or plate glass can then be found in Table A-2.

If the thickness of an existing window is not known but must be estimated to determine air blast response, the above procedure or the local building code can be used to obtain the minimum allowable thickness, which may be considered the most likely thickness used. If either side of an installed window pane is accessible, the thickness may be simply measured by light refraction.*

* An FHA Glass Thickness Gage, a two-inch by four-inch plastic card, was used to make glass thickness measurements for use in the applications chapter of this report. The card contains several lines corresponding to various glass thicknesses. Reflections of these lines from both glass surfaces readily indicate the glass thickness when the card is held at an angle of 45 degrees to the pane.

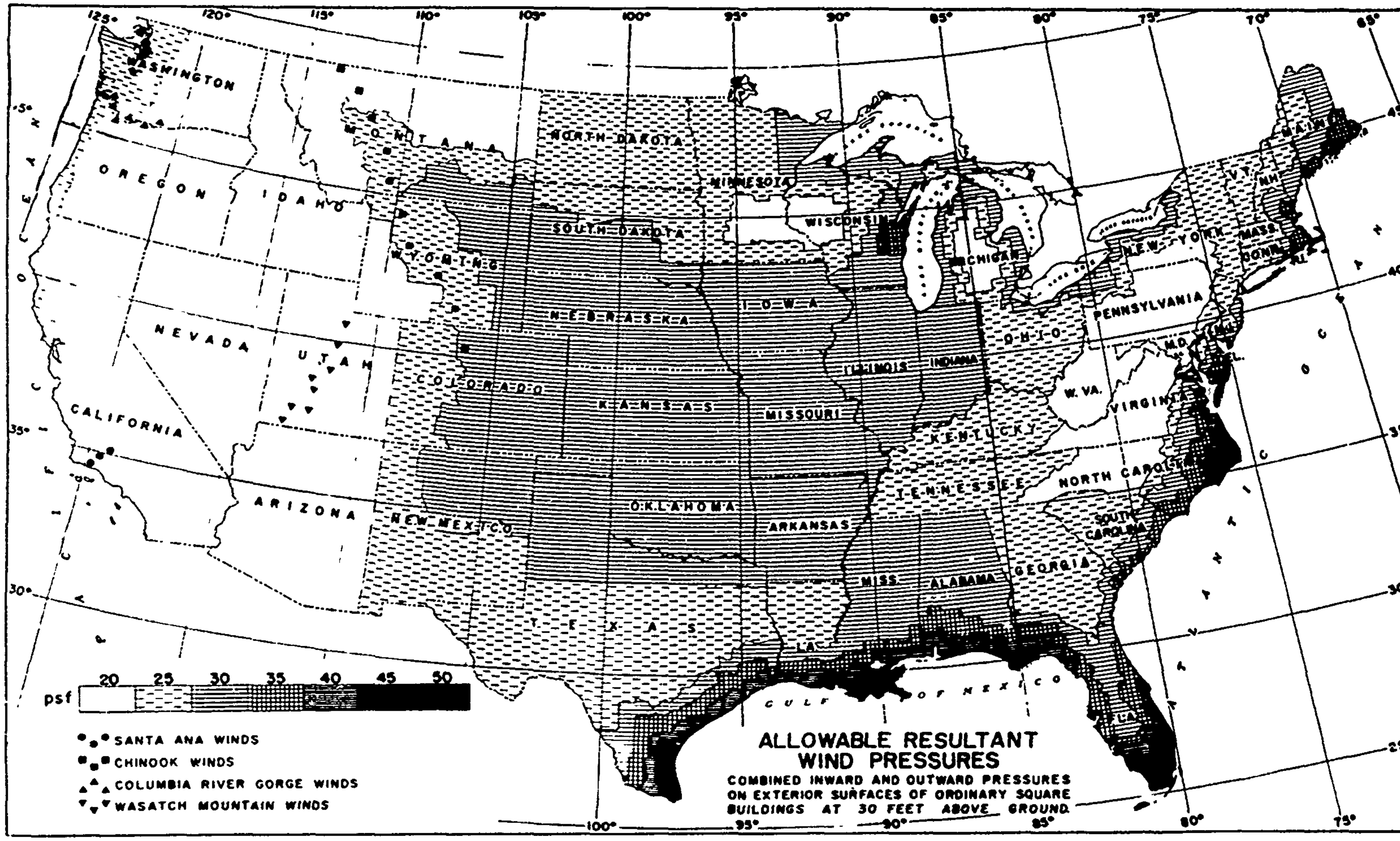

SOURCE: Reprinted through the courtesy of the International Conference of Building Officials (Ref. 28).

FIG. A-1 ALLOWABLE RESULTANT WIND PRESSURES

Table A-1

WIND PRESSURES AT VARIOUS ELEVATIONS ABOVE GRADE

Pressure from Figure A-1				20	25	30	35	40	45	50
Related pressure (psf) in various height zones:										
0-29	feet	above	grade	15	20	25	25	30	35	40
30-49	"	"	"	20	25	30	35	40	45	50
50-99	"	"	"	25	30	40	45	50	55	60
100-499	"	"	"	30	40	45	55	60	70	75
500-1199	"	"	"	35	45	55	60	70	80	90
1200 and over	"	"	"	40	50	60	70	80	90	100

Source: Reprinted through the courtesy of the International Conference of Building Officials (Reference 28).

Table A-2

MAXIMUM ALLOWABLE AREA OF GLASS*
(Square Feet)

Wind Load	Thickness (in.)										
(lb/ft^2)	SS	DS	3/16	7/32	13/64	1/4	5/16	3/8	1/2	5/8	3/4
10	25	37	72	84	72	114	156	198	270	365	465
15	16	25	48	58	48	72	104	131	192	260	330
20	12	19	36	43	36	54	78	98	144	195	245
25	10	15	29	35	29	43	62	78	115	156	195
30	8	12	24	29	24	36	52	65	96	130	165
35	7	11	21	25	21	31	45	56	82	112	140
40	6	9	18	22	18	27	39	49	72	98	124
45	5	8	16	19	16	24	35	44	64	87	110
50	4	7	14	17	14	22	31	39	58	78	98
60	--	6	12	15	12	18	25	32	48	65	81
70	--	--	10	12	10	15	22	28	40	55	70
80	--	--	9	11	9	13	19	24	35	47	61
90	--	--	8	9	8	12	17	22	32	42	55
100	--	--	7	8	7	11	16	20	29	39	50

* Maximum areas apply for rectangular lights of annealed glass firmly supported on all four sides in a vertical position. Glass mounted at a slope not to exceed one horizontal to five verticals may be considered vertical. Maximum areas based on minimum thicknesses set forth in Table No. 54-1-A, Volume III, U.B.C. Standard No. 54-1-67.

Source: Reprinted through the courtesy of the International Conference of Building Officials (Reference 28).

Appendix B

COMMON WINDOW TYPES AND SIZES

Appendix B

COMMON WINDOW TYPES AND SIZES

Single or double strength panes approximately 10" X 20" mounted in wood sash are typical of window installations used in houses today. Picture windows have panes as large as 110" X 80" and 7/32" or 1/4" thick. A common pane size for schools is 16" X 44" with a thickness of 3/16".[3]

Figure B-1 shows some of the common window types. The following list provides the standard sizes and types of windows used today.[40] An average pane size is indicated in some cases.

a. Aluminum casement windows

Commercial: height 2'9" to 8'1"; width 1'8-7/8" to 6'8-7/8"

Residential: height 2'2" to 5'3"; width 1'7-1/8" to 5'9-3/8"

b. Aluminum projected windows

Commercial: height 1'5" to 8'1"; width 2'0-7/8" to 4'0-7/8"

Residential: height 1'7-1/8" to 5'9-3/8"; width 2'2" to 4'2-5/8"

Approximate average size of glass: 12" X 32".

c. Steel casement windows

Residential: height 2'2" to 5'3"; width 1'7-1/8" to 7'7-3/8"

Approximate average size of glass: 10" X 16".

d. Steel commercial projected windows

Commercial: height 2'9" to 9'5"; width 1'8-7/8" to 6'8-7/8"

Approximate average size of glass: 14" X 18".

e. Double-hung wood windows (all applications)

Height 2'6" to 6'6"; width 1'4" to 4'4"; glass about 20" X 20"

f. Picture winaows are made to sizes desired, as limited by building codes.

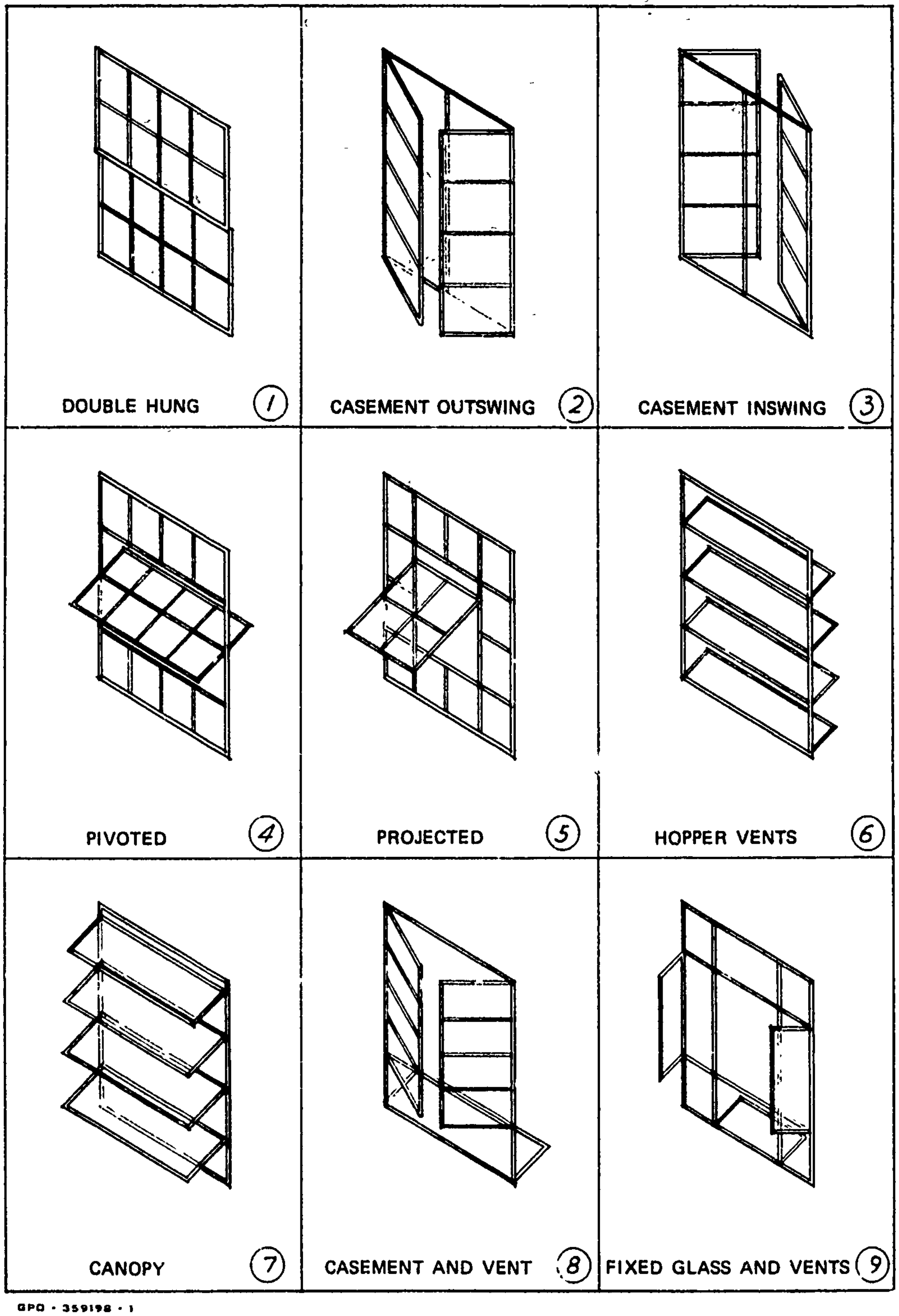

SOURCE: Ref. 41.

FIG. B-1 COMMON WINDOW TYPES

Appendix C

MODULUS OF RUPTURE DATA

Appendix C

MODULUS OF RUPTURE DATA

Tests to determine the modulus of rupture, σ_r, of plate glass have been made by the National Bureau of Standards.[12,42] The tests were performed on soda-lime-silica plate glass in varying conditions of anneal with as-cut edges. The test laths were all 10" X 1-1/2" X 1/4", the loading rate was 10,000 psi per minute, and the test temperature was 75°F. In an attempt to account for scratches, surface deterioration, and age, the surface of some of the laths was abraded by sand blasting. Results of the tests are shown in Table C-1. A sketch of the test loading arrangement is shown in Figure C-1.

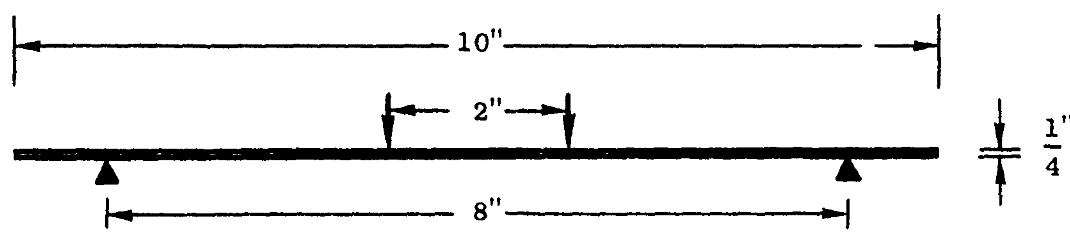

FIG. C-1 DIAGRAM OF TEST METHOD

Source: Reference 12.

A summary of the data presented in Table C-1 is given in Table C-2 for the purpose of having one value of the modulus of rupture, its standard deviation, and its coefficient of variation for each of the various conditions of anneal and abrasion.

Preceding page blank

Table C-1

MODULUS OF RUPTURE TESTS ON PLATE GLASS*

Type†	Condition of Anneal‡	Number Tested	Failure Type	Average σ_r (psi)	High σ_r (psi)	Low σ_r (psi)	Standard Deviation (psi)	Coefficient of Variation (percent)
1	A	30	--	14,700	21,900	6,400	4,400	29.9%
1	A	30	--	15,900	21,700	9,300	2,900	18.2
1	A	30	--	13,400	20,700	5,800	3,000	22.4
1	A	30	--	15,000	22,700	5,000	4,100	27.3
	A	24	Surface	19,208	--	--	4,338	22.6
	A	26	Edge	14,801	--	--	5,127	34.6
1	A	Σ = 50	All	16,917	--	--	5,215	30.8
	S	36	Surface	23,426	--	--	3,995	17.1
	S	14	Edge	28,587	--	--	5,265	18.4
2	S	Σ = 50	All	24,871	--	--	4,923	19.8
3	T	30	--	30,400	47,000	23,700	3,900	12.8
3	T	30	--	33,300	41,500	25,500	4,500	13.5
3	T	30	--	28,000	35,800	23,500	3,400	12.1
3	T	30	--	36,400	48,400	27,000	4,300	11.8
	T	40	Surface	35,590	--	--	5,073	14.3
	T	10	Edge	39,363	--	--	8,037	20.4
3	T	Σ = 50	All	36,345	--	--	5,888	16.2
4	Aa	30	--	10,100	11,200	8,500	600	5.9
4	Aa	30	--	9,700	11,600	8,200	700	7.2
4	Aa	30	--	10,100	11,400	6,200	800	7.9
4	Aa	30	--	10,400	12,400	7,200	1,100	10.6
5	Ta	30	--	23,400	28,500	20,500	1,100	4.7
5	Ta	30	--	23,800	27,600	20,700	900	3.8
5	Ta	30	--	24,600	26,500	21,600	900	3.6
5	Ta	30	--	25,700	30,200	23,800	1,100	4.3

* Some of the data in this table were taken from a table in Ref. 12. The remainder of the data were estimated to the nearest 100 psi from a floating bar chart in Ref. 42.

† Same numbered lines were combined in the preparation of Table C-2.

‡ A = annealed, S = semitempered, T = tempered, Aa = annealed and abraded, and Ta = tempered and abraded.

Table C-2

SUMMARY OF TABLE C-1 DATA

Condition of Anneal	Abraded	Modulus of Rupture (psi)	Standard Deviation (psi)	Coefficient of Variation (percent)
Annealed	No	15,400	4,300	27.9%
Semitempered	No	24,871	4,923	19.8
Tempered	No	33,300	5,700	17.1
Annealed	Yes	10,100	500	5.0
Tempered	Yes	24,400	800	3.3

Table C-3

MODULUS OF RUPTURE TESTS

Number of Samples	Surface Condition	Strength (psi)	Standard Deviation (psi)	Coefficient of Variation (percent)
247	Ground and polished	12,906	2,624	20.3%
293	Sandblasted	6,789	464	6.8
287	Ground and polished	8,400	1,865	22.2

Source: Reference 3.

The results of other tests[3] taken under similar conditions to those previously described are presented in the first two rows of Table C-3. One difference noted was that the glass laths in this case were 1/2 in. wide rather than 1-1/2 in. wide as in the other tests. The third row of data came from concentric ring[17] tests carried to destruction.

The results of modulus of rupture tests[43] reported in 1923 are reproduced in Table C-4. The glass laths in this case were 18" X 2", the supports were 16 in. apart, and the load was applied at midspan at a rate of 10 pounds per minute.

It can be seen that the modulus of rupture values shown in Table C-1 are more than two times larger than the values for 1/4-in. plate shown in Table C-4. Even the strengths of the abraded laths of Table C-1 are larger than those for the unabraded laths reported in Table C-4. This considerable difference illustrates the difficulty in assigning modulus of rupture values to a brittle material.

Table C-4

MODULUS OF RUPTURE TESTS

Type*	Number Tested	Average Modulus of Rupture (psi)	Deflection (in.)	Load (lb)
A grade SS	65	10,020	.423	6.4
A grade SS	74	10,770	.317	5.0
A grade SS	10	8,275	.338	4.9
A grade DS	70	9,692	.290	10.8
A grade DS	76	9,442	.316	12.37
A grade DS	8	7,880	.297	9.5
26-oz sheet	10	7,460	.213	10.8
29-oz sheet	10	6,111	.190	10.8
34-oz sheet	10	7,230	.182	15.2
39-oz sheet	10	6,980	.151	22.2
39-oz sheet	10	5,970	.127	18.8
1/4-in. polished plate	9	6,027	.109	33.0
1/4-in. polished plate	9	6,977	.124	33.4

* Types given in ounces may be converted to thicknesses by using Table 1 of this report.

Source: Reference 43.

Appendix D

WINDOWS SUBJECTED TO VARIOUS DYNAMIC LOADINGS

Appendix D

WINDOWS SUBJECTED TO VARIOUS DYNAMIC LOADINGS

The purpose of this appendix is to demonstrate the strength of glass in windows under various types of loading conditions. The most often quoted strength figures are reproduced in Table D-1. The table gives typical breaking stresses for large lights (panes) with normal surface quality, as glazed, thus accounting for temper, fabrication, support conditions, and type of loading. It is felt that breaking stress refers to the maximum tensile stress on the glass surface at the time of failure; however, a procedure for calculating such a large deflection plate stress for comparison with the tabulated values was not found in the literature.

Table D-1

THE RELATIONSHIP OF LOADING TO BREAKING STRESS

Type of Loading	Approximate Load Duration	Plate Glass (psi)	Window Glass (psi)
Sonic booms, blasts	0.1 second	6,000	6,600
Wind gusts	5-10 seconds	5,500	6,050
Fastest mile wind	60 seconds	4,000	4,400
Long term	2 hours--indefinite	3,000	3,300

Source: Reference 22.

Factors affecting the ability of windows to resist failure are numerous. Some factors affecting glass were mentioned in Chapter I. Other factors affecting the strength of glass panes in windows[9,10] are size,

Preceding page blank

thickness, shape, style, edge restraints, preloading, and uniformity of support. Of interest in sonic boom situations is that restraint may be different at different time points in the loading; that is, edge restraint may be different inward (frame) than outward (putty and glazers' points).[13] Again no method of applying a factor(s) to strength to account for each variable was found.

Nuclear Explosion Data

A nuclear device with a magnitude of nearly 30 kt was detonated atop a 500-foot tower at a distance of 10,500 feet from four test houses during Operation Teapot.[44] The resulting peak free-field overpressure at that distance was measured and calculated to be about 1.7 psi. All glass in all windows facing the blast was blown in, and most of the side and rear windows were destroyed. Phrases such as "remained in place but were distorted in shape," . . . "warped and twisted but remained in place," . . . and "in place with minor distortions" were used to describe the steel sashes in three of the four buildings.

During the Upshot-Knothole test series,[45] a two-story frame house was located 7,500 feet from a 16.4-kt atomic device detonated atop a 300-foot tower. Using Figure 3.67b of ENW,[25] the peak free-field overpressure at the house was calculated to be nearly 1.9 psi, which means a peak reflected pressure of about 4 psi. Wood, double-hung, multipane windows with single strength, grade B window glass were used. All front and side windows failed, with glass broken into small fragments and muntins broken from the sashes. The sashes in the front wall were pushed into the rooms but this may have been the result of unconventional mounting procedure. Slightly less than one-half of the glass in the rear wall was destroyed. It was concluded that "major damage to multilight double-hung wood sash may be expected at overpressures of 2 psi."

A test structure was located 10,328 feet from a 46.7-kt atomic device detonated atop a 300-foot tower in the Operation Greenhouse series.[46]

The pressures were estimated at p_{so} = 2 psi and p_r = 4.2 psi. Aluminum and steel sashes were only slightly damaged when glazed with double strength glass, which failed readily. However, this type of sash was more severely damaged when glazed with heavier glass, such as 1/4-in. plate, because of the high forces transmitted to the frames by the ability of the stronger glass to resist breakage. Commercial, lightweight, double-hung, wooden, multipane windows glazed with double strength glass were almost completely destroyed even though they were located at the sides of the test house where there was no reflection.

Nuclear test results have indicated that the resistance of windows to atomic blast appears to be "approximately proportional to their strength in supporting static loads."[46] This observation has been summarized into five rules:[47]

1. If $p_{so} < 1/4\, q_{sf}$, windows facing the blast "will almost surely survive the blast." A value of p_{so} = 0.25 psi was suggested for failure of usual lightweight, double-hung, wooden windows with ordinary glazing, facing ground zero.

2. If $p_{so} > q_{sf}$, windows facing the blast "will almost surely fail."

3. "Within these two extremes the situation is variable."

4. If $p_{so} < 1/2\, q_{sf}$, side windows "may have an excellent chance of surviving."

5. If the building interior is open, pressure equalization could reduce damage on rear windows.

Frame rigidity is important. A pane may survive in a rigid frame, whereas the same pane in a flexible frame would be broken by the frame as it distorted.[46] "Generally the weakest parts of a window assembly are the cross pieces (muntins) that divide the sashes into smaller glass areas. Sashes designed with intersecting muntins are particularly susceptible to blast."[41] Table D-2, although not conclusive, gives some idea of the reaction of various sashes to atomic blast. All pressures shown in the table are peak reflected pressures.

A formula for calculating the shatter pressures of flat glazing materials exposed to blast, apparently derived empirically from nuclear weapons effects data, is as follows:[41]

$$q_s = \frac{KRh^2}{A} \qquad \text{(D-1)}$$

where q_s = psi required to shatter,

K = a constant (approximately 10,500 for ordinary window glass)

h = thickness in inches

A = area in square inches

R = a shape factor

Aspect Ratio	R
1.0	1.000
.9	1.005
.8	1.02
.7	1.07
.6	1.14
.5	1.25
.4	1.45
.3	1.8
.2	2.6
.1	5.0

The formula assumes that the frame is substantial for the type of glass it supports and that the frame does not deform.

From the best available field test data, it has been estimated that both large and small glass windows facing ground zero will shatter with some frame failures at p_{so} = 0.5 - 1.0 psi.[25] Using scaling laws on other estimates presented in the same reference, it was found that p_{so} = 0.25 psi is given as the pressure at which glass breakage in front-facing windows is possible. Light damage to frames is estimated to occur at p_{so} = 0.75 psi.

Table D-2

BLAST EFFECTS ON WINDOW CONSTRUCTION AND GLAZING

Type of Window	Size	Frame and Sash Condition		Glass Breakage	
Lightweight wood, double-hung with 12 panes 10-1/2" X 15" double strength glass	3'0" X 5'6"	At 2 psi, muntins broken, frame intact		At 2 psi, all broken	
Lightweight aluminum outswinging casements 4 panes 1/8" glass 12" X 16" 4 panes 1/4" glass 12" X 16"	3'2" X 4'2"	At 4.2 psi, frame bent	At 2 psi, no damage	At 4.2 psi, all broken	At 2 psi, none of 1/4" broken; 1/8" not tested
Steel intermediate projected 2 panes 1/4" plate 15" X 40" 2 panes 1/4" safety in vent	3'6" X 5'6"	At 4.2 psi, muntin in vent bent	At 2 psi, no damage	At 4.2 psi, panes broken only in vent	None at 2 psi
Heavy aluminum inswinging casement 6 panes 18" X 22" X 1/4" tempered	4'8" X 5'1"	At 7.4 psi, wrecked	At 3.2 psi, no damage	At 7.4 psi, all broken	None at 3.2 psi
Hopper vents, inswinging, steel 4 panes 12" X 42": 3/16" glass, 1/4" plate, tempered & plastic	4'0" X 5'2"	At 7.4 psi, wrecked	At 3.2 psi, no damage	At 7.4 psi, all broken	At 3.2 psi, 1/4" plate and 3/16" broken
Hopper vents inswinging aluminum 4 panes 1/4" X 12" X 42" tempered	4'0" X 5'2"	At 7.4 psi, sash torn from frame	At 3.2 psi, no damage	At 7.4 psi, one pane broken	None at 3.2 psi
Heavy steel double-hung 3 panes 1/4" plate and 1 DS 20" X 30"	4'2" X 5'8"	At 4.2 psi, muntins bent	At 2 psi, no damage	At 4.2 psi, all broken	At 2 psi, only DS pane broken
Heavy steel double-hung 4 panes 3/16" glass 12" X 28"	2'8" X 4'5"	At 3.2 psi, no damage	At 3.2 psi, no damage	At 3.2 psi, all broken	At 1.5 psi, only 2 panes broken
Canopy aluminum 2 panes plate 1/4" X 19" X 33" 1 pane 1/8" X 19" X 33"	3'1" X 5'4"	At 4.2 psi, no damage	At 2 psi, latch broken	At 4.2 psi, all broken	At 2 psi, 1/8" pane broken

Source: Reference 41.

Conventional Explosion Data

Considerable work has been done, especially during World War II, on the problem of blast loading of windows; however, none of this previous work is believed to be applicable to this investigation. To clarify this statement, the work of Schardin[14] who indicated the similarity between the responses of a simple oscillator and a window pane to an explosive force must be considered. If t_o is the positive pressure phase duration and T is the natural period of vibration of the system, then:

> If the system has a large natural period, or if the strain is caused by a shock wave coming from a small explosive charge at a short distance $[t_o < T]$, then the destruction depends on the momentum of the shock wave. If the system has a low natural period, or if the strain is caused by a shock wave coming from large explosive charges at a great distance $[t_o > T]$, then the destruction depends on the maximum pressure of the shock wave. Between those two limits there is a transition range.[14]

The natural period of usual sizes of single and double strength panes varies from 10 to possibly 100 milliseconds. Positive phase durations for the conventional explosions reviewed during this investigation were all less than the natural period of the window being tested. On the other hand, the positive phase duration of a 1-Mt nuclear explosion exceeds several seconds. Therefore, on the basis of the above quotation, window failures caused by conventional explosions are a result of the momentum of the shock wave, while failures caused by nuclear detonations are dependent on p_{so}.

Since it has been shown above that window failures for a conventional explosion are not dependent on p_{so}, the results of only one, large magnitude conventional explosion with a considerable amount of window data are presented here. Other sources of conventional explosion data can be found in the bibliography.

An accidental detonation of conventional explosives occurred at Medina Facility near San Antonio, Texas, in November 1963.

> Storage records showed that 111,500 lbs. of chemical high explosives with a TNT yield equivalent of 145,000 lbs. were destroyed. The burst was partially contained in its storage bunker and it was not one uniform sphere, because many more missiles were ejected to the west. It is reasonable, however, to assume that its blast yield equalled its weight, free air burst. An ideal 145,000 lbs. TNT sphere, if surface burst, and restricted to hemispheric expansion, would have given a blast wave more like 290,000 lbs. TNT free air burst. . . . One million pounds of TNT, or one-half kiloton, is assumed to be the air blast generating equivalent of one-kiloton nuclear explosives.[48]

On the basis of the above quotation, the yield of the explosion was assumed to be 145,000 lb. TNT (equal to 0.0725 kt TNT). The air blast generating equivalent was therefore 0.145 kt nuclear. Prevailing weather conditions were carefully analyzed, and window damage claims were categorized by pane size and location.[48] One of the results of the extensive research performed is the following equation:

$$D = 3.71 \times 10^{-3} A^{1.22} \Delta p^{2.78} \tag{D-2}$$

where D = damage intensity in number of panes broken per 1,000 panes exposed

A = area of pane in square feet

Δp = incident overpressure in millibars.

Rewriting the above equation in terms of probability and psi, it becomes

$$\text{Probability of failure} = 0.48\ A^{1.22}\ p_{so}^{\ 2.78} \tag{D-3}$$

Equation D-2 was derived for windows with a wide range of areas and a pressure range of approximately 0.01 to 0.1 psi. The thickness of the window pane in the survey in Reference 48 is implied by the area. As an example, the 50 percent probability of failure of a 40" X 40" window, which would probably be a double strength window in San Antonio, is

$$0.50 = 0.48 \times 11.1^{1.22} p_{so}^{2.78}$$

$$p_{so} = 0.35 \text{ psi}$$

Shock Tube Test[49]

The shock tube used was designed to simulate the shock wave of a large bomb with one slight, inherent difference. The test specimens experienced reflected pressures for a longer time than a building since the specimens closed off the end of the tube. The tests were done on both 1/8-in. and 7/32-in. thick, 16-in. X 16-in. sheet glass panes, with a 1/4-in. engagement on all sides. It was found that the 1/8-in. specimens survived p_{so} = 0.7 psi and failed at p_{so} = 0.8 psi. The 7/32-in. specimens survived p_{so} = 0.9 psi and failed at p_{so} = 1.1 psi.

Sonic Boom Data

References concerned with the study of sonic booms generally agree that the window damage threshold is near p_{so} = 2 psf or 0.014 psi. Because of the pressure, the duration of the pulse, and the "N" shape of sonic boom pressure signatures, window natural frequency becomes important since resonance can increase the stress significantly.[3] Windows responding to sonic booms have been known to deflect inward and then fail on an outward deflection that has no comparison to nuclear explosion response; however, a few sonic boom test results are reported here.

The following results were taken from one series of tests.[50] A sonic boom with p_{so} = 0.26 psi caused deflections up to 1.5 in. in twelve 5 ft X 10 ft X 1/4 in. windows causing some molding damage in one of them, but none broke. One of five 32-1/2 in. X 48-1/2 in. X 0.115 in. windows broke at p_{so} = 0.15 psi. Glass fell equally on both sides of the window. When a greenhouse having 120 panes 0.085 in. thick was exposed to a boom with p_{so} = 0.26 psi, 12 panes broke and 4 cracked, mostly on the side facing the pressure wave.

A case of an accidental boom without warning over Cedar City, Utah, has been documented.[50] Claims for damage were reported in a path where the estimated overpressure ranged from about 0.125 psi to 0.04 psi at a lateral distance of about 2,000 feet. No claims were reported beyond 2,000 feet laterally from the flight path.

Two airplanes were used to create sonic booms with overpressures much higher than usual for normal supersonic flight.[11] One of the planes produced a pressure signature with a longer duration than the other. The data concerning that plane, which caused greater damage, are given in Table D-3. The number of window units (not panes) is reported for multi-pane windows.

Table D-3

SONIC BOOM EXPOSURE

3' X 3' Double Strength Window			
p_{so} (psi)	Number Exposed	Number Broken	Percent Broken
0.16 } 0.24 }	28	9	32%
0.29	3	2	67
0.33	10	4	40
0.39	6	6	100
0.50	2	2	100
0.53	1	1	100
0.65	6	6	100

Nine 11" X 11" Single Strength Panes in 3' X 3' Wooden Frame			
p_{so} (psi)	Number Exposed	Number Broken	Percent Broken
0.16 } 0.18 }	13	3	23%
0.29	3	0	0
0.43	10	4	40
0.50	3	2	67
0.60	6	3	50

Source: Reference 11.

Appendix E

TIME TO FAILURE

Appendix E

TIME TO FAILURE

The purpose of this appendix is to provide a measure of the elapsed time between loading and failure for windows.

The computer program described in Chapter II was used to provide the data plotted in Figures E-1 through E-4. The times associated with the lowest overpressure are for incipient failure. To plot other points for determining the curves for each window size shown, use was made of the program feature which permits overpressures above the incipient failure overpressure to be used as inputs.

No test data were found to confirm or deny the values provided in the figures. It is suggested that these values be used in the interim until test data become available.

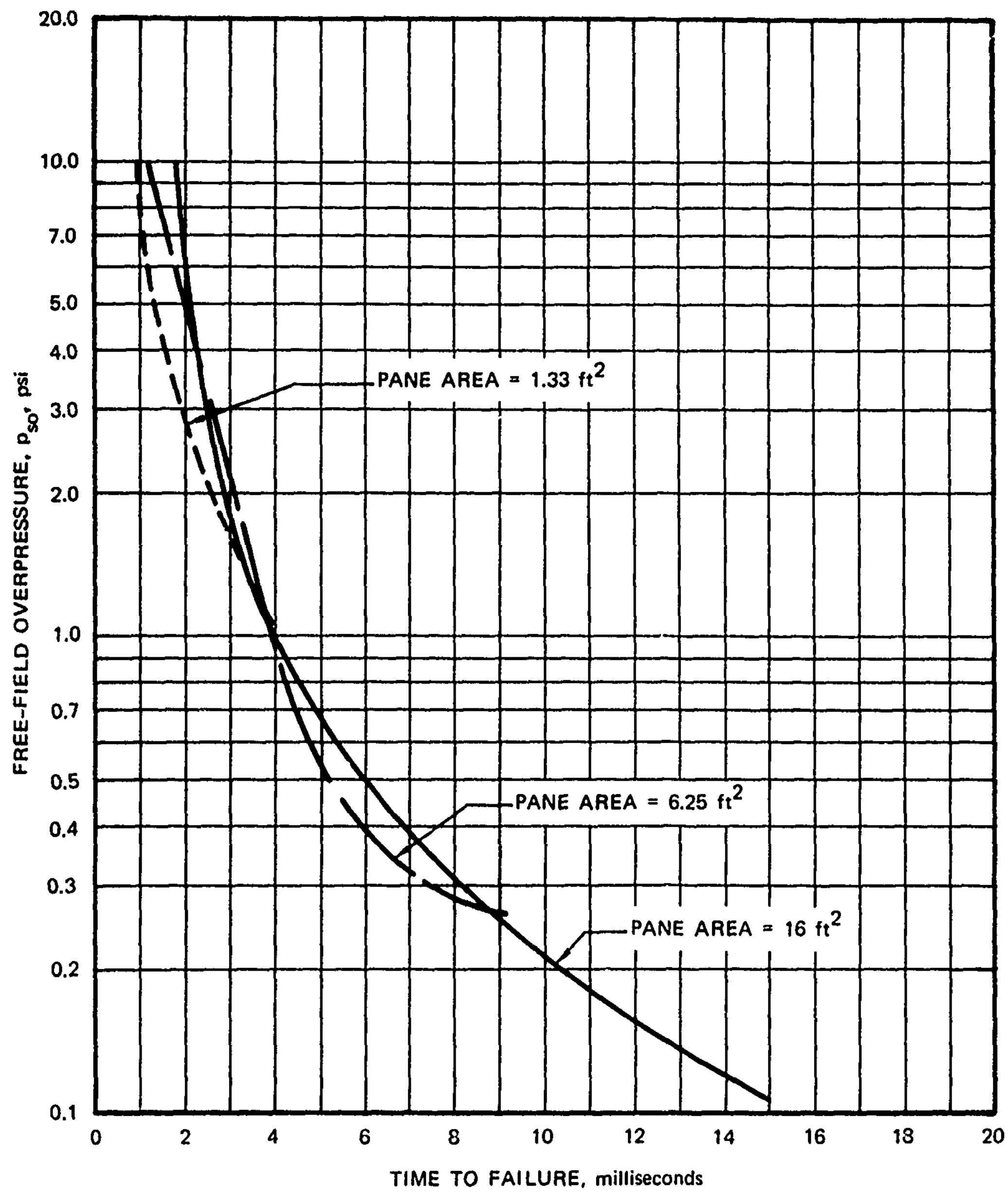

FIG. E-1 FREE-FIELD OVERPRESSURE VERSUS TIME TO FAILURE FOR PANES OF GLASS MOUNTED IN HOUSE WALLS
Single Strength Glass, Front-Face Loading

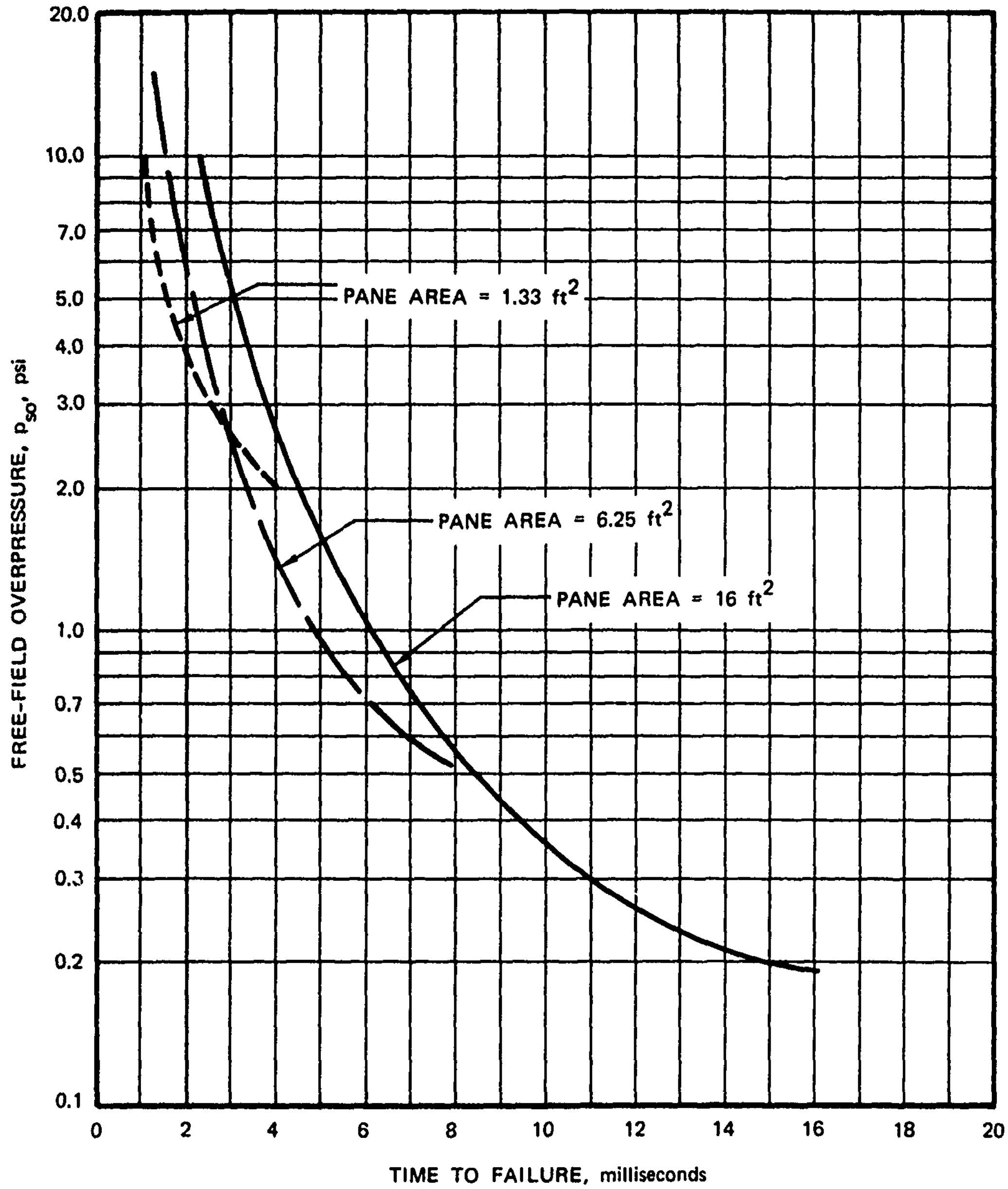

FIG. E-2 FREE-FIELD OVERPRESSURE VERSUS TIME TO FAILURE FOR PANES OF GLASS MOUNTED IN HOUSE WALLS
Single Strength Glass, Side-Face Loading

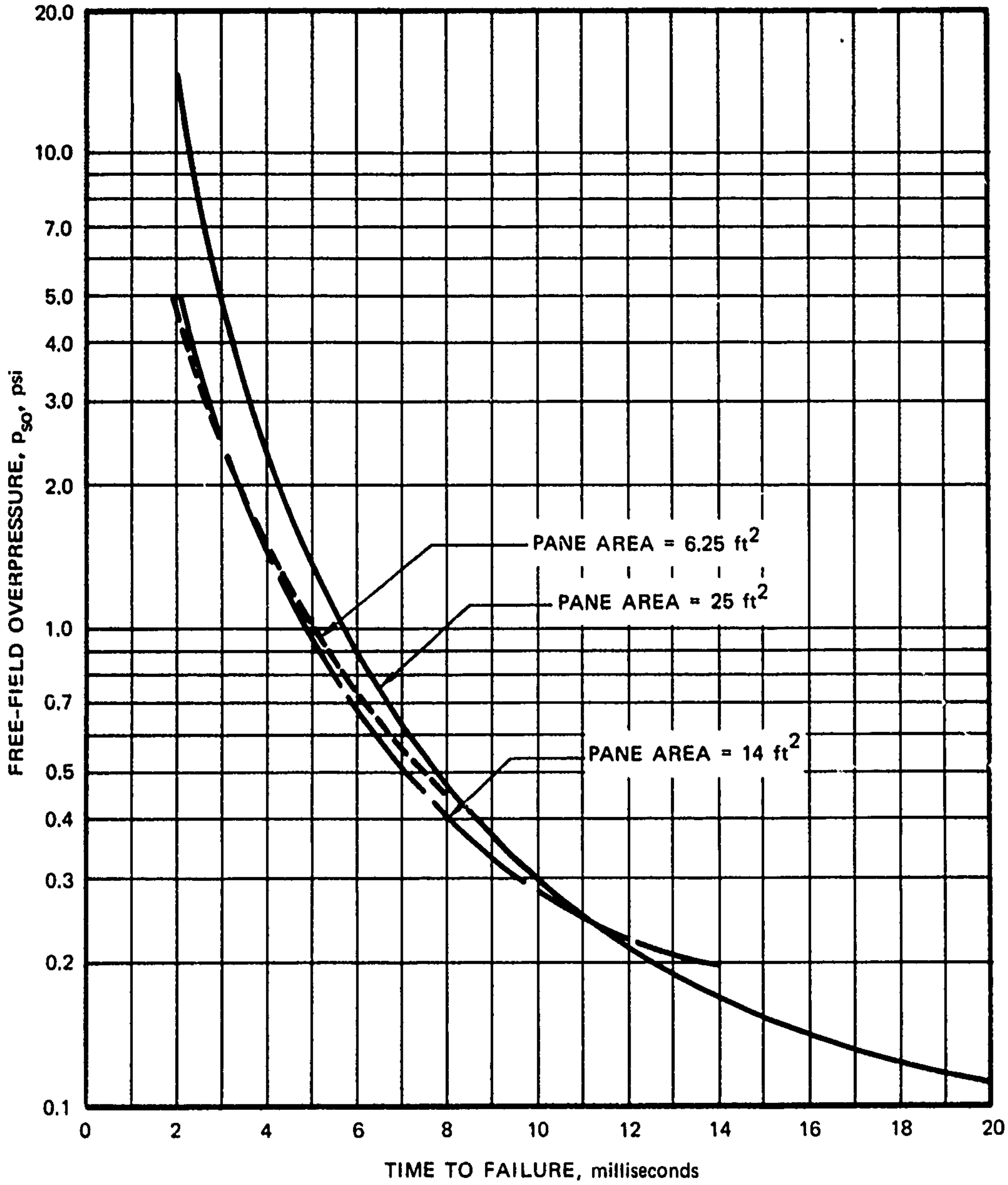

FIG. E-3 FREE-FIELD OVERPRESSURE VERSUS TIME TO FAILURE FOR PANES OF GLASS MOUNTED IN HOUSE WALLS
Double Strength Glass, Front-Face Loading

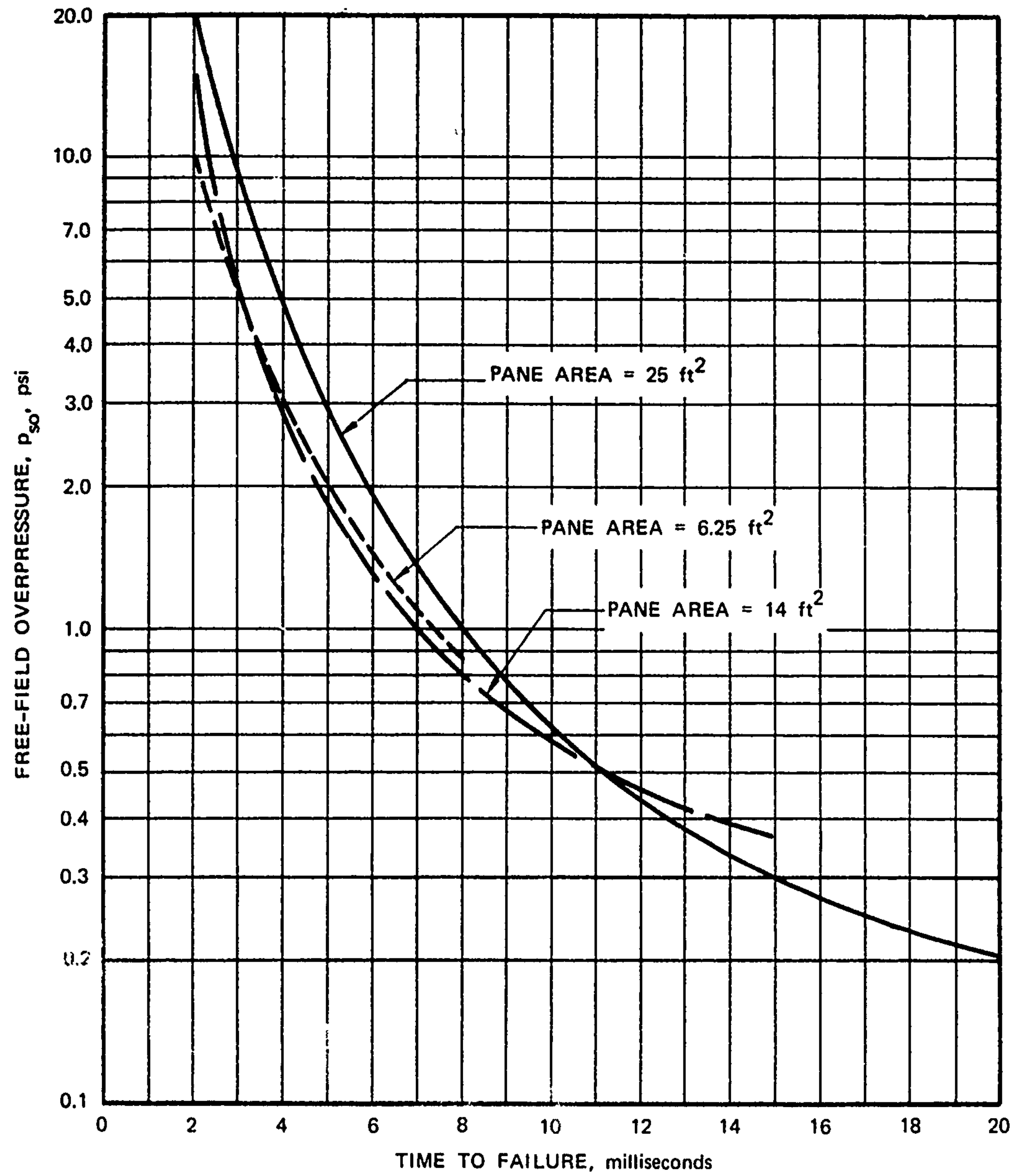

FIG. E-4 FREE-FIELD OVERPRESSURE VERSUS TIME TO FAILURE FOR PANES OF GLASS MOUNTED IN HOUSE WALLS
Double Strength Glass, Side-Face Loading

Addendum

A MULTIPLE REGRESSION ANALYSIS APPROACH

By H. L. Murphy

Addendum

A MULTIPLE REGRESSION ANALYSIS APPROACH

By H. L. Murphy

As stated in the report, one must conclude from the literature that the fracture behavior of window glass principally depends on the flaws and scratches in the glass, and the unevenness and other variations in the mounting and frame. A brief statistical study, therefore, appeared to be indicated for at least part of the problem. Such an approach was undertaken following the technical work reported; results are described in the following paragraphs.

For incipient collapse prediction in terms of free-field air blast overpressure, no further study was made - the approach described in the report appeared to be supported by many tests and much research.

When higher overpressures than sufficient for incipient collapse were assumed, prediction of window glass behavior must be based on sparse nuclear test data and thus was considered appropriate for a simple statistical analysis. Table An-1 shows TEAPOT nuclear test data (Table 7 plus average and geometric mean velocity data at the trap).

Independent variables involved were:

Free-field air blast peak overpressure	A
Total glass area of window	C
Window pane area	D
Thickness of glass	E
Total volume of glass	F
Glass travel distance to point of interest	K
Unit weight of glass	Y

Preceding page blank

It was desired to predict values for four dependent variables in a statistical (multiple regression analysis) approach:

Average fragment weight	B
Total number of glass fragments	G
Geometric mean fragment weight	H
Geometric mean velocity (at K)	J

Since F can be calculated as a function of C and E, or F = f(C,E), and G can be calculated from B, F and γ, or G = f(B,F,γ), both F and G merited no further study.

It was reasoned that the following relationships for predicting the dependent variables should be tried:

B = f(A,C,D,E) or f(A,C,E) or f(A,D,E) or f(A,E) or f(A)

H = same functional equations as for B

J = f(A,H,K) or J = $[f(A,H,K)]^{1/2}$

The latter was actually handled as J^2 = f(A,H,K). It may be noted that J as a function of H was considered sounder, technically, than J as a function of B.

Because Equation 6 indicates that the glass behavior is closer to a linear function of glass thickness, than to some (whole-numbered) power or root, only the linear function of this variable was tried. Time did not permit trial of nonlinear functions for any of the other variables except as indicated for J and for both B and H as functions of several roots of A. The latter were all poorer fits than obtained for B and H as functions of A.

Tables An-2 through An-6 show the results of trying the functions shown above for B, using a library program of a commercial time-sharing computer service and the Table An-1 data on seven windows. All things considered, the best function for use seemed to be the last one shown above, i.e., $B = f(A)$. Similar results were obtained in trying the five functions shown above for H; Table An-7 shows the data on the function considered best for use, i.e., $H = f(A)$.

The two functions shown above for J were tried, with the results for the first one being somewhat the better of the two. However, considering that the user must, in practice, calculate H before using one of these functions for J, results of a trial of $J = f(A,H,K)$, with H values computed from $H = f(A)$, were compared with results of a trial of $J = f(A,K)$ which needs no H calculation. The latter results were considered best for use and are shown in Table An-8.

For the nonstatistician: the smaller the absolute value of beta, the lower the influence of that independent variable in the linear equation for the dependent variable; the "F-ratio test statistic" must be considered in connection with an F Table from standard statistical texts, and together with the index of determination (higher values equal better least squares fit), indicates the overall statistical merit of the derived linear equation.

From all of the foregoing, the most useful linear equations derived appear to be the following:

$$B = 2.96068 - 0.537311A$$

$$H = 1.97486 - 0.368371A$$

$$J = 132.36 + 17.8936A - 5.12857K$$

That the computer program routinely prints out six significant figures should not be taken as an implication of prediction accuracy, of course.

Much more confidence would be engendered by this approach if it could be based on more than seven test windows; however, that was all that seemed to be available.

Table An-1

WINDOW GLASS FRAGMENT WEIGHT DATA*

Free-Field Overpressure, P_{so} (psi)	Trap Designation	Average Thickness of Panes h (in.)	Number of Fragments Caught in Traps†	Geometric Mean Weight, M_{50} (gm)	Average Weight, $\bar{M}$ (gm)	Distance from Window to Trap, x (ft)	Size of Individual Panes (in.)	Number of Panes per Window	Frame Material	Average Velocity at Trap (fps)	Geometric Mean Velocity at Trap (fps)
5.0	2A	.092	254	.140	.226	8.83	12 × 12	16	Wood‡	176	171
5.0	2C	.096	423	.140	.282	13.50	12 × 16	20	Steel	151	146
5.0	$2D_1$	.094	247	.113	.307	9.00	12 × 16	12	Steel	180	176
5.0	$2D_2$	.089	231	.095	.140	9.00				184	180
			478	.104	.226					182	178
5.0	$2E_1$	.124	242	.153	.415	10.50	12 × 23.5	9	Steel§	170	166
5.0	$2E_2$	.122	732	.142	.241	10.50				186	178
			974	.145	.284					182	175
3.8	$3C_1$	.120	61	.810	1.275	7.00	12 × 12	16	Wood‡	148	146
3.8	$3C_2$	.118	259	.540	.993	7.00				179	175
			320	.580	1.047					173	169
1.9	$4B_1$	.124	1	2.125	2.125	10.67	15 × 18	20	Steel‡	111	111
1.9	$4B_2$	.123	11	1.322	1.677	10.67				98	94.8
1.9	$4B_3$	.124	5	1.596	1.704	10.67				99	98.7
1.9	$4B_4$	.124	5	4.407	5.260	10.67				109	107.4
			22	1.854	2.518					101.3	99.2
1.9	4D	.088	15	.694	1.312	13.50	12 × 16	20	Steel‡	111	107.8

* All data were taken from 13 traps located behind 7 windows mounted in house walls that faced ground zero. In cases of more than one trap per window, data from traps have been combined to provide results for each window as well as each trap.

† The number of fragments given is limited to the number for which the velocity could be calculated.

‡ Window covered with venetian blinds.

§ Window covered with curtains.

Source: Reference 29.

Table An-2

B = f(A,C,D,E)

VARIABLE	REGR COEFF	BETA	MEAN VALUE	STD DEV
0 (DEP VAR)	2.58206 $-2	(=CONSTANT)	.842143	.86176
1	-.374546	-.635738	3.94286	1.46271
2	2.52484 $-4	.348795	3218.57	1190.48
3	-2.71972 $-3	-.173108	202.286	54.8504
4	19.3855	.366469	.10475	.016291

SOURCE OF VARIATION	DEGREES OF FREEDOM	SUM OF SQUARES	MEAN SQUARE
TOTAL	6	4.45578	.742629
REGRESSION	4	4.28226	1.07056
ERROR	2	.173521	8.67605 $-2

INDEX OF DETERMINATION	.961057
F-RATIO TEST STATISTIC	12.3393

Y-ACTUAL	Y-CALCULATED	DIFFERENCE	PERCENT
.226	.126636	-9.93644 $-2	-78.4649
.282	.461446	.179446	38.8877
.226	-1.36035 $-2	-.239604	1761.34
.284	.411345	.127345	30.9583
1.047	1.0995	5.24987 $-2	4.77478
2.518	2.34222	-.175778	-7.50473
1.312	1.46746	.155455	10.5935

Table An-3

B = f(A,C,E)

VARIABLE	REGR COEFF	BETA	MEAN VALUE	STD DEV
0 (DEP VAR)	.330447	(=CONSTANT)	.842143	.86176
1	-.406869	-.690601	3.94286	1.46271
2	1.73418 $-4	.23957	3218.57	1190.48
3	14.8712	.281131	.10475	.016291

SOURCE OF VARIATION	DEGREES OF FREEDOM	SUM OF SQUARES	MEAN SQUARE
TOTAL	6	4.45578	.742629
REGRESSION	3	4.219	1.40633
ERROR	3	.236773	7.89242 $-2

INDEX OF DETERMINATION	.946862
F-RATIO TEST STATISTIC	17.8188

Y-ACTUAL	Y-CALCULATED	DIFFERENCE	PERCENT
.226	6.38125 $-2	-.162188	-254.163
.282	.389668	.107668	27.6307
.226	5.63769 $-2	-.169623	-300.874
.284	.565401	.281401	49.7701
1.047	.953579	-9.34215 $-2	-9.79694
2.518	2.33417	-.183829	-7.87554
1.312	1.53199	.219992	14.3599

Table An-4

B = f(A,D,E)

VARIABLE	REGR COEFF	BETA	MEAN VALUE	STD DEV
0 (DEP VAR)	1.17925	(=CONSTANT)	.842143	.86176
1	-.508773	-.863568	3.94286	1.46271
2	-2.79582 $-4	-1.77952 $-2	202.286	54.8504
3	16.4722	.311396	.10475	.016291

SOURCE OF VARIATION	DEGREES OF FREEDOM	SUM OF SQUARES	MEAN SQUARE
TOTAL	6	4.45578	.742629
REGRESSION	3	4.10103	1.36701
ERROR	3	.354742	.118247

INDEX OF DETERMINATION	.920386
F-RATIO TEST STATISTIC	11.5606

Y-ACTUAL	Y-CALCULATED	DIFFERENCE	PERCENT
.226	.110572	-.115428	-104.392
.282	.163041	-.118959	-72.9629
.226	8.89157 $-2	-.137084	-154.173
.284	.582629	.298629	51.2554
1.047	1.16585	.11885	10.1942
2.518	2.17553	-.342466	-15.7417
1.312	1.60846	.296459	18.4313

Table An-5

B = f(A,E)

VARIABLE	REGR COEFF	BETA	MEAN VALUE	STD DEV
0 (DEP VAR)	1.17116	(=CONSTANT)	.842143	.86176
1	-.507385	-.861212	3.94286	1.46271
2	15.9573	.301661	.10475	.016291

SOURCE OF VARIATION	DEGREES OF FREEDOM	SUM OF SQUARES	MEAN SQUARE
TOTAL	6	4.45578	.742629
REGRESSION	2	4.1001	2.05005
ERROR	4	.355672	.088918

INDEX OF DETERMINATION	.920177
F-RATIO TEST STATISTIC	23.0555

Y-ACTUAL	Y-CALCULATED	DIFFERENCE	PERCENT
.226	.102309	-.123691	-120.899
.282	.166138	-.115862	-69.7379
.226	9.43308 E-2	-.131669	-139.583
.284	.596985	.312985	52.4276
1.047	1.14202	9.50175 E-2	8.32015
2.518	2.18185	-.336154	-15.4069
1.312	1.61137	.299373	18.5788

Table An-6

B = f(A)

VARIABLE	REGR COEFF	BETA	MEAN VALUE	STD DEV
0 (DEP VAR)	2.96068	(=CONSTANT)	.842143	.86176
1	-.537311	-.912008	3.94286	1.46271

SOURCE OF VARIATION	DEGREES OF FREEDOM	SUM OF SQUARES	MEAN SQUARE
TOTAL	6	4.45578	.742629
REGRESSION	1	3.70613	3.70613
ERROR	5	.749649	.14993

INDEX OF DETERMINATION	.831758
F-RATIO TEST STATISTIC	24.7191

Y-ACTUAL	Y-CALCULATED	DIFFERENCE	PERCENT
.226	.274128	.048128	17.5568
.282	.274128	-7.87201 E-3	-2.87165
.226	.274128	.048128	17.5568
.284	.274128	-9.87201 E-3	-3.60124
1.047	.918902	-.128098	-13.9404
2.518	1.93979	-.578207	-29.8077
1.312	1.93979	.627793	32.3639

Table An-7

H = f(A)

VARIABLE	REGR COEFF	BETA	MEAN VALUE	STD DEV
0 (DEP VAR)	1.97486	(=CONSTANT)	.522429	.634543
1	-.368371	-.849146	3.94286	1.46271

SOURCE OF VARIATION	DEGREES OF FREEDOM	SUM OF SQUARES	MEAN SQUARE
TOTAL	6	2.41587	.402645
REGRESSION	1	1.74196	1.74196
ERROR	5	.673909	.134782

INDEX OF DETERMINATION	.721049
F-RATIO TEST STATISTIC	12.9243

Y-ACTUAL	Y-CALCULATED	DIFFERENCE	PERCENT
.14	.133008	-6.99197 $-3	-5.2568[illegible]
.14	.133008	-6.99197 $-3	-5.25681
.104	.133008	.029008	21.8092
.145	.133008	-.011992	-9.01598
.58	.575053	-4.94704 $-3	-.860275
1.854	1.27496	-.579043	-45.4166
.694	1.27496	.580957	45.5668

Table An-8

J = f(A,K)

VARIABLE	REGR COEFF	BETA	MEAN VALUE	STD DEV
0 (DEP VAR)	132.36	(=CONSTANT)	149.429	33.1315
1	17.8936	.789976	3.94286	1.46271
2	-5.12857	-.375367	10.4286	2.42494

SOURCE OF VARIATION	DEGREES OF FREEDOM	SUM OF SQUARES	MEAN SQUARE
TOTAL	6	6586.2	1097.7
REGRESSION	2	6167.96	3083.98
ERROR	4	418.235	104.559

INDEX OF DETERMINATION	.936498
F-RATIO TEST STATISTIC	29.4952

Y-ACTUAL	Y-CALCULATED	DIFFERENCE	PERCENT
171	176.543	5.543	3.13975
146	152.593	6.59259	4.32039
178	175.671	-2.32885	-1.32569
175	167.978	-7.02171	-4.18013
169	164.456	-4.54399	-2.76304
99.2	111.636	12.4364	11.1401
107.8	97.1226	-10.6774	-10.9938

REFERENCES

1. Garden, G. K., "Characteristics of Window Glass," Canadian Building Digest, Division of Building Research, National Research Council, Canada, December 1964.

2. Shand, E. B., Glass Engineering Handbook, 2nd Edition, McGraw-Hill Book Company, Inc., New York, 1958.

3. McKinley, R. W., "Response of Glass in Windows to Sonic Booms," Materials Research and Standards, November 1964.

4. Architectural Data Handbook, Fifth Edition, Pittsburgh Plate Glass Company, Pittsburgh, Pa., 1965.

5. Sakhnovsky, A. A., "New ASTM Structural Testing Procedures for Sash and Glass," Building Research, the Journal of the Building Research Institute, Vol. 4, No. 3, May-June 1967.

6. Preston, F. W., "The Mechanical Properties of Glass," Journal of Applied Physics, Vol. 13, No. 10, October 1942.

7. Swarts, E. L., "Fundamental Strength Considerations," Building Research, The Journal of the Building Research Institute, Vol. 4, No. 3, May-June 1967.

8. Haward, R. N., The Strength of Plastics and Glass, Cleaver-Hume Press, Ltd., New York, 1949.

9. Parrott, T. L., "Experimental Studies of Glass Breakage due to Sonic Booms," Sound, Vol. 1, No. 3, May-June 1962.

10. Gurney, C., "Sources of Weakness in Glass," Royal Society Proceedings, A, Vol. 282, 1964.

11. Maglieri, D. J., V. Huckel, and T. L. Parrott, Ground Measurements of Shock-Wave Pressure for Fighter Airplanes Flying at Very Low Altitudes and Comments on Associated Response Phenomena, NASA TN D-3443, Langley Research Center, July 1966.

12. Kerper, M. J., T. G. Scuderi, and E. H. Eimer, Strength of Glass as Related to Edge Finish, National Bureau of Standards Report No. 9069, December 1965. (AD 480 215L)

13. Freynik, H. S., Jr., "Response of Windows to Random Noise," Sound, May-June 1963.

14. Schardin, H., "The Physical Principles of the Effects of a Detonation," German Aviation Medicine, World War II, Chapter XIV - A, Vol. 2, U.S. Government Printing Office, Washington, D.C., 1950.

15. Orr, L., "Engineering Properties of Glass," Windows and Glass in the Exterior of Buildings, Building Research Institute, NAS-NRC, Publication 478, March 1957.

16. Bowles, R. and B. Sugarman, "The Strength and Deflection Characteristics of Large Rectangular Glass Panels Under Uniform Pressure," Glass Technology, Vol. 3, No. 5, October 1962.

17. Seely, F. B. and J. O. Smith, Advanced Mechanics of Materials, Second Edition, John Wiley and Sons, Inc., New York, 1952.

18. Timoshenko, S. and S. Woinowsky - Krieger, Theory of Plates and Shells, McGraw-Hill Book Company, Inc., New York, 1959.

19. Greene, C. [illegible], "Fundamental Strength Considerations," Building Research, The Journal of the Building Research Institute, Vol. 4, No. 3, May-June 1967.

20. Mould, R. E., "The Strength of Inorganic Glasses," Fundamental Phenomena in the Materials Sciences, Vol. 4, Fracture of Metals, Polymers, and Glasses, Plenum Press, New York, 1967.

21. Seaman, L., Response of Windows to Sonic Booms, prepared by Stanford Research Institute for the Dept. of the Air Force, SRI Project ETU-5897, June 1967.

22. "Glass Product Recommendations - Structural," Technical Service Report No. 101, Pittsburgh Plate Glass Company, Pittsburgh, Pa., March 1964.

23. Glass Performance Under Wind Load, Part II - Supplementary Data, Technical Memorandum, Product Development Dept., Pittsburgh Plate Glass Company, Pittsburgh, Pa., February 1962.

24. Fitzgerald, J. E., Blast Loading and Response of Prototype Structures and Quarter Scale Model, Operation Greenhouse WT-86 Interim Report, prepared by Armour Research Foundation of Ill. Inst. of Tech. for the U.S. Air Force, August 1951. (AD 460 274)

25. Glasstone, S., The Effects of Nuclear Weapons, Department of Defense and Atomic Energy Commission, 1962 edition, reprinted February 1964.

26. Kaplan, K. and C. Wiehle, Air Blast Loading in the High Shock Strength Region (U), Part II - Prediction Methods and Examples (U), DASA 1460-1, URS Corporation (for Defense Atomic Support Agency), Burlingame, California, February 1965.

27. Newmark, N. M., "A Method of Computation for Structural Dynamics," J. Engineering Mechanics Div., Proceedings Vol. 85, American Society of Civil Engineers, New York, July 1959; ASCE Transactions, Paper No. 3384, Vol. 127, 1962, Part I.

28. "Glass and Glazing," Uniform Building Code, Chapter 54, International Conference of Building Officials, Pasadena, California, 1967 Edition.

29. Bowen, I. G., A. F. Strehler, and M. B. Wetherbe, Distribution and Density of Missiles from Nuclear Explosions, Operation Teapot WT-1168, prepared by Lovelace Foundation for the AEC, March 1956.

30. Bowen, I. G., D. R. Richmond, M. B. Wetherbe, and C. S. White, Biological Effects of Blast from Bombs. Glass Fragments as Penetrating Missiles and Some of the Biological Implications of Class Fragmented by Atomic Explosions, AECU-3350, prepared by Lovelace Foundation for the AEC, June 1956.

31. Bowen, I. G., et al., A Model Designed to Predict the Motion of Objects Translated by Classical Blast Waves, Report CEX-58.9, prepared by Lovelace Foundation for the AEC, June 1961.

32. Fletcher, E. R., et al., Determination of Aerodynamic Drag Parameters of Small Irregular Objects by Means of Drop Tests, Report CEX-59.14, prepared by Lovelace Foundation for the AEC, October 1961.

33. Bowen, I. G., et al., Secondary Missiles Generated by Nuclear-produced Blast Waves, Operation Plumbbob WT-1468, prepared by Lovelace Foundation for the AEC, October 1963. (AD 436 391)

34. Goldizen, V. C., D. R. Richmond, and T. L. Chiffelle, Missile Studies with a Biological Target, Operation Plumbbob WT-1470 Report, prepared by Lovelace Foundation for the AEC, January 1961.

35. Bowen, I. G., private communication.

36. White, C. S., I. G. Bowen, and D. R. Richmond, Biological Tolerance to Air Blast and Related Biomedical Criteria, Report CEX-65.4, prepared by Lovelace Foundation for the AEC, October 1965.

37. Liber, T. and R. L. Barnett, An Experimental Investigation of Frangible Plate Fragmentation, IITRI Project M6095 for OCD, October 1966.

38. Barnett, R. L., J. F. Costello, and D. I. Feinstein, Debris Formation and Translation, IITRI Project M6103 for OCD, November 1966. (AD 657 603)

39. Hill, E. L., A. A. Qadeer, and A. B. Nicholls, Structural Characteristics of NFSS Buildings, Volume V - San Jose, California, Research Triangle Institute Final Report R-OU-237 prepared for OCD, June 1967.

40. Ramsey, C. G. and H. R. Sleeper, Architectural Graphic Standards, Fifth Edition, John Wiley and Sons, Inc., New York, 1956.

41. Clark, W. C., Window and Glass Hazards Under Wartime Conditions and Recommended Protective Measures, U.S. Atomic Energy Commission, AECU-3037, 1954.

42. Kerper, M. J. and T. G. Scuderi, "Mechanical Properties of Glass at Elevated Temperatures," American Ceramic Society Bulletin, December 1963.

43. Williams, A. E., "The Mechanical Strength of Glazing Glass," Journal of the American Ceramic Society, Vol. 6, No. 9, 1923.

44. Randall, P. A., Damage to Conventional and Special Types of Residences Exposed to Nuclear Effects, Operation Teapot WT-1194 Report, Office of Civil and Defense Mobilization, March 1961. (AD 611 160)

45. Byrnes, J. B., Effects of an Atomic Explosion on Two Typical Two-Story-and-Basement Wood-Frame Houses, Operation Upshot-Knothole WT-792 Report, Federal Civil Defense Administration, September 1953.

46. Clark, W. C., The Effect of Atomic Weapons on Glazing and Window Construction, Operation Greenhouse WT-7 Report, Public Buildings Service, August 1951. (AD 482 990L)

47. Chilton, CDR A. B., USN, "Resistance of Glass Windows to Atomic Blast," Chapter 12 of Studies in Atomic Defense Engineering, Navdocks P-290, Revised June 1962.

48. Reed, J. W., Evaluation of Window Pane Damage Intensity in San Antonio Resulting from Medina Facility Explosion on 13 November 1963, Sandia Laboratory and Southwest Research Institute supported by USAEC.

49. Taylor, W. J. and R. O. Clark, Shock Tube Test of Glazing Materials, BRL Memorandum Report No. 626, November 1952.

50. Wiggins, J. H. Jr., "Effect of Sonic Boom on Structural Behavior," Materials Research and Standards, June 1967.

BIBLIOGRAPHY*

Background information

Archer, J. S., E. A. Lawlor, and C. F. Long, Study of Atomic Blast Damage to Buildings at Hiroshima and Nagasaki, Department of Civil and Sanitary Engineering, MIT, AFSWP-808, July 1954 (regraded unclassified December 1966).

Brode, H. L., A Review of Nuclear Explosion Phenomena Pertinent to Protective Construction, prepared by Rand Corporation for the U.S. Air Force, May 1964.

Fletcher, E. R. et al., Nuclear Bomb Effects Computer, Report CEX 62.2, February 1963.

"Flexure Testing of Glass," ASTM Standards, Part 13, ASTM Designation C158-43, April 1965.

Keefer, J. H., Air Blast Predictions for Operation Distant Plain, Ballistic Research Laboratories, Tech. Note No. 1612, June 1966.

Levy, S., Bending of Rectangular Plates with Large Deflections, National Bureau of Standards, Report No. 737, 1942.

Weibull, W., A Statistical Theory of the Strength of Materials, Generalstabens Litografiska Anstalts Forlag, Stockholm, 1939.

Wiehle, C. K., and W. L. Durbin, Combined Effects of Nuclear Weapons on NFSS Type Structures, URS Corporation, September 1966.

General glass and window information

Building Research, the Journal of the Building Research Institute, Vol. 4, No. 3, May-June 1967. (A collection of articles concerning glass in windows.)

---

* These books, reports, and articles were reviewed during the course of this investigation but not used specifically in preparing the report.

Haward, R. N., "The Behaviour of Glass under Impact and Static Loading," Society of Glass Technology-Journal, Vol. 28, 1944.

Haward, R. N., "The Behaviour of Laminated and Toughened Glass under Impact by a Falling Bolt," Journal of the Society of Glass Technology, Vol. 29, 1945.

Reinhart, F. W., R. A. Kronstadt, and G. M. Kline, Antiscatter Treatments of Glass, National Bureau of Standards Miscellaneous Publication M175, June 1944.

Shand, E. B., "Experimental Study of Fracture of Glass: I, The Fracture Process, and II, Experimental Data," Journal of the American Ceramic Society, Vol. 37, No. 2, February 1954, and Vol. 37, No. 12, December 1954.

"Testing Window Glass for Concussion Damage," Engineering News-Record, Vol. 128, 521, April 2, 1942.

Conventional Explosion information related to glass

Adams, F. W., "Behavior of Glazing Material Subjected to Explosion," ASTM Bulletin No. 122, May 1943.

Eilenberg, T. R., and W. K. Jones, "Discussion of Paper on Behavior of Glazing Material Subjected to Explosion," ASTM Bulletin No. 124, October 1943.

Grossman, J. R., Methods of Reducing the Flying Glass Hazard From Blast Shattered Windows, Atlantic Research Corporation, TR-PL-9222, for the Dept. of State, December 1966.

Ilsley, R., Glass and Plaster Damage from Small Explosions, Armed Services Explosives Safety Board, Technical Paper No. 7, March 1950. (AD 637 835)

Moore, H., "Physics and Windows in War-time," Journal of Scientific Instruments, Vol. 17, 237-241, October 1940.

Report of Blast Tests on Glass, prepared by the Fortification Section, Construction Division, Office of Chief of Engineers, War Dept., March 1943.

Thompson, N. J., and E. W. Cousins, "Explosion Tests on Glass Windows; Effect on Glass Breakage of Varying the Rate of Pressure Application," Journal of the American Ceramic Society, Vol. 32, 1949.

"Windows and Bomb Blast," Nature, Vol. 146, 435-6, September 28, 1940.

Wise, J. A., Rupture of Glass by Blast, Monthly Report EWT-5e (OSRD-5405e), Div. 2, NDRC, August 1945.

Sonic boom information

Bailey, D., A Sonic Boom Study for the Structural Engineer, Air Force Weapons Laboratory, Tech. Report No. AFWL-TR-66-154, March 1967.

Structural Response to Sonic Booms, Vols. 1 and 2, prepared by Andrews Associates, Inc. and Hudgins, Thompson, Ball and Associates, Inc. for the Federal Aviation Agency, February 1965.

Proceedings of the Sonic Boom Symposium, Acoustical Society of America, November 1965.

Young, J. R., "Energy Spectral Density of the Sonic Boom," The Journal of the Acoustical Society of America, Vol. 40, No. 2, 1966.

Biological information

McDonnell, G. M., W. H. Crosby, C. F. Tessmer, et al., Effects of Nuclear Detonation on a Large Biological Specimen (Swine), Operation Plumbbob Report WT-1428, Project 4.1, prepared by Walter Reed Army Institute of Research, For Official Use Only, August 1961. (AD 460 308)

Missile Effects of Flying Glass, OCD, MPM #263-276, PSD-Project No. NF-55, October 1963.

Richmond, D. R., and C. S. White, Biological Effects of Blast and Shock, Technical Progress Report on Contract No. DA-49-146-XZ-055, DASA-1777, April 1966.

White, C. S., Biological Blast Effects, presented before the Special Subcommittee on Radiation of the Joint Committee on Atomic Energy During Public Hearings on the Biological and Environmental Effects of Nuclear War, Washington, D.C., Report TID-5564, June 24, 1959.

White, C. S., I. G. Bowen, and D. R. Richmond, "A Comparative Analysis of Some of the Immediate Environmental Effects at Hiroshima and Nagasaki," Health Physics, Vol. 10, pp. 89-150, March 1964.

White, C. S., I. G. Bowen, D. R. Richmond, and R. L. Corsbie, Comparative Nuclear Effects of Biomedical Interest, Report CEX-58.8, January 1961.

NOTATION

a	Short side dimension of a rectangular window pane
A	Pane area; nondimensional missile parameter in translation model
A_f	Area of fragment presented to the wind
b	Long side dimension of a rectangular window pane
c_o	Speed of sound in undisturbed air
C_d	Drag coefficient
$D(n)$	Nondimensional fragment displacement in translation model
E	Modulus of elasticity
g	Acceleration of gravity
h	Average thickness of a glass pane
m	Mass of an entire window (Equation 1); glass fragment weight
$\overline{M}$	Average weight of a number of fragments
M_{50}	Geometric mean weight of a number of fragments
n	Decimal point locator in translation model equations
N	Estimated total number of glass fragments produced by the failure of a given window
N_x	Spatial density of fragments at x feet from a window, fragments/unit area
N_0	Spatial density of fragments zero feet from a window, fragments/unit area (x may be replaced by a number to denote a specific distance from a window)
N_{10}	Spatial density of fragments 10 feet from a window, fragments/unit area

$p(t)$ Time dependent pressure against any surface

p_c Pressure exerted at time t_c

p_d Dynamic pressure varying with time

p_{do} Peak dynamic pressure

p_r Reflected pressure

p_s Free-field overpressure varying with time

p_{so} Peak free-field overpressure

P Nondimensional peak free-field overpressure used in translation model; probability of penetration or serious injury

P_o Ambient atmospheric pressure of undisturbed air

q Applied pressure to glass panes

q_{sf} Static failure pressure for glass panes

q_{df} Dynamic failure pressure for glass panes

s Length of a side of a square glass pane

S Clearing distance

t Time

t_c Clearing time, front-face

t_o Duration of positive overpressure phase

t_u Duration of dynamic pressure phase

T Nondimensional time used in translation model

U Shock front velocity

v Fragment velocity

v_m Maximum fragment velocity

$\dot{v}$ Fragment acceleration

$V(n)$ Nondimensional fragment velocity used in translation model

$\dot{V}(n)$ Nondimensional fragment acceleration used in translation model

w_o Mean central deflection of a glass pane

W Weapon yield, kilotons

x Pane displacement at center during loading (Equation 1); distance of travel for a glass fragment

α Fragment acceleration coefficient, area/weight

γ Unit weight

ν Poisson's ratio

σ Stress

σ_r Modulus of rupture

UNCLASSIFIED

Security Classification

DOCUMENT CONTROL DATA - R & D			
(Security classification of title, body of abstract and indexing annotation must be entered when the overall report is classified)			
1. ORIGINATING ACTIVITY *(Corporate author)* STANFORD RESEARCH INSTITUTE Menlo Park, California 94025		2a. REPORT SECURITY CLASSIFICATION Unclassified	
		2b. GROUP Not applicable	
3. REPORT TITLE EXISTING STRUCTURES EVALUATION - PART II: WINDOW GLASS AND APPLICATIONS			
4. DESCRIPTIVE NOTES *(Type of report and inclusive dates)* Final Report			
5. AUTHOR(S) *(First name, middle initial, last name)* James H. Iverson			
6. REPORT DATE December 1968	7a. TOTAL NO. OF PAGES 164		7b. NO. OF REFS 50
8a. CONTRACT OR GRANT NO. OCD-DAHC20-67-C-0136	9a. ORIGINATOR'S REPORT NUMBER(S) None		
b. PROJECT NO. Work Unit No. 1126C			
c.	9b. OTHER REPORT NO(S) *(Any other numbers that may be assigned this report)*		
d.			
10. DISTRIBUTION STATEMENT This document has been approved for public release and sale; its distribution is unlimited.			
11. SUPPLEMENTARY NOTES	12. SPONSORING MILITARY ACTIVITY Office of Civil Defense Office of the Secretary of the Army Washington, D.C. 20310		

13. ABSTRACT

This report covers one portion of a research project to evaluate existing National Fallout Shelter Survey (NFSS) structures for resistance to combined nuclear weapons effects. The objective of this investigation was to determine the response of windows to air blast overpressures generated by nuclear explosions, including glass fragment characteristics (weights, velocities, numbers produced, and spatial densities) that could be used to predict statistically the effects of window glass failure on humans.

The analysis leading to the presentation of graphs, which can be used to predict the free-field overpressure at incipient failure for sheet and plate glass, was based on the theoretical load-deflection equation for large deflections of plates, modified by test results found in the literature. Glass panes were changed to equivalent single-degree-of-freedom systems in the analysis. The analysis was also used to estimate the time to failure for windows at various overpressures. Methods for predicting glass fragment characteristics were obtained empirically from Operation Teapot nuclear test data. The procedures for estimating incipient failure overpressures and fragment weights, spatial densities, numbers, and velocities were applied to windows in 14 buildings (located in San Jose and Palo Alto, California) that were part of the NFSS.

DD FORM 1 NOV 65 1473 REPLACES DD FORM 1473, 1 JAN 64, WHICH IS OBSOLETE FOR ARMY USE.

UNCLASSIFIED

Security Classification

14. KEY WORDS	LINK A		LINK B		LINK C	
	ROLE	WT	ROLE	WT	ROLE	WT
Nuclear weapon effects						
Response of windows to air blast						
Glass fragment characteristics						
Window glass failure						
Incipient failure for sheet and plate glass						
Time to failure for window						